KILOHERTZ ULTRASOUND AS A POTENTIAL THERAPY FOR DENTAL REPAIR

by

UPEN SACHIN PATEL

BDS, AHEA, MFDS (RCS Edin), MJDF (RCS Eng)

A thesis submitted to the University of Birmingham for the degree of

DOCTOR OF PHILOSOPHY

Institute of Clinical Sciences
School of Dentistry
College of Medical and Dental Sciences
University of Birmingham

April 2016

ABSTRACT

Biological effects are known to occur with ultrasound energy at kilohertz frequencies. This has led to research into its use as a non-invasive tool for tissue healing and repair. The aim of this research is to investigate the *in vitro* application of kilohertz ultrasound and to measure the biological responses using models of dental pulp cells which play an important role in dental repair. Ultrasound emitted from a longwave therapy instrument (DuoSon, SRA Developments Ltd) was characterised and measured identifying the range and intensity of the field. These measurements, coupled with biological data, identified the difficulties when conducting research with kilohertz ultrasound *in vitro* and indicated that the use of multi-well culture plates is not appropriate when investigating the effects of kilohertz ultrasound in cell culture. An improved method for *in vitro* kilohertz ultrasound application was devised enabling the investigation of non-thermal ultrasound effects on primary human dental cells. Cell proliferation, viability and gene expression, including the dental-related and biomechanically-responsive gene, dentine matrix protein-1, responded in a dose-dependent manner with respect to the duration of ultrasound application. At seven days after the application of kilohertz ultrasound, mineral formation was not found in *in vitro* human dental pulp cultures, however, sham control samples demonstrated few small deposits with the same culture time period. The challenges of maintaining viable primary cell cultures *in vitro* precluded longer culture times, which may have demonstrated an effect of kilohertz ultrasound. This finding highlights the complexity of the biophysical interaction of kilohertz ultrasound with cells and demonstrates the need for further clarification of specific ultrasound settings for optimal therapeutic application. This study has demonstrated a positive effect of kilohertz ultrasound on human dental pulp cells and has identified methods to improve *in vitro* cell culture models to capture robust data to develop a novel therapy for dental repair.

|| SHREE GANESHAYA NAMAH ||

|| JAI SHRI KRISHNA || JAI SIYA RAM || RADHE RADHE || HAR HAR MAHADEV ||

DEDICATED TO MY DAUGHTER

PRIYANA JYOTI PATEL

AND MY LOVING FAMILY

ACKNOWLEDGEMENTS

To begin with, I would like to express my sincerest thanks to my supervisors Dr Ben Scheven and Professor Damien Walmsley for their guidance, advice and support to complete this study. I would like to thank all the technical staff in the Oral Biology and Biomaterials research laboratories, in particular Gay Smith and Michelle Holder, who kindly gave up their time to train and support me with laboratory work. I would like to thank collaborators, Professor Sleiman Ghorayeb and his team at HOFSTRA University (NY, USA) for their support in the mathematical analysis of the ultrasound field measurements. I would also like to thank Dental Technicians, Mr Glyn Thomas and Mr Martyn Baylis, and the technicians from the Biosciences Workshop for their practical advice in the development and construction of apparatus for the application of ultrasound.

Finally I would like to acknowledge my family for their understanding and patience during this period of my life, and in particular my wife Jyoti, who's loving, unconditional and never-ending support has been the keystone to the success of my endeavours. Thank you for being my unreservedly accepting and 'non-boring' rock in this increasingly demanding world.

TABLE OF CONTENTS

LIST OF FIGURES

LIST OF TABLES

LIST OF ABBREVIATIONS

°C	Degrees centigrade
AA	Ascorbic acid
ADM	Adrenomedullin
ALP	Alkaline phosphatase
AmpB	Amphotericin B
ANOVA	One way analysis of variance
ARS	Alizarin Red S
BDNF	Brain-derived neurotrophic factor
bFGF	Basic fibroblast growth factor
β-GP	Beta-glycerol phosphate disodium salt pentahydrate
β-ME	Beta-mercaptoethanol
BMP-2	Bone morphogenetic protein-2
BMP-7	Bone morphogenetic protein-7
BNR	Beam non-uniformity ratio
BSP	Bone sialoprotein
C1α1	Collagen type 1 alpha 1
CGRP	Calcitonin gene related peptide
cm	Centrimetre
cm^2	Square centimetre
CT	Calcitonin
DEX	Dexamethasone
DMEM	Dulbecco's modified eagle medium

DMEMsup	DMEM supplemented with 4.5 g/l glucose, 10% FBS, 1% penicillin/streptomycin and a 2 mM concentration of glutamine
DMEMmin	DMEMsup supplemented with 10 mM β-GP, 50 μg/ml AA and 10nM DEX
DMP-1	Dentine matrix protein-1
DMSO	Dimethyl sulfoxide
DNA	Deoxyribonucleic acid
DPP	Dentine phosphoprotein
DSP	Dentine sialoprotein
DSPP	Dentine sialophosphoprotein
EDTA	Ethylenediaminetetraacetic acid
EDX	Energy dispersive x-ray spectrometry
ERK	Extracellular signal-regulated kinase
FBS	Heat inactivated foetal bovine serum
FDA	Food and drug administration
FGF-2	Fibroblast growth factor-2
g	Gram
g/l	Grams per litre
GAPDH	Glyceraldehyde-3-phosphate dehydrogenase
GDNF	Glial cell line-derived growth factor
h	Hour
HSP	Heat shock protein
HDPC	Human dental pulp cells
Hz	Hertz
IEC	International electrotechnical commission

IL-1β	Interleukin-1β
IL-6	Interleukin-6
IL-8	Interleukin-8
IL-10	Interleukin-10
ILGF-1	Insulin-like growth factor-1
ILGF-2	Insulin-like growth factor-2
J	Joule
J/s	Joules per second
kHz	Kilohertz
kV	Kilovolt
l	Litre
LIPUS	Low intensity pulsed ultrasound
m	Metre
mA	Milliamp
MAPK	Mitogen-activated protein kinase
MMP-13	Matrix metalloproteinase-13
MDPC-23	Mouse-derived dental pulp cells-23
MEPE	Matrix extracellular phosphoglycoprotein
µA	Microamp
µCT	Micro-computed tomography
µg	Microgram
µg/ml	Microgram per millilitre
µl	Microlitre
min	Minute

mg	Milligram
mg/l	Milligrams per litre
MHz	Megahertz
ml	Millilitre
mm	Millimetre
mm^2	Square millimetre
mm^3	Cubic millimetre
mm/s	Millimetres per second
mM	Millimolar
mmol	Millimole
ms	Millisecond
MTA	Mineral trioxide aggregate
mW	Milliwatt
mW/cm^2	Milliwatts per centimetre squared
NCP	Non-collagenous proteins
NICE	National institute for health and care excellence
ng	Nanogram
NGF	Nerve growth factor
nM	Nanomolat
NPY	Neuropeptide Y
OCN	Osteocalcin
ON	Osteonectin
OPN	Osteopontin
PA	Pulse average

PBS	Phosphate buffered solution
PDGF	Platelet derived growth factor
RANKL	Receptor activator of nuclear factor κ-B ligand
RDT	Residual dentine thickness
RNA	Ribonucleic acid
ROS	Reactive oxygen species
rpm	Revolutions per minute
RUNX2	Runt-related transcription factor 2
s	Second
SA	Spatial average
SATA	Spatial average temporal average
SEM	Scanning electron microscopy
SIBLING	Small integrin-binding ligand N-linked glycoproteins
SPA	Spatial peak average
SP	Spatial peak
SPTA	Spatial peak temporal average
sqRT-PCR	Semi-quantitative reverse transcriptase polymerase chain reaction
SubP	Substance P
TA	Temporal average
TAE	Tris-acetate-EDTA
TGF-β1	Transforming growth factor beta 1
TNF-α	Tumour necrosis factor-α
V	Volt
VEGF	Vascular endothelial growth factor

VIP	Vasoactive intestinal polypeptide
W	Watt
W/cm^2	Watts per centimetre squared

CHAPTER 1

INTRODUCTION

1.1 ULTRASOUND

The human auditory sensory organ is capable of sensing vibrations when particles oscillate at a frequency within the range of 20 Hz and 20,000 Hz. This is known as acoustic sound. The detection of particles oscillating at a frequency greater than 20,000 Hz is categorised as ultrasound. This is outside the detectable range of human hearing but can be sensed by certain species of the animal kingdom, such as dogs, bats and dolphins.

1.1.1 GENERATION, PROPAGATION AND PHYSICAL PROPERTIES OF A SOUND WAVE

Particle oscillation at a frequency greater than 20,000 Hz can be generated naturally by many animals. Bats and dolphins navigate using ultrasound and echolocation. These animals emit ultrasound and listen for their echoes as the ultrasonic wave is reflected from objects in their vicinity. Dogs are unable to generate ultrasound, but they can hear sound at ultrasonic frequencies. Ultrasound is produced by dog whistles where the air blown through the whistle is made to vibrate at high frequencies only heard by the animal. Ultrasound can also be generated by converting electrical energy into mechanical energy via a transducer. Two methods to generate ultrasound in this way utilise magnetostrictive or piezoelectric technologies. Industrial uses of ultrasound include non-destructive testing of materials to identify imperfections, motion sensing technology such as parking sensors in vehicles and range finding for underwater navigation. The most commonly used application of ultrasound in the medical field is ultrasonography. This is used to produce a real-time image of organs and tissues, such as the unborn foetus or the heart and its blood vessels. It can also be used to

guide surgery for tumour removal or stent placement. Ultrasonography can be considered a safer method of diagnostic testing compared to conventional imaging techniques which utilises X-rays because ultrasound does not deliver ionising radiation to the patient (Barnett et al. 2000). In the field of physiotherapy, ultrasound has been used in the treatment of soft tissue injuries (ter Haar et al. 1987) involving muscles and tendons (Speed 2001) as well as hard tissues such as bone fractures (Heckman et al. 1994).

Magnetostriction is the change in dimension of a metal when exposed to a magnetic field and was first observed by James Joule (Joule 1842). The piezoelectric effect was first documented nearly 40 years later, in 1880, by brothers Jacques and Pierre Curie (Curie and Curie 1880). The Curie brothers initially observed that certain crystals, such as quartz, would generate electricity when placed under compression or tension stress. They later demonstrated the converse was true when crystals were exposed to an electrical current (Curie and Curie 1881).

An ultrasound wave is generated when these materials are made to change shape more than 20,000 times a second. The resulting oscillatory action creates a wave of pressure arising from the material which displaces the surrounding particles. Energy is transferred through the vibration of particles. Such motion is only possible in a medium composed of particles such as gas, liquid, solid or plasma. Sound cannot travel in a vacuum. The rate of particle displacement is related to the frequency at which the material is vibrating and generates localised areas of compression followed by rarefaction of particles in the medium. Sound waves are mechanical pressure waves, and the energy is transferred from particle to particle. There is no net movement of the particle and it is the energy that is transferred along the wave

(O'Brien 2007). A typical sound wave follows a sinusoidal pattern as shown in Figure 1.1 which demonstrates its oscillatory nature.

The frequency of a sound wave can be calculated using Equation 1. The amplitude determines the degree by which the sound wave oscillates and therefore particle displacement (Hykes et al. 1985).

Equation 1.

$$f = \frac{v}{\lambda}$$

Where wavelength is represented by lambda (λ), velocity (v) is the speed of the sound wave and frequency (f).

The frequency of the sound wave remains constant, whether in the same medium, or as it propagates from one type of medium to another (Cracknell 1980a). However the velocity of the sound wave is dependent on the density and compressibility of the medium it is travelling through (Hykes et al. 1985). Material density and sound velocity values from Table 1.1 show that materials with particles organised into solids have a higher sound velocity compared to liquids and gases.

Figure 1.1 A sine waveform showing two properties of a sound wave; (A) wavelength, (B) amplitude. Two wavelengths are shown.

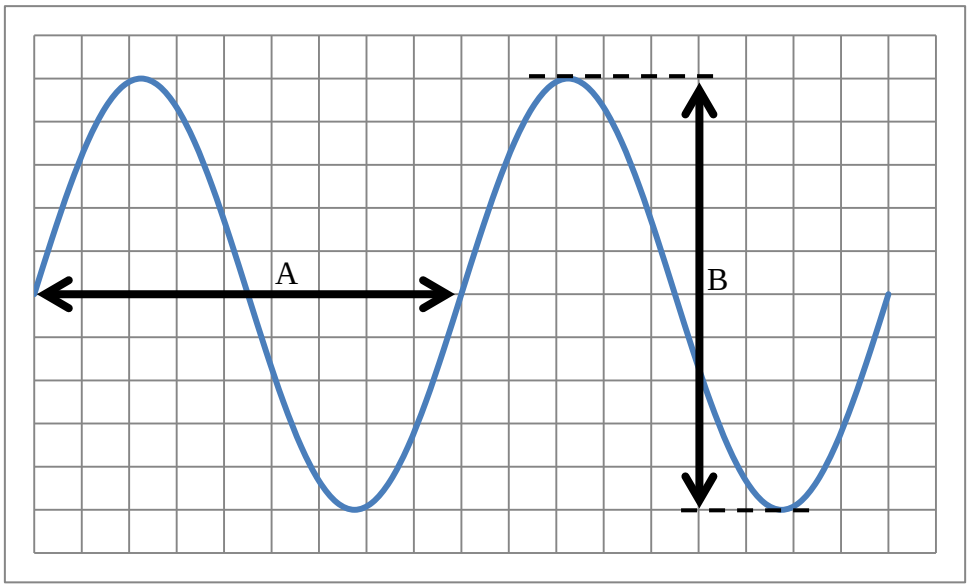

Acoustic impedance is the degree by which a material restricts the flow of ultrasound, essentially the momentum of ultrasound through the material (Hykes et al. 1985). Dense materials, such as enamel, exhibit a faster ultrasound transmission speed resulting in a larger acoustic impedance value (Table 1.1). The relationship of a material's acoustic impedance, density and the speed at which ultrasound propagates through it is demonstrated by Equation 2.

Equation 2.

$$Z = \rho v$$

Where acoustic impedance is represented by *Z*, velocity (v) is the speed of the sound wave and density (ρ).

Table 1.1 Acoustic properties of biological materials in different physical states. Adapted from various sources (Blodgett 2002, Hykes et al. 1985, Lees 1971).

Material	**Density (kg/m^3)**	**Velocity (m/s)**	**Acoustic Impedance ($kg/m^2s \times 10^6$)**
Air	1.2	330	0.0004
Water (20 °C)	1000	1480	1.48
Liver	1060	1550	1.64
Muscle	1080	1580	1.70
Fat	952	1459	1.38
Dentine	2000	3800	7.6
Enamel	3000	6250	18.8
Bone	1912	4080	7.8

1.1.2 ATTENUATION AND DEFLECTION OF ULTRASOUND

A collection of sound waves travelling in a similar direction can be considered to be a beam of sound. When the frequency of each wave is greater than 20,000 Hz, it is considered to be an ultrasound beam. As the ultrasound propagates through a medium, the amplitude of each wave within the beam is reduced. This is called attenuation and is a result of the medium absorbing energy from the wave and deflection of the wave by reflection, refraction, diffraction and scattering (Cracknell 1980b).

Much of the absorbed energy is converted to heat and dissipated from the medium (ter Haar 1999). The degree to which the energy of the ultrasound beam is absorbed is determined by the frequency of the ultrasound wave and the properties of the medium in which it is travelling. The absorption of ultrasound and hence the production of heat in biological tissues is also dependent upon its molecular composition. The amount of absorption in biological tissues increases as a function of protein content (Goss et al. 1979). However, estimating the overall temperature rise in these tissues is complex and should also take into account the balance between heat loss and heat gain as a result of the thermal conductivity and the degree of vascular perfusion (Barnett et al. 1997, Miller et al. 2012). Higher viscosity materials will require more energy to move their particles compared to those materials with a lower viscosity, which in turn generates heat. The rate of energy absorption is directly related to the frequency of the ultrasound wave. At higher frequencies, particles do not get the time to return to their normal resting positions once exposed to an ultrasound wave. Hence, particle movement will occur against the force of a particle returning to its rest position. Changing the

direction of a particle already in motion requires more energy which is absorbed by the material and lost as heat (Hykes et al. 1985).

Deflection of ultrasound waves usually occur at a medium boundary, where the wave passes from one type of material to another. A wave is reflected if there is a significant mismatch in the acoustic impedance between two materials (Hykes et al. 1985). Table 1.1 shows the acoustic impedance of some biological materials. The greatest mismatch would occur when a wave is travelling from one physical state to another, such as gas to liquid or liquid to solid. If the medium boundary is perpendicular to the direction the wave is travelling, the reflected wave would travel back in the opposite direction towards the source of the wave. The reflected wave has the effect of causing either constructive or destructive interference, enhancing or nullifying, respectively, the incident ultrasound wave (Hykes et al. 1985). This is known as a standing wave (O'Brien 2007).

The independent advisory group on non-ionising radiation (Health Protection Agency) reported that the potential for the generation of standing waves within the human body as a result of an ultrasound field is very rare (AGNIR 2010). However Schlieren imaging has demonstrated the presence of standing waves during the application of 500 kHz ultrasound to a cadaver human skull submerged in water but found no evidence of standing waves when ultrasound with a frequency of 2 MHz was applied (Azuma et al. 2004). The study concluded that the increased attenuation of high frequency ultrasound prevented significant reflection at the soft-hard tissue interface. Lower frequency ultrasound demonstrates better penetration and thus more potential for reflection and standing wave generation (O'Reilly et al. 2010). A biological study utilising 300 kHz ultrasound to treat stroke with transcranial

sonothrombolysis was halted after brain haemorrhages were discovered in five patients (Daffertshofer et al. 2005). A simulation study based on the biological study later identified standing waves as a possible cause of the injury and simulations using 2 MHz ultrasound demonstrated a significant reduction in standing waves (Baron et al. 2009). Transcranial sonothrombolysis requires the use of high intensity focused ultrasound and the risks of standing wave generation are high. Low-power applications of ultrasound (Table 1.2) pose a much lower risk of *in vivo* standing waves. Using a low intensity and keeping the source of ultrasound in motion helps to reduce the risks of generating a standing wave.

1.1.3 THE ULTRASOUND BEAM

To generate a beam of ultrasound, the dimensions of the transducer should be higher than the wavelength of sound being produced. Energy is applied to the piezoelectric material producing a dimensional change which in turn generates multiple mechanical pressure ultrasound waves at the transducer face. The number of individual waves generated is dependent on the wavelength and the surface area of the transducer face. If the diameter of the transducer face was equal to one wavelength, only one wave would be generated. The ultrasound beam is a collection of these individual ultrasonic waves which interact with each other close to the transducer face (Huygens' principle). This region is called the near field or the Fresnal zone. Within this zone there is a lack of homogeneity resulting in both increased and decreased energy levels in the ultrasound beam as shown in figure 1.2 (Hykes et al. 1985). Equation 3 describes the relationship between the velocity and frequency of an ultrasound wave and how this relates to the length of the near field from the transducer face for an unfocussed transducer.

Equation 3.

$$L = \frac{d^2 f}{4v}$$

Where L is the length of the near field, velocity (v) is the speed of the sound wave, frequency (f) and diameter (d) of the transducer face.

Figure 1.2 Diagrammatic representation of an ultrasound beam indicating the position of the near field and far field relative to the transducer face. The diagram also shows a typical intensity profile versus distance from the transducer face (Hykes et al. 1985).

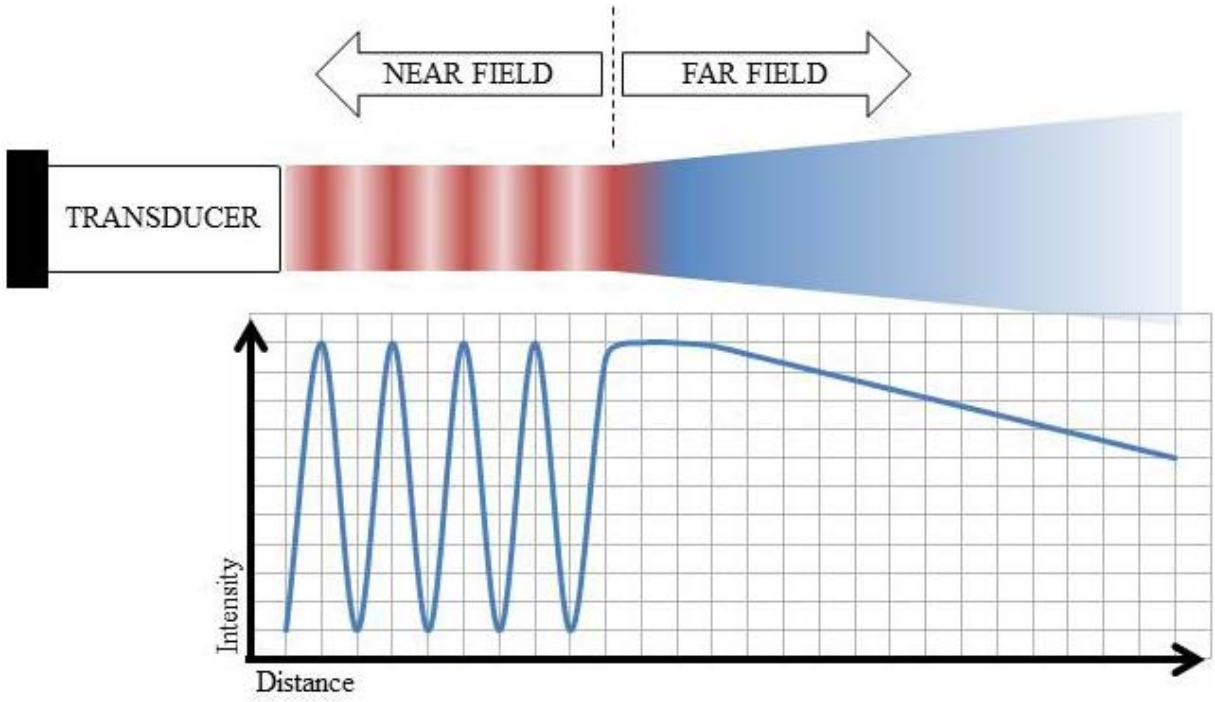

1.1.3.1 MEASURING ULTRASONIC ENERGY

Energy is expressed as a Joule (J) and combined with a period of time as Joules per second (J/s), is the equivalent to 1 watt (W) (O'Brien 2007). The total amount of energy exerted by a beam of ultrasound per second is called the acoustic power and is expressed in watts (Zeqiri 2007). The intensity describes the amount of energy transferred through a unit cross-sectional area per second with the unit W/cm^2. The intensity of ultrasound refers to a specific area within the ultrasound beam and whilst this value is not homogenous in the near field, due to wave interaction, there is better reproducibility of the intensity measurement in the far field or Fraunhofer zone as shown in Figure 1.2 (Hykes et al. 1985).

Depending on the electrical input, transducers are able to emit ultrasound in a continuous beam, or in repeating packets of energy producing a pulsing beam. A pulsed beam will reduce heat generation when a high frequency or a high power ultrasound beam is used. Due to these variations and the inhomogeneity of the ultrasound beam, recording the energy output of an ultrasound transducer is not straightforward. The terms; spatial peak, spatial average, pulse average and temporal average can be used to describe the intensity of the ultrasound beam. Spatial peak (SP) and spatial average (SA) values refer to the maximum intensity and average intensity (respectively) in the ultrasound field. Temporal average (TA) refers to a measurement taken over a period of time, and when using a pulsed beam of ultrasound, the term pulse average (PA) should be used. This terminology allows standardisation for the reporting of ultrasound energy (ter Haar 2007, Wu and Nyborg 2006).

The energy levels of an ultrasound beam can be recorded using devices that detect changes in pressure. A hydrophone converts pressure to electrical voltage using the piezoelectric effect. The voltage measurements are recorded and interpreted by an oscilloscope and the core frequency of the ultrasound beam can be calculated. The hydrophone must first be calibrated against a reference hydrophone to determine its accuracy and thus generate a calibration factor or sensitivity level for a range of predetermined ultrasonic frequencies. These values are used to carry out the calculations to determine the intensity level. It is assumed that the frequency of ultrasound generated by the transducer is a single component however multiple frequencies can exist within a single ultrasound beam. This requires the use of a deconvolution method, such as Fourier Transform, to ensure the correct intensity is calculated from measurements of the ultrasound field (Zeqiri 2007).

1.1.4 THE EFFECTS OF ULTRASOUND ON BIOLOGICAL TISSUES

Ultrasound waves are used in diagnostic medicine to visualise internal structures within the human body and this imaging modality is termed ultrasonography. Ultrasound waves are reflected at tissue boundaries (section 1.1.2) and the transducer which emits the initial ultrasound beam also receives the reflected waves. The ultrasound waves received by the transducer are converted into electrical signals and an image is generated. Ultrasound waves used in ultrasonography are generated with a frequency usually greater than 2.5 MHz, however the frequency used is related to the depth of the area in the body that requires investigation. The ultrasonic examination of internal organs such as the liver or kidney use low (<3 MHz) ultrasound frequencies whilst investigations of more superficial tissues such as muscles, mammary glands and neonatal investigations can be carried out with higher

frequencies (>2.5 MHz). These higher frequencies also improve the resolution of the image (O'Brien 2007). Ultrasonography is considered a safe diagnostic tool with no irreversible biological effects. However, the interaction of ultrasonic waves with biological tissues has the potential to cause harm due to the heating and mechanical effects of ultrasound with high-power applications (Table 1.2) (Child et al. 1990, Connor and Hynynen 2004, Daffertshofer et al. 2005). The risk of harm with low-power applications (Table 1.2) is low (Miller et al. 2012). The risks of these effects are reduced by limiting the duration of the examination and in some instances, ensuring the transducer is kept in motion to prevent an accumulation of heat. Ultrasound beams used in ultrasonography are pulsed and are regulated to ensure the spatial peak temporal average (SPTA) intensity used for investigation is set at 720 mW/cm^2. This reduces the energy of the ultrasound beam decreasing the occurrence of heating and mechanical effects (ter Haar 2011a).

Whilst it is intended for the ultrasound used in ultrasonography to have very little interaction with biological tissues, ultrasonic energy can generate physical interactions in biological tissues via heating and mechanical effects resulting in a therapeutic benefit. Therapeutic ultrasound is a general term describing the use of ultrasound to produce a healing or curative effect in biological tissues. There are two broad categories for the applications of therapeutic ultrasound; high-power and low-power (Table 1.2). This study will consider low-power therapeutic ultrasound, focusing on its application and mechanisms for the repair and regeneration of biological tissues.

Table 1.2 Applications of therapeutic ultrasound in biological tissues (Ahmadi et al. 2012, Mason 2011, ter Haar 2007).

High-power	**Low-power**
Ablation therapy (High Intensity Focused Ultrasound)	Drug activation (Sonodynamic therapy)
Extra-corporeal Shockwave Therapy (e.g. Lithotripsy)	Drug delivery (Sonophoresis & Sonoporation)
Sonothrombolysis	Gene therapy
	Physiotherapy
	Tissue repair / regeneration

1.1.4.1 HEATING EFFECTS

A heating effect is created when ultrasound interacts with biological tissues as a result of absorption of the wave energy. Decreasing the frequency of the ultrasound wave allows for better penetration of tissues and in turn reduces heating as there is less energy absorption. Both increasing the time that ultrasound is applied and using a continuous ultrasound beam (opposed to a pulsing beam) increases the heating effect in tissues. The adsorption of the wave energy results in an increase in blood flow and tissue extensibility. This produces a beneficial effect which has been used to treat a range of disorders including reducing joint stiffness and muscle spasm, modulation of pain and the production of a mild inflammatory response (Speed 2001).

Robertson (2002) conducted a review of randomised controlled trials where ultrasound was used to treat pain and promote soft tissue healing (Robertson 2002). These treatments can be considered to be within the field of physiotherapy which aims to increase tissue temperatures above 39.6 °C and has been shown to generate a therapeutic physiological effect (Hayes et al. 2004). Robertson (2002) found 24 suitable randomised control studies which utilised low-power therapeutic ultrasound with a spatial average temporal average (SATA) intensity in the region of 0.16 and 0.5 W/cm^2 (Robertson 2002). Statistically significant improvements in the group treated with ultrasound where reported in 7 out of the 24 studies (Binder et al. 1985, Callam et al. 1987, Dyson et al. 1976, Ebenbichler et al. 1999, Ebenbichler et al. 1998, Hasson et al. 1990, Roche and West 1984) whereas the remaining 17 studies did not report a significant outcome (Bradnock et al. 1996, Craig et al. 1999, Downing and Weinstein 1986, Eriksson et al. 1991, Everett et al. 1992, Falconer et al. 1992, Grant et al. 1989, Haker and

Lundeberg 1991, Hashish et al. 1988, Hashish et al. 1986, Lundeberg et al. 1988, Lundeberg et al. 1990, Mcdiarmid et al. 1984, McLachlan et al. 1991, Nykanen 1995, Plaskett et al. 1999, ter Riet et al. 1996). Studies which reported a significant outcome showed that 0.2 W/cm^2 would be the most appropriate SATA intensity and in all 7 of these studies, ultrasound was pulsed. Robertson (2002) summarised that whilst this study identified an effective window of SATA intensity for soft tissue therapeutic use, variables such as the equipment used, method and site of ultrasound application, the frequency of ultrasound and treatment times will affect outcomes.

High-power applications, such as ablation therapy for cancer treatment, focus the ultrasound beam to a specific localised area within biological tissues. This generates localised hyperthermia and results in coagulative tissue necrosis (Malcolm and ter Haar 1996). This method has been used for the treatment of solid malignant tumours (Zhou 2011) as well as the arrest of bleeding from blood vessels around the heart (Vaezy et al. 2001). Whilst ablation therapy relies on the generation of heat, mechanical effects should not be ignored. Damage to leukemic cells has been shown with the use of low energy 1.8 MHz ultrasound where no heat is generated (Lagneaux et al. 2002). A recent study has demonstrated the ablation of brain tissue in rats by generating localised cavitation and microstreaming using a contrast agent with low power overlapping applications of ultrasound (McDannold et al. 2016). Ultrasound at higher frequencies, as used in tissue ablation, has been shown to generate significant levels of cavitation and the release of energy can result in profound cell and tissue damage (Hill 1971). When considering the effects of ultrasound, both mechanical and thermal effects can take place at the same time.

1.1.4.2 MECHANICAL EFFECTS

As well as heating effects, Speed (2001) also proposed non-thermal (also known as mechanical) effects of therapeutic ultrasound; cavitation and acoustic microstreaming. These mechanical effects are a result of the changes in pressure generated by an ultrasound wave (Section 1.1.1). It is postulated that cell membranes and cytoskeletal structures are affected either directly by the ultrasound wave oscillation, or indirectly via cavitation and acoustic microstreaming (Baker et al. 2001, Feril and Kondo 2004). The pulsing nature of ultrasound (frequency) provides a repetitive stimulus that may sufficiently stress the cell into upregulating its internal cell processes resulting in a biological effect. The subsequent effect of mechanical stimulation is thought to be the activation of intracellular signalling resulting in gene transcription (Johns 2002, Scheven et al. 2009b).

Externally, the cellular membrane is composed of a variety of molecules that are sensitive to mechanical stimulation (Padilla et al. 2014), whilst internally, the cytoskeleton has been shown to be responsive to differing mechanical load from the extracellular matrix (Geiger et al. 2001, Robling et al. 2006). Calcium ion channels found in the cell membrane have been shown to respond to mechanical stimulation affecting the intracellular concentration of calcium ions (Parvizi et al. 2002). Fluctuations in the concentration of calcium ions have been shown to trigger differentiation in stem cells (den Dekker et al. 2001, Sun et al. 2007). Integrin-mediated focal adhesions link the extracellular matrix to the cytoskeleton and allow for the signalling of mechanical force through protein modulation (del Rio et al. 2009). The exposure of protein binding sites on the integrin-mediated focal adhesion molecules, as a result of mechanical stimulation (Whitney et al. 2012) has been shown to activate the

integrin/phosphatidylinositol 3-OH kinase/Akt pathway (Takeuchi et al. 2008). This pathway has been linked with increasing cell proliferation and activation of extracellular signal-regulated kinases (ERK) and mitogen-activated protein kinases (MAPK) which has been shown to influence cell migration and the regulation of gene expression (Whitney et al. 2012). Bandow et al. (2007) has shown that ultrasonic mechanical activation of the angiotensin II type I receptor found on osteoblasts induces cytokine expression and ERK phosphorylation activation (Bandow et al. 2007). Stretch activated ion channels (Liedert et al. 2006), G-protein coupled receptors (Morris et al. 2010) and primary cilia (Malone et al. 2007) have also been shown to be receptive to mechanical stimulation however their activation of internal cell processes are as yet unclear. Cell membranes have also been shown to increase their porosity when stimulated with ultrasound allowing the improved transfer of drugs (sonoporation), mineral ions and genes to stimulate cell processes (Deng et al. 2004, Mehier-Humbert et al. 2005, Mitragotri 2005).

The application of low intensity ultrasound (considered non-thermal) to osteoblastic cells *in vitro* has been shown to upregulate chemokines such as monocyte chemoattractant protein, macrophage-inflammatory protein and receptor activator of nuclear factor κ-B ligand (RANKL) (Bandow et al. 2007). Harle et al. (2001) showed the upregulation of alkaline phosphatase and osteopontin was dependent on the intensity of 3 MHz ultrasound applied to osteoblasts *in vitro* (Harle et al. 2001). A later study (Harle et al. 2005) by the same group found upregulation of transforming growth factor-beta was again dependent on ultrasound intensity in a similar manner as the first study. The later study also measured the streaming velocity in culture media using Doppler shift and found an increase in the streaming velocity with an increase in intensity. Temperature changes were also negligible. These findings

strongly indicate that mechanical effects have a role in the regulation of gene expression. The stimulation of microbubbles by ultrasound gives rise to acoustic microstreaming through cavitation. This mechanical effect has been shown to upregulate genes involved in apoptosis and ceramide-induced apoptotic pathways in endothelial cells (Al-Mahrouki et al. 2012).

1.1.4.2.1 CAVITATION

Cavitation is the excitation of gas filled bubbles by ultrasonic pressure waves. When ultrasound passes through the medium, these bubbles will either undergo inertial (transient) or non-inertial (stable) cavitation depending upon the pressure amplitude of the wave (Wu and Nyborg 2008). High-pressure amplitudes above a threshold level will result in inertial cavitation usually resulting in the bubble imploding violently and subsequently releasing further mechanical energy and highly reactive free radicals (Edmonds and Sancier 1983, Lea et al. 2005). Non-inertial cavitation allows the bubble to remain intact with only moderate changes in size and a degree of oscillation (Wu and Nyborg 2008). When a bubble collapses, the energy produced is extremely high but only for a very small period of time (Ahmadi et al. 2012). Multiple bubbles collapsing continuously can give rise to large energy releases which can damage tissues. This effect, in conjunction with a focused ultrasound beam, is used in ablation therapy to generate high temperatures at specific points within the body (ter Haar 2007). Proving the presence of cavitation at therapeutic (low-power) intensities *in vivo* is challenging and only a few studies have demonstrated cavitation *in vivo* (ter Haar et al. 1982, ter Haar and Daniels 1981). However the findings from these studies have been challenged due to the interpretation of ultrasound imaging to determine the presence of cavitation (Watmough et al. 1991). Regardless, high-power applications, such as extra-corporeal

lithotripsy, are known for inducing cavitation *in vivo* (Barnett et al. 1997, Coleman et al. 1996, Coleman et al. 1995, Vakil and Everbach 1993). Cavitation generated by an ultrasonic scaling tip is used to remove hard debris cemented to the tooth surface during a dental scaling procedure (Lea et al. 2005, Walmsley 1988).

1.1.4.2.2 ACOUSTIC MICROSTREAMING

Acoustic microstreaming has been described as the flow of liquid as a result of non-inertial cavitation (ter Haar et al. 1987, Wu and Nyborg 2008). Expanding and contracting bubbles, as a result of the pressure changes within an ultrasound field, can generate intercellular and intracellular oscillations (Ahmadi et al. 2012, ter Haar 2007). These movements result in a shear stress being applied to the cells' membranes and organelles within the cell (Johns 2002, Laird and Walmsley 1991, Nyborg 1982, Williams and Chater 1980) resulting in the activation of various mechano-transduction pathways discussed in section 1.1.4.2. Johns (2002) has proposed that microstreaming stresses biological cells significantly in order for the cell to respond. The cell membrane can be influenced to affect permeability, adhesion and proliferation resulting in changes to signalling pathways and gene regulation within the cell (Johns 2002). Acoustic microstreaming has been shown to take place around ultrasonic dental scaling tips (Khambay and Walmsley 1999, Laird and Walmsley 1991) where it is employed to remove plaque and calculus (Walmsley et al. 1984) and has been shown to disrupt the bacterial biofilm that forms on teeth (O'Leary et al. 1997). Sonothrombolysis utilises acoustic microstreaming to breakdown clots in the body to reduce the risk of stroke. Saqqur et al. (2014) undertook a systematic review of the literature and concluded that sonothrombolysis was a safe and effective method of treatment (Saqqur et al. 2014).

1.1.4.2.3 FREQUENCY RESONANCE HYPOTHESIS

It is further postulated that the vibrations generated from the ultrasound wave are absorbed by proteins within the cell, triggering a conformational change. This change may also come about due to the resonant frequency of each protein matching that of the ultrasound wave. A conformational change in a protein, such as an enzyme, may activate or deactivate the enzyme resulting in changes to gene expression and ultimately influencing the biological function of the cell (Johns 2002). The principles of this theory have been investigated by Chetverikova et al. (1985). Chetverikova et al found that ultrasound decreased the activity of creatine kinase and suggested that ultrasound had disrupted the multi-molecular form of this enzyme (Chetverikova et al. 1985). A more recent study investigating the effectiveness of sonothrombolysis discovered that whilst fibrinogen activity was upregulated, no conformational changes were induced (Cherniavsky et al. 2011). Marchioni et al. (2009) investigated the effect of ultrasound on six proteins; cytochrome, lysozyme, myoglobin, bovine serum albumin, trypsinogen and α–chymotrypsinogen A. They summarised that conformational changes in proteins were evident, however rather than resonance, cavitation resulting in free radical production was the more influential factor (Marchioni et al. 2009). Whilst the findings from these studies are based on *in vitro* experiments, *in vivo* findings are as yet unreported.

1.2 DENTAL REGENERATION

Most biological tissues in the human body are able to respond to harmful stimuli to ensure the structure, functioning and survival of that tissue is maintained. Some of the tooth's structures have an inherent capacity to repair but the environment of the oral cavity presents mechanical and chemical challenges to the survival of dental tissues. Hence the capacity to repair is limited and there is the potential that the insult will overwhelm the tissue defences leading to irreversible damage. The different tissues that make up teeth are organised into layers allowing for each individual tooth to respond effectively to slowly progressing mild stimuli. Maintaining the biological functions of a tooth will allow for its long-term survival, giving it the ability to respond to future stimuli. However the mechanism by which ultrasound energy generates a beneficial response remains unclear. Ultrasound stimulation has been linked to the differentiation of pulp cells *in vitro* (Nakashima et al. 2003, Scheven et al. 2009a) whilst *in vivo* studies have shown dentine production in association with mechanical distraction (El-Bialy et al. 2003). Understanding the various reparative and regenerative processes that occur within dental tissues is important to support the development of novel therapies and techniques that prevent the need for complex dental procedures and tooth extractions.

1.2.1 TOOTH STRUCTURE

The crown is that part of the tooth that is directly exposed to the oral environment whilst the root portion is embedded within the alveolar bone of the jaw. The central compartment of a tooth is made up of pulp tissue which is encased by dentine but for a small opening at the apex of the root; the apical foramen. The dentine in the crown of the tooth is covered by

Figure 1.3 Diagrammatic representation of a coronal cross section through a two rooted molar tooth. The diagram demonstrates the relationship of the major structures in a tooth.

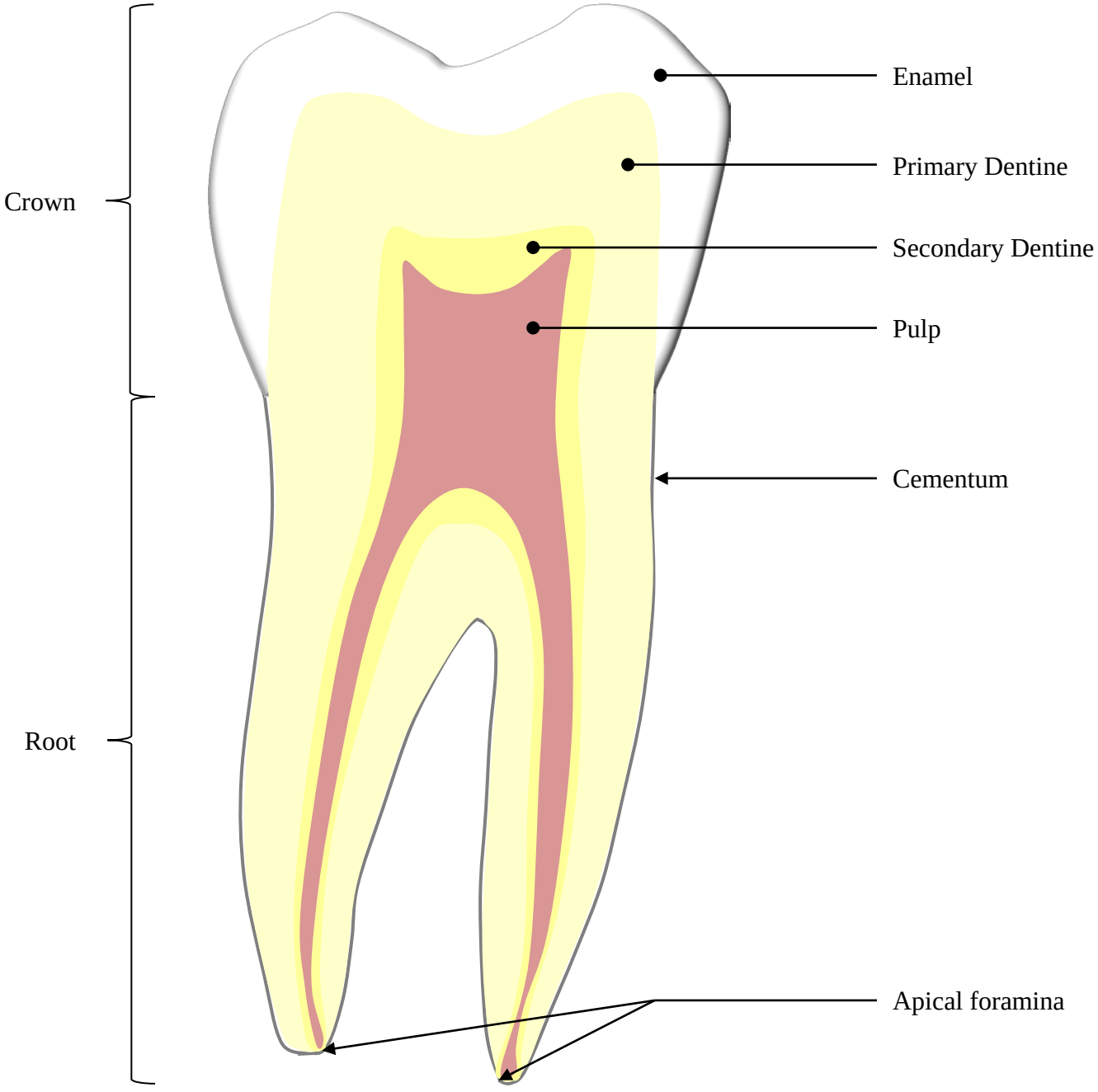

enamel, whereas in the root, it is covered by cementum (Figure 1.3). Enamel, dentine and cementum are mineralised tissues whereas the dental pulp is a fibrous connective tissue containing vascular, neural and connective tissue (Ten Cate 1998). Enamel is considered to be the hardest mineralised tissue in the human body with a mineral content of 96% and a hardness similar to steel (Gwinnett 1992, Ten Cate 1998). This covering protects the underlying structure of the tooth from the recurring processes of mastication, tooth-brushing and attack from dietary food products, such as acid, however due to its low water and high mineral content, enamel is a brittle material (Caldwell et al. 1957, Meckel et al. 1965, Staines et al. 1981). Dentine has a lower mineral content (Mjor 1966), which is comparable to bone, and although softer than enamel, dentine supports the overlying enamel preventing fracture under heavy and sudden occlusal load, such as during mastication (Craig and Peyton 1958). Cementum is considered to be part of the periodontium together with the gingivae, periodontal ligament and bone which support the tooth in the mouth. The categorisation of different types of cementum is complex and is based on the presence of cells (cementocytes), time of formation and the source of collagenous fibres within its matrix. Whilst the role of acellular cementum is to ensure its attachment to the tooth, cellular cementum is responsible for replenishing its surface layer adjacent to the periodontal ligament and is adaptive to tooth wear and movement (Ten Cate 1998). In humans, enamel is secreted and mineralised only whilst the tooth is developing. Once the tooth has erupted into the oral cavity, the cells responsible for enamel production, ameloblasts, are lost and no further enamel is deposited (Ten Cate 1998). Enamel can be lost from the tooth either by dental caries, tooth wear or trauma. The tooth is unable to generate new enamel and, in order to protect the pulp, the tooth responds to this stimulation by upregulating the production of dentine at the interface between

the pulp and the dentine layer (Smith 2002). Unlike ameloblasts, the cells that generate dentine, odontoblasts, remain at the dentine-pulp complex.

1.2.1.1 DENTINE-PULP COMPLEX

Dentine is secreted and mineralised (dentinogenesis) by odontoblasts which line the entire internal border of the pulp chamber adjacent to the dentine layer. The shape of this boundary matches that of the overall form of the tooth resulting in pulp horns in the crown beneath the peaked cusps of teeth and a taper to the apical foramen at the apex of the root (Figure 1.3). Nerve and blood vessel branches pass through this opening and supply the pulp tissue which is composed of collagen fibres, ground substance, fibroblasts, undifferentiated ectomesenchymal cells, macrophages, lymphocytes and dendritic cells (Ten Cate 1998). Their main function is to support the production of dentine by odontoblasts in the dentine-pulp complex. The dentine deposited by the odontoblasts after the root is completed is called secondary dentine (Figure 1.3). Secondary dentine is produced throughout the lifetime of the tooth (Baume 1980). Prior to root completion, odontoblasts generate primary dentine which makes up the majority of the dentine in a tooth (Figure 1.3) (Smith et al. 1995). Dentine secreted by odontoblasts has a tubular structure to accommodate for the odontoblasts' cell processes and can be categorised into intertubular and peritubular (intratubular) dentine. As the odontoblast migrates towards the centre of the tooth depositing dentine, the cell process elongates and maintains a tapered tract (dentinal tubule), narrower at its origin, the enamel-dentine junction, due to peritubular dentine deposition (Garberoglio and Brannstrom 1976, Mjor 1966, Ten Cate 1998). These tracts are sinusoidal in shape, markedly so in the crown of the tooth, due to the crowding of odontoblasts as the size of the pulp chamber is reduced by

the continuous formation of dentine. The reduction of the internal surface area of the pulp chamber results in a higher tubule density in dentine closest to pulp (inner dentine) compared to dentine near enamel (outer dentine). Individual dentinal tubules may also be interconnected by branches which increases the permeability of dentine and provides an effective means of communication between the dentine-pulp complex, the enamel layer and the environment of the oral cavity (Pashley 1996). This network of tubules traversing across the entire dentine layer allows a specific area of the dentine-pulp complex to respond to a stimulus affecting that part of the tooth. Superficial and mild stimuli, such as tooth-brushing, mastication and cavity preparation into the outer dentine tend not to trigger a response from the dentine-pulp complex (Smith et al. 1994). However, cavity preparation close to the pulp, dental caries and tooth wear involving dentine are significant threats resulting in the production of dentine, termed tertiary dentine. These repair processes can only continue to respond to stimuli whilst the living tissue of the pulp remains healthy. Stronger and more severe stimuli, such as trauma or disease, that exposes the pulp chamber to the oral environment, will result in infection and ultimately death of the pulp. It is therefore important to understand the repair processes within teeth and promote the production of tertiary dentine when required to maintain pulp vitality.

1.2.2 TERTIARY DENTINOGENESIS

Whereas the production of primary and secondary dentine is controlled by innate processes within the developing and mature tooth, tertiary dentine is generated as result of external stimuli acting on the dentine-pulp complex. Two types of tertiary dentine have been recognised; reactionary and reparative (Lesot et al. 1993, Smith et al. 1995). Whilst both types aim to preserve the structural integrity of the pulp chamber and provide a protective barrier to

prevent the loss of pulp vitality, they are produced by two different cell types. Mild stimulation would trigger odontoblasts lining the pulp chamber to produce reactionary dentine. A stronger stimulus may damage these cells resulting in the recruitment of undifferentiated ectomesenchymal pulp cells and their subsequent differentiation into odontoblast-like cells. These cells migrate to the damaged area in the pulp and produce reparative dentine (Figure 1.4).

Figure 1.4 Diagrammatic representation of the crown portion of a tooth indicating the process of tertiary dentinogenesis. Reactionary dentinogenesis is shown on the left side of the tooth where caries has provided a mild stimulus and triggered odontoblast cells to produce reactionary dentine. On the right, deep cavity preparation into the pulp has damaged odontoblast cells at the site of the exposure resulting in odontoblast-like cells producing reparative dentine.

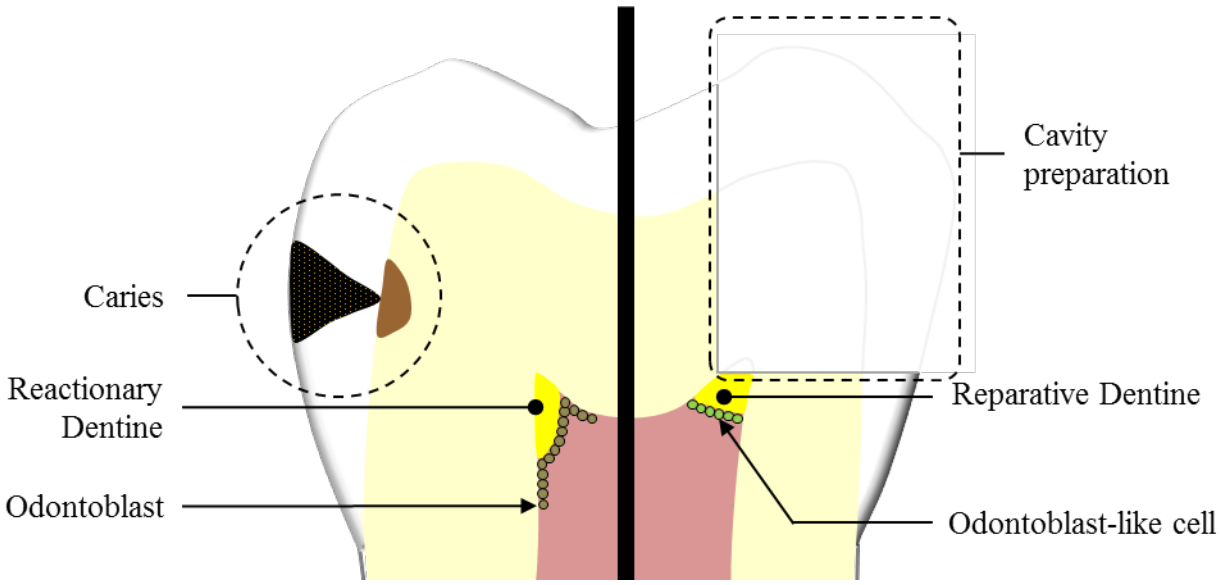

1.2.2.1 REACTIONARY DENTINOGENESIS

Odontoblasts lining the pulp chamber at the dentine-pulp complex respond to damage to the hard dental tissues by producing tertiary, reactionary, dentine. Once the root of a tooth has fully formed, odontoblasts are usually in a relatively quiescent state producing secondary dentine, however when stimulated, they are required to up-regulate dentine production which is usually proportional to the severity of the stimulus (Ten Cate 1998). The trigger to initiate reactionary dentinogenesis is related to the type of damage sustained by the tooth. Carious destruction of tooth tissue is mainly due to acid producing bacteria found in the oral environment. These bacteria convert dietary sugars to acid and can be found in high numbers in the microbial biofilm that adheres to teeth (Marsh and Bradshaw 1995). Effective oral hygiene measures, such as tooth brushing and interproximal cleaning, can help to prevent caries by disturbing and removing the dental plaque biofilm. Failure of these measures can result in the acid dissolution of enamel, destroying its structure, and allowing bacteria access to the underlying dentine. The destruction of dentine by caries is much quicker compared to enamel. This is due to a lower mineral content and the presence of dentinal tubules which allows the bacteria to track down to the pulp. Dissolution of dentine is thought to release molecules which may have an effect on the dentine-pulp complex resulting in tertiary dentinogenesis. These bioactive molecules can also be released by restorative procedures. Both cutting dentine during cavity preparation and the dental materials used to restore the tooth can produce these molecules (Ferracane et al. 2010, Smith et al. 2012a). Table 1.3 lists the bioactive molecules released by dentine, and their roles in the regulation of tertiary dentinogenesis.

Table 1.3 A selection of bioactive molecules found in dentine and a summary of their roles in tertiary dentinogenesis (Goldberg et al. 2008, Smith et al. 2001b, Smith et al. 2012a)

Bioactive molecule	Role in tertiary dentinogenesis
Non-collagenous proteins (NCP) – Dentine sialoprotein (DSP) – Dentine phosphoprotein (DPP) – Bone sialoprotein (BSP) – Dentine matrix protein-1 (DMP-1) – Osteopontin (OPN) – Matrix extracellular phosphoglycoprotein (MEPE) – Osteocalcin (OCN)	Cell signalling (i.e. stem or progenitor cells in the pulp). Regulation of mineralisation by controlling the formation of hydroxyapatite crystals. (Butler et al. 2003, Butler and Ritchie 1995, Fisher et al. 2001).
Growth factors – Adrenomedullin (ADM) – Bone morphogenetic protein-7 (BMP-7) – Fibroblast growth factor-2 (FGF-2) – Insulin-like growth factor-1 (ILGF-1) – Insulin-like growth factor-2 (ILGF-2) – Platelet derived growth factor (PDGF) – Transforming growth factor-β1 (TGF-β1)	Signalling for the upregulation of dentine secretion. Cell signalling (i.e. stem or progenitor cells in the pulp). Promotes the differentiation of pulp cells into dentine producing cells. Stimulates mineralisation. Stimulation of angiogenesis and cell proliferation in the dentine-pulp complex. (Cassidy et al. 1997, Dobie et al. 2002, Rutherford et al. 1993, Six et al. 2002,

– Vascular endothelial growth factor (VEGF)	Sloan and Smith 1999, Smith et al. 1998, Smith et al. 1994).
Cytokines – Interleukin-1β (IL-1β) – Interleukin-6 (IL-6) – Interleukin-8 (IL-8) – Interleukin-10 (IL-10)	Cell signalling (i.e. stem or progenitor cells in the pulp). Regulation of the immune and inflammatory response within the pulp during the repair process. Receptor binding to modulate gene expression. (Cooper et al. 2010, Levin et al. 1999).
Neuropeptides – Calcitonin (CT) – Calcitonin gene related peptide (CGRP) – Neuropeptide Y (NPY) – Substance P (SubP) – Vasoactive intestinal polypeptide (VIP)	Regulation of angiogenic and neurogenic events in the pulp. Stimulation of osteodentine deposition. (El Karim et al. 2009, Kline and Yu 2009).
Neurotrophic factors – Brain-derived neurotrophic factor (BDNF) – Glial cell line-derived growth factor (GDNF) – Nerve growth factor (NGF)	Neurogenic / neurotrophic effects and may promote the differentiation of pulp cells into dentine producing cells. (Arany et al. 2009, de Vicente et al. 2002, Gale et al. 2011, Mitsiadis and Luukko 1995, Nosrat et al. 1998).

A large number of bioactive molecules have been identified to be involved in the process of tertiary dentinogenesis (Table 1.3) however it has been shown that certain molecules are critical to the various stages of the repair process. The NCP group are comprised of non-phosphorylated proteins (such as OCN) and phosphorylated small integrin-binding ligand N-linked glycoproteins (SIBLING) such as DSP, DPP, DMP-1, BSP, OPN and MEPE (Goldberg and Smith 2004). As a group of proteins, SIBLINGs have been shown to regulate the process of hydroxyapatite crystal formation by behaving as nucleation factors during mineralisation (Fisher et al. 2001, Goldberg et al. 1996, He et al. 2003). However individual proteins within the SIBLING group have been shown to be involved in other aspects of the repair process. Tartaix et al. (2004) found that DMP-1 was critical to the mineralisation process due to its role as a signalling molecule and mineralisation inhibitor and nucleator. This group found that the role DMP-1 plays is dependent on its size, concentration and the degree of phosphorylation (Tartaix et al. 2004). Feng et al. (2003) found that DMP-1 was critical in the maturation of predentine (Feng et al. 2003). It has been postulated that DMP-1 may initiate differentiation of undifferentiated mesenchymal cells (Almushayt et al. 2006) and the molecule is known to be expressed in differentiating odontoblasts (Toyosawa et al. 2004a). Like many of the other SIBLINGs, DMP-1 has also been shown to be involved in the mineralisation processes of bone and cementum tissues (Gluhak-Heinrich et al. 2003, MacDougall et al. 1998, Sawada et al. 2012, Toyosawa et al. 2004b). Dentine sialophosphoprotein (DSPP) is required to regulate dentine mineralisation and is expressed by odontoblasts (Sreenath et al. 2003) however proteolytic processing of DSPP results in the generation of DSP and DPP which are found in dentine extracellular matrix (MacDougall et al. 1997, Ritchie et al. 1995). Whilst both DSPP and DMP-1 are considered to be positive regulators of mineralisation, it is been suggested that DSPP induces intra-fibril collagen

mineralisation, whereas DMP-1 induces collagen mineralisation along the collagen fibril axis (Deshpande et al. 2011). Osteopontin (OPN) has been found entombed within mineralised dentine and at the junction between pre-existing dentine and newly formed tertiary dentine (Moses et al. 2006, Qin et al. 2001). Saito et al. (2011) have shown that OPN is found at the predentine-dentine border prior to odontoblast differentiation suggesting a possible role in the differentiation process (Saito et al. 2011). A further study by this research group has shown that OPN is essential for newly differentiated odontoblasts to produce type I collagen; required for the generation of reparative dentine (Saito et al. 2016). The non-phosphorylated NCP, OCN, is reported to be present more so in primary dentine compared to secondary dentine (Gorter de Vries et al. 1987) and expression of OCN is considered to be high in differentiating odontoblasts (Goldberg et al. 2011, Papagerakis et al. 2002).

Growth factors are considered to be signalling molecules which induce an effect by binding to cell surface receptors and trigger a series of intracellular processes. These processes may result in gene expression which can determine cell characteristics and spectrum of activity. Growth factors play a critical role in stimulating and regulating the processes of tooth development and repair (Smith et al. 2012a). Growth factors, secreted by odontoblasts (Smith and Lesot 2001a), are found entombed within the dentine extracellular matrix during mineralisation (Sloan et al. 2002, Smith et al. 1998). Protein binding improves growth factor bioavailability (Arai et al. 1996, Kuang et al. 2006, Wakefield et al. 1990) once released from the mineralised matrix. The presence of growth factor, TGF-β1, in dentine extracellular matrix has been reported by multiple studies (Cassidy et al. 1997, Finkelman et al. 1990, Smith et al. 1998) and has been identified as a chemoattractant for pluripotent cells in the dental pulp (Kwon et al. 2010) and bone (Macdonald et al. 2007). Studies have also shown

TGF-β1 to initiate differentiation of odontoblast-like cells and dentinogenesis (Hu et al. 1998, Melin et al. 2000, Sloan and Smith 1999).

The identification of these bioactive molecules assists in understanding the triggering mechanisms of the repair processes within the dentine-pulp complex. Investigating the response of bioactive molecules to biophysical factors may yield novel therapies for the application of ultrasonic energy for tooth repair.

The degree by which the dentine-pulp complex responds to injury is determined not only by the stimulus, but the age of the tooth and the consistency of the dentine structure. The dentinal tubule network provides an efficient means of communication, not only for bioactive molecules to stimulate repair processes, but also for bacteria and their toxins, increasing the potential for damage. Young teeth tend to have larger pulp chambers and an increased dentinal tubule density compared to older, heavily restored teeth. Carrigan et al. (1984) reported that an average of 242,775 tubules/mm^2 were found in teeth from people in the 20 to 34 years age group compared to 149,025 tubules/mm^2 in the 80 years and above age group (Carrigan et al. 1984). This is partly due to the deposition of secondary dentine throughout the lifetime of the tooth but also the production of reparative dentine as a response to tooth wear, cavity preparation and subsequent restoration. This is more likely to affect tubules in the crown of the tooth whereas tubules in root dentine are less prone to external stimuli (Nalbandian et al. 1960). Tubules ultimately become blocked with the continual deposition of peritubular dentine decreasing the permeability of dentine (Senawongse et al. 2008, Symons 1961). Conversely, whilst it is known that peritubular dentine is deposited on the walls of the dentinal tubule, it has been shown that there is no correlation between tubule diameter and

age, however tubule density and age have a strong correlation (Whittaker and Kneale 1979) as reported by Carrigan et al. (1984). Large pulp chambers have a higher regenerative capacity owing to a greater number of pulp cells and odontoblasts lining the pulp chamber due to a large internal surface area. Younger pulps are made up of cells with a higher metabolism with the ability to respond to injury quicker than older pulp tissue (Morse 1991, Moxham et al. 1998, Murray et al. 2000, Murray et al. 2002b). Repair processes in younger teeth are more efficient however the dentine structure is less resilient and allows for the rapid spread of caries to the dental pulp. Upregulation of the repair processes within teeth is important, both for the young and older tooth, to ensure the vitality of the tooth is maintained.

Research into the therapeutic nature of dental materials and the preparation of cavities prior to restoration has helped us to increase our understanding of the factors involved that give rise to the release of bioactive molecules from dentine and the response from the dentine-pulp complex. Calcium hydroxide and mineral trioxide aggregate (MTA) are two materials used in modern dentistry that have been shown to extract these molecules from dentine (Graham et al. 2006, Tomson et al. 2007). However cavity preparation agents such as ethylene diamine tetra acetic acid (EDTA) and phosphoric acid have been shown to be more effective compared to dental materials to promote the release of bioactive molecules (Ferracane et al. 2013, Tezvergil-Mutluay et al. 2013, Tomson et al. 2007, Zhao et al. 2000). The thickness of dentine remaining between the pulp and cavity after preparation; residual dentine thickness (RDT), has been observed to have a strong influence on the survival of odontoblasts beneath cavities (About et al. 2001, Camps et al. 2000, Smith et al. 1994, Stanley et al. 1975). Cavities with an RDT between 0.25 mm and 0.5 mm have demonstrated the presence of more reactionary dentine compared to an RDT greater or smaller than these dimensions (Murray et

al. 2002a). Indeed, a distance greater than 0.5 mm does not provide sufficient stimulation to the odontoblasts to produce a significant response whereas an RDT smaller than 0.25 mm damages the odontoblasts to the extent that they cannot produce reactionary dentine (Murray et al. 2002c). Further research in this field will help to further our understanding of the effects dental disease and their treatments have on teeth and how they are important to preserve the tooth's ability to maintain its vitality and protect itself from future harm.

1.2.2.2 REPARATIVE DENTINOGENESIS

The dentine-pulp complex has the capacity to respond to injuries, however severe damage, usually exposing the pulp, can result in the loss of odontoblasts, which are post-mitotic cells unable to divide to produce further dentine secreting cells. To continue the healing response of the tooth, undifferentiated ectomesenchymal pulp cells are recruited to take the place of the dead odontoblast (Fitzgerald 1979, Fitzgerald et al. 1990, Gronthos et al. 2002, Gronthos et al. 2000, Nakashima 1994, Tziafas et al. 2000). Whilst the events that take place during reparative dentinogenesis are unclear (Sloan and Waddington 2009), cell labelling studies have demonstrated that initially, cells deep within the dental pulp below the site of injury undergo proliferation (Fitzgerald et al. 1990). It is thought that growth factor signalling may initiate this response (Smith et al. 2012a) and that the cells involved are pluripotent stem cells that reside in niches within the dental pulp (Gronthos et al. 2000) or may be transported to the pulp tissue by the blood supply (Stocum 2001). These cells have been found to be highly proliferative indicating their role in the repair process (Casagrande et al. 2011, Sloan and Smith 2007). Subsequently, it has been shown that these cells migrate towards the site of injury and further proliferation takes place (Fitzgerald et al. 1990, Murray et al. 2002a,

Murray et al. 2002b, Murray et al. 2002c, Tziafas 2004). Finally, these cells differentiate into odontoblast-like cells which secrete reparative dentine at the site of injury (Figure 1.4) (Smith et al. 1990). This is also referred to as a dentine bridge, essentially reparative dentine 'bridging' the site of injury and producing a physical barrier of tertiary dentine to maintain the vitality of the pulp. The quality of reparative dentine varies from a tubular structure (as in reactionary dentinogenesis) to osteodentine which is a calcified tissue with a non-tubular structure and morphologically has the characteristics of bone (Goldberg and Smith 2004). Osteodentine is considered porous and can give rise to tunnel defects within the dentine bridge reducing the ability of the repair process to seal the exposure (Cox et al. 1996). Upon pulp exposure, the process of reparative dentinogenesis has been shown to occur regardless of intervention. However controlling infection is an important factor in its success (Cotton 1974, Kakehashi et al. 1965), as is the degree of inflammation of the pulp tissues (Mjor 2002). A procedure known as direct pulp capping is performed in dentistry to promote the formation of a dentine bridge after an exposure. The material traditionally used is calcium hydroxide however research has shown MTA to provide better treatment outcomes when used as a pulp capping material (Aeinehchi et al. 2003, Faraco and Holland 2001, Mente et al. 2010, Nair et al. 2008). MTA has been shown to release calcium hydroxide (Okiji and Yoshiba 2009) and the nature of the MTA material allows it to provide a better seal, preventing bacterial ingress, compared to calcium hydroxide resulting in more favourable treatment outcomes (Cox et al. 1999). These materials, whilst ensuring the exposure is sealed, have also been shown to have antibacterial properties by increasing the pH of the environment to help reduce the amount of bacteria irritating the pulpal tissue and the ability to promote dental repair by being biocompatible. It also has the ability to free bioactive molecules (Table 1.3) which are entombed within the dentine matrix (Graham et al. 2006, Tomson et al. 2007). The release of

calcium ions from these materials has also been shown to induce mineralisation (Narita et al. 2010).

Whereas in reactionary dentinogenesis, dentine production is upregulated by pre-existing odontoblasts, the repair process in reparative dentinogenesis is more complex (Smith et al. 1995). It follows the conventional model of tissue healing; haemostasis, inflammation, proliferation and remodelling (Gosain and DiPietro 2004). The remodelling phase is distinct in reparative dentinogenesis as dentine is not resorbed, it is only deposited. In the healthy pulp, exposure of the pulp chamber will result in the formation of a spontaneous blood clot assisting the tissue healing process. However, the inflammatory status of the pulp is dependent on the amount of bacteria and irritants that have diffused through the dentine and stimulated the pulp (Mjor 2002, Seltzer et al. 1963). Achieving haemostasis from an inflamed pulp is challenging due to vasodilation of blood vessels and increased blood flow. Dental intervention involves removal of the infected dentine and placement of therapeutic material over the exposure. This will prevent further bacterial ingress and aims to resolve inflammation and prevents necrosis of pulp tissue from chronic inflammation. Indeed, a degree of balance must be achieved between inflammation and its resolution to ensure the success of the repair mechanisms of the dental pulp. It is known that inflammation is needed to clear the damaged area of microbes and debris, and for the release of inflammatory signalling molecules (Staquet et al. 2008) that have been shown to stimulate cell differentiation and tertiary dentinogenesis after the inflammation has resolved (Bergenholtz 1981, Cooper et al. 2010, Goldberg et al. 2008). Two potent inflammatory markers, tumour necrosis factor-α (TNF- α) and reactive oxygen species (ROS), that were originally thought to disrupt the healing process, have now been shown to promote odontogenic differentiation and

stimulate mineralisation under certain conditions (Lee et al. 2006, Paula-Silva et al. 2009). Inflammation plays a key role in the repair process and further research is needed to determine future treatment strategies to promote healing.

The interactions between bioactive molecules and the pulp tissue resulting in reparative dentinogenesis are still unclear and it is thought that the mechanisms involved are similar to those that occur during tooth development (Mitsiadis and Rahiotis 2004, Smith and Lesot 2001a). Ultrasonic energy has the potential to stimulate these interactions or directly up-regulate cellular responses to enhance the repair processes. Further research in this area has the potential for the application of ultrasound to stimulate the biological processes involved in bioengineering teeth.

1.3 ULTRASOUND ENHANCED BIOLOGICAL REPAIR

An effective ultrasound treatment regime to promote tooth repair aims to provide repeated mechanical stimulation to cells within the dentine-pulp complex whilst maintaining the structural integrity of the pulp chamber and the hard tissue structures of the tooth. The investigation of this potential treatment modality presents many challenges from both the biological and the physical sciences standpoint. Regardless, the scientific and medical literature both demonstrate an awareness of a therapeutic effect of ultrasound with biological repair. The number of studies investigating the effect of ultrasound on tooth repair is limited; however an abundance of research is available in the literature investigating ultrasound stimulated bone fracture healing (Claes and Willie 2007, Griffin et al. 2014, Hannemann et al. 2014, Heckman et al. 1994, Khan and Laurencin 2008, Malizos et al. 2006, Rubin et al. 2001, Watanabe et al. 2010). Many of the processes, such as mineralisation and cell signalling, that apply to bone repair, may be applicable to dental repair.

Padilla et al. (2014) carried out an extensive review of the possible mechanical effects of ultrasound that can promote bone fracture repair. Multiple mechanisms were identified with supporting evidence for the stimulation of gene expression, release of signalling molecules and mechano-transduction of signalling pathways which influenced and enhanced the stages of bone healing; inflammation, soft callus formation, bone formation and remodelling (Padilla et al. 2014). Angiogenesis is a key requirement for healing in biological tissues, and in the inflammation stage of bone healing, bioactive molecules such as VEGF (Ferrara et al. 2003) and PDGF (Canalis et al. 1989, Kilian et al. 2004) have been shown to be upregulated and enhancing angiogenic activity with ultrasound treatment (Doan et al. 1999, Ito et al. 2000,

Reher et al. 1999, Wang et al. 2004). Cell proliferation is considered to be an important precursor to healing and studies have shown that ultrasound can upregulate mitogenic activity in both murine (Gleizal et al. 2006, Li et al. 2003, Suzuki et al. 2009) and human (Doan et al. 1999, Reher et al. 1998, Wang et al. 2004) osteoblasts. Osteogenic growth factors regulate the bone healing process by influencing cell differentiation, proliferation and tissue maturation. Ultrasound mediated upregulation of various osteogenic markers may enhance the bone healing process with various studies having reported an upregulation of alkaline phosphatase (ALP), bone morphogenetic protein-2 (BMP-2), BSP, collagen type 1 alpha 1 (C1α1), OCN, osteonectin (ON) and OPN in osteoblast cells (Bozec et al. 2010, Gleizal et al. 2006, Maddi et al. 2006, Naruse et al. 2003, Yang et al. 2005). Whilst ultrasound has not been shown to stimulate only a specific single process during bone healing, the combination of cell proliferation and gene expression demonstrates an anabolic effect to the rate of fracture repair. Endochondral ossification takes places during bone repair converting the initially formed callus (cartilage) into bone tissue. Cell differentiation is a prerequisite to soft callus and bone formation with specific markers, as in dentine mineralisation (Sreenath et al. 2003), having been identified to regulate bone mineralisation. Runt-related transcription factor 2 (RUNX2) has been identified to be critical in both intramembranous and endochondral ossification (Komori et al. 1997, Otto et al. 1997). Encoded by the core-binding factor-1 gene (Ducy et al. 1999), RUNX2 has been shown to be upregulated by ultrasound in osteoblast cell lines and mesenchymal stem cells (Sant'Anna et al. 2005, Suzuki et al. 2009). A preosteoblast (MC3T3-E1) murine cell line treated with ultrasound has reported to demonstrate enhanced mineral production with increased ALP and matrix metalloproteinase-13 (MMP-13) gene expression (Unsworth et al. 2007). Ultrasound has also been shown to enhance chondrogenesis with animal and human studies reporting chrondocyte differentiation from mesenchymal stem cells

(Lee et al. 2006, Mukai et al. 2005, Schumann et al. 2006). The RANKL protein is thought to influence bone remodelling by upregulating osteoclastogenesis (Lacey et al. 1998). Osteoblasts have been shown to increase RANKL gene expression when exposed to ultrasound (Bandow et al. 2007). This study showed that RANKL gene expression peaked at a similar time in the repair process to woven bone resorption and the formation of lamellar bone, indicating a possible enhancement to reducing the duration of fracture repair.

Whilst we have identified that ultrasound can stimulate a response from bone cells, the mechanism by which this occurs is unclear. Integrins are transmembrane receptors which are thought to convert mechanical stimulation, such as the mechanical effects of ultrasound, to an intracellular chemical response (Ingber 1991, Pounder and Harrison 2008). Ultrasound has been shown to upregulate integrin surface expression in primary murine osteoblasts (Tang et al. 2006, Watabe et al. 2011, Yang et al. 2005) indicating ultrasound mediated positive feedback and may explain the stimulation for the changes in cell proliferation, differentiation and gene expression exhibited by osteoblasts. Signalling pathways involving MAPK have been identified to be responsive to mechanical stress, and ultrasound (Gao et al. 2016), and inhibiting their activation has led to preventing ultrasound mediated cell differentiation (Ikeda et al. 2006, Louw et al. 2013, Ren et al. 2013). Indeed, activation of the integrin-P38 MAPK pathway in ultrasound treated chondrocytes has shown an increase in extracellular matrix production (Xia et al. 2015) whilst cell proliferation has been linked to the phosphatidylinositol 3-OH kinase/Akt pathway (Takeuchi et al. 2008).

Whilst *in vitro* studies provide a sound basis for scientific research, working with cells in two-dimensional culture can limit the potential for investigating the mechanical effects of

ultrasound. Three-dimensional culture scaffolds better mimic *in vivo* conditions allowing for improved cell-to-cell and cell-to-matrix interactions (Mazzoleni et al. 2009). Studies culturing osteoblasts in three dimensional collagen scaffolds have shown that the MC3T3-E1 cell line mineralise the extracellular matrix earlier than conventional *in vitro* culture (Matthews et al. 2014). The porous nature of collagen scaffolds allow for the scaffold to be impregnated with hydroxyapatite to better mimic bone extracellular matrix (Jones et al. 2010). The number of ultrasound studies comparing conventional two-dimensional culture and three-dimensional scaffolds in the literature are limited however Appleford et al. (2007) found that osteoblast precursor cells cultured on scaffolds increased signalling activity resulting in elevated integrin expression compared to conventional culture (Appleford et al. 2007). Kang et al. (2011) cultured MC3T3-E1 preosteoblasts on three-dimensional scaffolds and compared cyclic strain and ultrasound exposure. They observed that MC3T3-E1 differentiation was significantly enhanced when both cyclic strain and ultrasound were applied to the three-dimensional culture (Kang et al. 2011). Cell culture on three-dimensional structures allows for advances to be made in tissue engineering applications and should be regarded as the way forward for future work.

At present, low intensity pulsed ultrasound (LIPUS) has been found to be the most effective at stimulating bone fracture repair. The Food and Drug Administration (FDA) in the United States of America (USA) and the National Institute for Health and Care Excellence (NICE) in the United Kingdom (UK) have both approved the use of LIPUS for bone fracture healing (Higgins et al. 2014, NICE 2010, Roussignol et al. 2012). The frequency of ultrasound used in LIPUS is commonly between 1 and 3 MHz and it is produced in packets (pulsed) resulting in low SATA intensities between 30 and 150 mW/cm^2. Continuous (non-pulsed) ultrasound at

these frequencies can produce higher SA intensities (~ 1 W/cm^2) and is utilised in physiotherapy where tissue heating is the mechanism employed to bring about a therapeutic effect. LIPUS is traditionally pulsed at a ratio of 1:4; 200 μs in every millisecond, thus repeating at a frequency of 1 kHz. Whilst the core ultrasound frequency of LIPUS is in the megahertz range, the pulsing effect at a kilohertz frequency may play a role in the biological effect of ultrasound (Argadine et al. 2006, Man et al. 2012, Sarvazyan et al. 2010).

1.3.1 ULTRASOUND TRANSMISSION IN DENTAL TISSUES

Ultrasound technology has been identified as a useful dental diagnostic tool (Marotti et al. 2013), however the transmission of ultrasound through a tooth poses a significant challenge due to its non-homogenous and anisotropic multi-layered structure (Ghorayeb et al. 2008, Hall and Girkin 2004, Singh et al. 2008). Tissue boundaries, such as that found between enamel and dentine, generate scattering effects as ultrasound is reflected and scattered at the boundaries of materials with significantly different acoustic impedance (Section 1.1.1 and Table 1.1). The high density of enamel increases attenuation of the ultrasound beam (Section 1.1.2) resulting in less energy being transmitted to the dentine-pulp complex, the target area within the tooth for ultrasonic energy to promote dental repair. Ultrasound with a lower frequency is able to transmit energy more efficiently through dense material, such as enamel, compared to higher frequencies of ultrasound as discussed in Section 1.1.2. Lowering the frequency of ultrasound increases its wavelength as it is transmitted through the material (Equation 1). A study using finite element analysis methodology demonstrated the transmission of ultrasound at various frequencies through a tooth when applied to the enamel surface (Ghorayeb et al. 2013). The study found that while ultrasound with a frequency higher

than 500 kHz is more prone to scattering effects as it is transmitted through the tooth, ultrasound with a lower frequency (30 and 45 kHz) is able to propagate more efficiently through the hard tissues to the pulp chamber.

1.3.2 THE EFFECTS OF ULTRASOUND ON DENTAL CELLS

The mechanical effects of ultrasound have been theorised to stimulate bone repair however the exact mechanism of this treatment modality is still unknown. Bone tissue may lend itself to ultrasound mediated repair due to its sensitivity to mechanical stimulation (Carter et al. 1987, Huiskes et al. 2000, Perry et al. 2009, Rubin and Lanyon 1984). Distraction osteotomy, a surgical procedure to correct limb and other abnormalities, places the bone under tensile stress during the distraction process to elongate the bone. Studies investigating LIPUS and distraction osteotomy in rabbits found that overall the healing process was accelerated, however there is a lack of agreement as to which phase of the repair process ultrasound has its effect (Chan et al. 2006, El-Bialy et al. 2003, Sakurakichi et al. 2004, Tobita et al. 2011).

Whilst the literature includes many studies investigating the effects of ultrasound on dental cells and tissues, few studies have reported the effects on cells from the dental pulp. Al-Daghreer et al. (2012) reported the effects of LIPUS (1.5 MHz, 30 mW/cm^2, 1:4 pulse) on *in vitro* tooth slice organ culture of human premolar teeth. Odontoblast cell numbers were shown to significantly increase compared to control after 5 days culture with a single LIPUS application of 5, 10 and 15 min. However, the application of LIPUS once a day for 5 days decreased cell numbers (Al-Daghreer et al. 2012). This study also reported that cells from the single LIPUS application groups were histologically similar, whereas cells from the daily

application groups had a loss of cellular integrity and tissue architecture. This would indicate that odontoblasts *in vitro* culture can endure a single application of LIPUS whereas multiple exposures, 24 h apart, may be excessive and result in cell damage or death. Further work by the same group showed that LIPUS application to a human premolar tooth slice organ culture upregulated the expression of C1α1 and DMP-1 (Table 1.3 Section 1.2.2.1) with a 10 min ultrasound application and C1α1 could also be upregulated with a 5 min application. Dentine sialophosphoprotein (DSPP) was shown to be poorly expressed in all groups, with its lowest levels found in the group where ultrasound was applied for 20 min (Al-Daghreer et al. 2013). It can be inferred from this work that shorter ultrasound treatments may be more beneficial for dental repair than the 20 min treatments applied in bone fracture healing using LIPUS. This research group has also applied LIPUS technology to the mouths of animals *in vivo* whilst investigating the effects of LIPUS on tooth movement by orthodontic realignment. After LIPUS application, the animals' mandibles were dissected and studied. El-Bialy (2011) reported that LIPUS application resulted in a dose dependent response in the mineralisation of dentine (El-Bialy et al. 2011) whilst Al-Daghreer et al. (2014) found an increase in the number of odontoblasts in the coronal and mid-third of teeth exposed to LIPUS for 20 min daily for 4 weeks (Al-Daghreer et al. 2014). Indeed, whilst *in vitro* studies may demonstrate a positive effect with shorter LIPUS exposure, it may not be immediately transferrable to *in vivo* investigations.

Earlier studies have demonstrated biological effects of ultrasound on immortalised cell lines from dental origin. Scheven et al. exposed mouse odontoblast-like cells from the immortalised MDPC-23 cell line (Hanks et al. 1998) with ultrasound produced from a dental scaler. Unlike LIPUS, the ultrasound used in this study was continuous and had a frequency of 30 kHz

producing an ultrasonic intensity in the range of 0.17 to 0.92 mW/cm^2. Cell viability was shown to reduce with increasing intensity and VEGF expression was upregulated (Scheven et al. 2009a). A separate study from the same group demonstrated an increase in the expression of heat shock protein (HSP) 25/27 (Scheven et al. 2007). These findings indicate that dental cells are responsive to ultrasonic energy with a frequency in the kilohertz range and it is important to investigate these further. A later study (Man et al. 2012) from the same group investigated the effects of continuous ultrasound with a frequency of 45 kHz and SATA intensity of 25 mW/cm^2. Cells from the MDPC-23 cell line were exposed with ultrasound and this promoted cell proliferation, differentiation and the production of a mineralised matrix. Single ultrasound exposures were found to be more beneficial than multiple exposures in the upregulation of gene expression specific to dental repair. This correlates with the findings from a previously discussed study (Al-Daghreer et al. 2012) by the ultrasound research group at the University of Alberta in Canada and it is interesting that both LIPUS with a 1.5 MHz frequency and continuous ultrasound with a 45 kHz frequency, resulted in similar outcomes. Whilst the frequencies used in these studies are different, the intensity of ultrasound applied to the cells are similar: 25 and 30 mW/cm^2. This highlights that the SATA intensity used may be more relevant than the frequency of ultrasound to generate a biological effect.

Bradnock et al. compared the effects of 45 kHz and 3 MHz ultrasound applications of 5 min duration when used for the treatment of soft tissue injuries to the ankle (Bradnock et al. 1996). This prospective randomised trial on 47 human patients showed that treatment outcomes were improved when the kilohertz ultrasound group was compared to the sham and megahertz groups; however there was no significant improvement when comparing the MHz and sham group. Reher et al. (1998) compared the effects of 45 kHz and 1 MHz ultrasound on human

cells harvested from the oral cavity. Bone and gingival cells were treated with ultrasound for 5 min *in vitro* with ultrasound at different intensities (1 MHz, pulsed 1:4, 100/400/700/1000 mW/cm^2 SAPA and 45 kHz, continuous, 5/15/30/50 mW/cm^2 SAPA). Whilst this study reported that 45 kHz and 1 MHz ultrasound upregulated cell proliferation and collagen synthesis, megahertz ultrasound appeared to demonstrate a dose-dependent relationship between ultrasound intensity and cell proliferation; increase in intensity equals an increase in cell proliferation. This effect was more prominent with bone cells compared with gingival cells, however, the effects are comparable between the two frequencies (Reher et al. 1998). Further work by the same research group showed that whilst cell proliferation was increased in fibroblasts and osteoblasts with both frequencies, 45 kHz ultrasound further enhanced collagen production in osteoblasts compared to 1 MHz ultrasound (Doan et al. 1999). This study also showed that whilst cytokine production was upregulated in all three cell types investigated (osteoblast, fibroblast and monocyte), 45 kHz ultrasound produced the most significant increase of IL-1β in monocytes. Angiogenesis is an important part of the healing process and this study demonstrates that angiogenesis-related factors (VEGF and bFGF) were found to be significantly increased with exposure to both 45 kHz and 1 MHz ultrasound. This was most significant at the lower intensities for the two ultrasound frequencies. Whilst the cells treated in this study were not harvested from the dental pulp, these findings corroborate with those of Scheven et al. (Scheven et al. 2009a) discussed earlier.

Taken together, whilst emerging evidence supports an anabolic effect of ultrasound in dental tissues, little research has been conducted to investigate the use of ultrasound to stimulate dental pulp cells and tertiary dentinogenesis. The studies discussed in this section have demonstrated that ultrasound can stimulate a biological response at a cellular and molecular

level, but further *in vitro* investigations are needed to quantify these findings in dental pulp cells to allow for *in vivo* controlled trials.

1.4 RESEARCH AIMS

The aim of this PhD study was to develop an *in vitro* cell culture system for the application of low intensity 45 kHz ultrasound and investigate the mechanical effects of ultrasound as a potential treatment modality for the repair of the dental pulp.

- Research Questions:
    - Can ultrasound with a frequency of 45 kHz be applied to cells *in vitro* in a controlled and reproducible manner?
    - Can primary cells cultured *in vitro* survive exposure to ultrasound with a frequency of 45 kHz at various intensities?
    - Do dental pulp cells respond differently to changes in the duration and intensity of ultrasound?
    - Does ultrasound with a frequency of 45 kHz stimulate dental pulp cells to express markers to stimulate tertiary dentinogenesis?

- Objectives:
    - To develop and use a system to characterise the ultrasonic output of a therapeutic ultrasound machine and quantify the dose exposure of ultrasound.
    - To develop a system to deliver 45 kHz ultrasound in a controlled and reproducible manner to cells *in vitro* culture.
    - To investigate the cellular and molecular effects of low intensity 45 kHz ultrasound on cells derived from the dental pulp of a human tooth.

CHAPTER 2

MATERIALS AND METHODS

2.1 ULTRASOUND GENERATION

Ultrasound was generated at a frequency of 45 kHz by a DuoSon longwave therapy instrument (SRA Developments Ltd, Ashburton, UK). The system was preprogrammed by the manufacturer to provide 3 customised modes of continuous ultrasonic output at spatial peak (SP) intensities of 10, 25 and 75 mW/cm^2. The instrument was calibrated using a radiation force balance (SRA Developments Ltd, Ashburton, UK). The DuoSon transducer is unfocused and the manufacturer reports an effective radiating area of 16.3 cm^2 at a frequency of 45 kHz. A beam plot (Figure 2.1) demonstrates a divergent beam profile with a frequency of 45 kHz which extends up to 40mm laterally from the central axis of the DuoSon transducer. The manufacturer also reports a beam non-uniformity ratio (BNR) of less than 6:1. This is the ratio between the peak and average ultrasonic intensity within the ultrasound field and determines the quality of ultrasound. The International Electrotechnical Commission (IEC) standard 60601-2-5:2009 requires that the BNR should be no greater than 8:1 as this could create potentially damaging ‘hot spots’ in the field. This standard states that the ideal BNR for a circular plane piston source should be 4:1. As the BNR approaches 1:1 the intensity within the beam becomes more homogenous providing a more consistent ultrasound exposure.

Figure 2.1 Spatial beam plot of the ultrasound field generated from the DuoSon at a frequency of 45 kHz (reproduced with permission from manufacturer documentation).

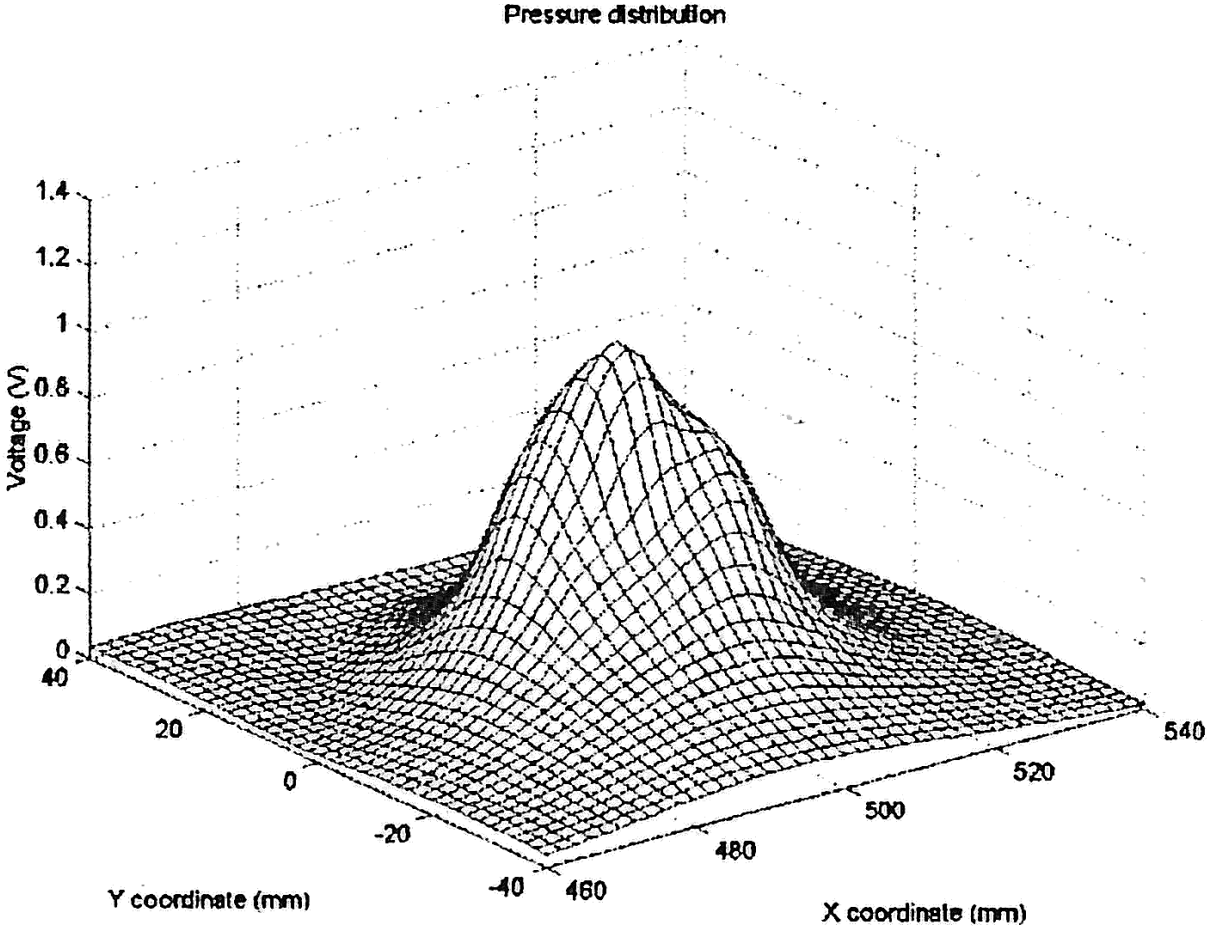

2.2 ULTRASOUND FIELD CHARACTERISATION

A vacuum degassing chamber was constructed from plastic (Applied Vacuum Engineering, Bristol, UK) with a curved internal surface to reduce direct ultrasonic reflections. An acoustically absorbing base was constructed from a combination of rubber and Apltile SF5048 (Precision Acoustics, Dorchester, UK). A 1.0 mm needle hydrophone probe (Model 1452; Precision Acoustics, Dorchester, UK) connected to a HP Series Submersible Preamplifier (PA09022, Precision Acoustics, Dorchester, UK) was held in place vertically by the Apltile SF5048 material. The chamber was filled with 12 l of double distilled deionized water and air evacuated to achieve a vacuum. The water was degassed for 12 h with a vacuum of -28 mmHg to eliminate bubbles of air within the water. Their removal will reduce any scattering effects of the ultrasound. The DuoSon transducer was positioned vertically in line over the hydrophone, with their central axes aligned, and its movement was controlled by an XYZ manual travel translation stage (Thorlabs Inc., Newton, NJ, USA) (Figure 2.2). Both the transducer and needle hydrophone probe were submerged for 4 h prior to use, simulating the conditions present when the hydrophone was calibrated. Voltage measurements were recorded using a PC oscilloscope (PicoScope 5203; Pico Technology, St Neots, UK). The hydrophone and preamplifier were connected to a DC Coupler (DCPS038; Precision Acoustics, Dorchester, UK) and the signal was passed through a 50 ohm Terminator (TA051 Feed-Through Terminator; Pico Technology, St Neots, UK) prior to connecting to the PC oscilloscope (Figure 2.2). The transducer face was positioned 50 mm below water level and maximum voltage measurements and frequency were recorded at 10 vertical points from the transducer at 1 mm intervals from the transducer face. The transducer was displaced

Figure 2.2 Annotated diagram illustrating the set-up of equipment for measuring the ultrasound field generated from the DuoSon longwave therapy instrument.

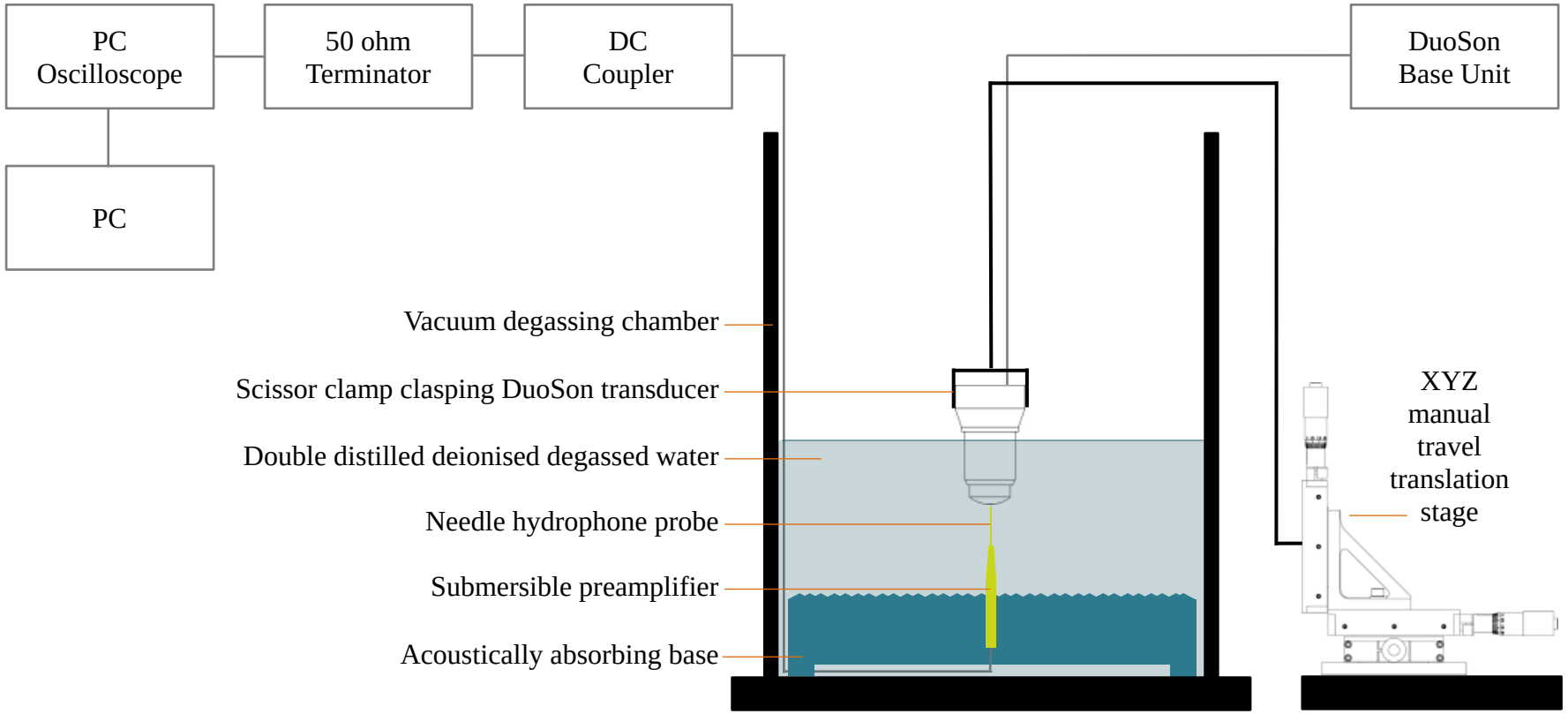

horizontally and 10 vertical measurements were taken at a further 5 positions from the transducer face at 5 mm intervals.

2.3 ULTRASOUND FIELD CALCULATION

The maximum voltage measurements and frequency were recorded for all three of the pre-set and manufacturers calibrated ultrasound intensities (10, 25 and 75 mW/cm^2) and were used to calculate the SP intensity of the ultrasound field at each horizontal position from the transducer. Initially, the pressure value was calculated using Equation 4.

Equation 4.

$$p = \frac{V}{K}$$

Where p is the acoustic pressure, V is the maximum voltage measured and K is the calibration factor (certificate: U3105, calibration carried out by National Physics Laboratory, London, UK). The needle hydrophone was calibrated over a frequency range of 10-100 kHz at 5 kHz intervals. Interpolation was initially used to determine the equivalent calibration factor based on the frequency recorded during the measurement. Subsequently, the SP acoustic intensity (I) was calculated using Equation 5.

Equation 5

$$I = \frac{1}{T_{prf}} \int \frac{p^2(t)}{\rho\, c}\, dt$$

Where T_{prf} is the pulse repetition period, ρ is the density of the propagating medium and c is the velocity of sound in the same medium (1480 m/s). Hydrophone sensitivity is rarely

constant as a function of frequency, and interpolation to determine the correct calibration factor may cause erroneous results. Further analysis using full-waveform deconvolution was employed and Equation 4 was modified to utilise Fourier transformation. This is shown in Equation 6.

Equation 6.

$$\Im^{-1}\left\{\frac{\Im(V(t))}{K(f)}\right\} = p(t)$$

Intensity was again derived using the acoustic pressure calculated using Equation 6 and compared with the intensity derived using Equation 4.

2.4 CELL CULTURE

Mouse derived dental pulp cells-23 (MDPC-23) (Hanks et al. 1998, Man et al. 2012, Scheven et al. 2007) were exposed to 45 kHz ultrasound to investigate the effects on cell viability and cell proliferation. Primary human dental pulp cells (HDPC) were cultivated from the explant of human dental pulp tissue and the effect of ultrasound on cell viability, cell proliferation, gene expression and mineralised nodule formation was investigated.

2.4.1 MOUSE ODONTOBLAST-LIKE (MDPC-23) CELL LINE

An immortalized mouse cell line of odontoblast-like dental pulp cells, MDPC-23 (Hanks et al. 1998, Man et al. 2012, Scheven et al. 2007), was cultured with DMEMsup (Dulbecco's modified eagle medium (DMEM; Biosera, UK) containing 4.5 g/l glucose, 10% heat-inactivated foetal bovine serum (FBS; Biosera, UK), 1% penicillin/streptomycin (Sigma-

Aldrich®, UK) and a 2 mM concentration of glutamine (GlutaMAX™-1; Gibco®, Invitrogen™, UK). The initial culture of MDPC-23 cells was carried out in 25 cm^2 tissue culture flasks (Appleton Woods, UK) in a humidified incubator (Galaxy S+, RS Biotech Ltd, UK) with 5% carbon dioxide in air at 37 °C. Subsequently, these cells were sub-cultured into larger 75 cm^2 culture flasks (Appleton Woods, UK) for expansion in preparation for ultrasound application.

2.4.2 PRIMARY HUMAN DENTAL PULP CULTURE

Human dental pulp tissue was harvested from extracted third molars of healthy individuals aged between 18 and 40. Teeth that were intact and had a healthy pulp were selected for the study and ethical approval was obtained from the UK National Research Ethics Service for the use of human tooth tissue (09/H0405/33). Selected teeth were extracted on the Oral Surgery department of the Birmingham Dental Hospital after the appropriate informed consent had been obtained from the patient. Immediately after extraction, the selected tooth was placed in a sterile universal tube (Fisher Scientific, UK) containing 10 ml of sterile phosphate buffered solution (PBS). Within an hour of extraction, the tooth underwent a series of washing steps, to reduce the incidence of microbial infection, in the following order:

- 2 min submerged in a 2% solution of chlorhexidine digluconate (Sigma-Aldrich®, UK)
- 1 min submerged in a 70% solution of ethanol
- 30 s submerged in sterile PBS (repeated 5 times)

The tooth was transferred from each washing step using sterile tweezers. After washing, the tooth was wrapped in sterile gauze and placed on a sterile metal tray. The tooth was crushed with a sterilised dental hammer to expose the pulp chamber and access the pulp tissue. The

pulp tissue was transferred to a 35 mm culture dish (Sarstedt, UK) which contained 2 ml of DMEMsup without FBS and supplemented with 2.5 mg/l Amphotericin B (AmpB; Sigma-Aldrich®, UK), using sterile tweezers and immediately after, covered with the lid of the culture dish. The outside of the culture dish containing pulp tissue was disinfected with a 70% solution of ethanol and transferred to a laminar flow hood and the pulp tissue was relocated to another 30 cm^2 culture dish containing DMEMsup without FBS and supplemented with 2.5 mg/l AmpB, with a disposable sterile scalpel (Swann-Morton, UK). The pulp tissue was washed for 30 s in the culture medium and this was repeated a further 3 times transferring the pulp tissue into a new 30 cm^2 culture dish containing DMEMsup without FBS and supplemented with 2.5 mg/L AmpB. A disposable sterile scalpel was used to transfer the pulp tissue to a sterile glass microscope slide (Surgipath Europe Ltd) held in a 100 mm culture dish (Corning®, NY, USA). A drop of DMEMsup supplemented with 20% FBS and 2.5 mg/l AmpB was added to the pulp tissue to prevent dehydration in the laminar flow hood. Disposable sterile scalpels were used to cut the pulp tissue into approximately 1 mm^3 sections and transfer the pieces to a 25 cm^2 culture flask. The sections of pulp tissue were arranged on the culturing surface of the culture flask as shown in Figure 2.3. To aid attachment of the pulp tissue sections to the culture surface and prevent them from floating off, only 1 ml of DMEMsup supplemented with 20% FBS and 2.5 mg/l AmpB was added to the culture flask. The culture flasks were individually stored in a culture box (Biosciences Stores, University of Birmingham, UK) with a vented lid and then placed in a humidified incubator with 5% carbon dioxide in air at 37 °C. After the sections of pulp tissue had attached to the culture surface of the 25 cm^2 culture flask, the culture medium was topped up with 4 ml of DMEMsup supplemented with 20% FBS and 2.5 mg/l AmpB. Initial attachment of the sections of pulp tissue to the culture surface took approximately 24 h. The explant cultures were monitored

daily and observed for signs of infection. Once attached outgrowth of cells were seen around the pulp tissues with a light microscope (Zeiss Axiovert 24), as in Figure 2.4, the culture medium was replenished with DMEMsup supplemented with 20% FBS. The pulp tissue was removed from its original 25 cm^2 culture flask and transferred to a new 25 cm^2 culture flask for attachment and cell proliferation. Methods described earlier in this section were followed. In the original culture flask (with pulp tissue removed), culture medium was replenished every 2 to 3 days until the culture flask was confluent and ready for sub-culture (approximately 3 to 4 weeks) for cell expansion. The initial sub-culture after explant was considered as passage 1 with subsequent sub-culture as an additional passage. The use of fifty teeth was approved from the UK National Research Ethics Service (09/H0405/33) and dental pulp cell populations from individual teeth were kept isolated. Each experiment (with duration of application as the variable) used cells from a single population.

2.5 IN VITRO APPLICATION OF ULTRASOUND

Ultrasound produced by the DuoSon was applied directly to dental cells *in vitro* culture by submerging the transducer head into the culture medium in which the cells were bathed. The transducer face, where ultrasound is produced, was directed towards the cells attached to the culture plastic of the well or dish. An advantage of this approach is the lack of an intervening layer of polystyrene culture plastic which is a boundary, resulting in attenuation, reflection and scattering of the ultrasound beam (see Section 1.1.2). This method allows for the investigation of the full output of the ultrasound transducer.

2.5.1 STATIONARY TRANSDUCER IN A MULTI-WELL CULTURE PLATE

A support structure was constructed out of silicone rubber (Centri Duplika; WHW Plastics, UK) in a square plastic box to hold in place a six-well culture plate (Costar® tissue-culture treated; Corning®, Tewksbury, MA, USA) for the application of ultrasound from the DuoSon transducer. Silicone rubber and a plastic box were used to construct this chamber to absorb ultrasound that may pass through the bottom of the six-well culture plate and prevent reflections thereby reducing the incidence of standing waves (Section 1.1.2). Figure 2.5 shows the stages of construction of the ultrasound absorbing chamber. Modelling wax (Tenatex Pink; Associated Dental Products Ltd Kemdent Works, UK) was used to construct a scaffold to allow for a six-well culture plate to be suspended within the chamber allowing for water to occupy the space below and maintain the temperature of the cells in culture. A base of silicone rubber was created first and then silicone was poured around the scaffold and six-well culture plate. The silicone rubber was allowed to set with pressure on the modelling wax scaffold to ensure chamber and support elements were correctly formed. Once the silicone rubber had set, the modelling wax scaffold and excess silicone were removed. The chamber was disinfected with a 70% solution of ethanol and filled with sterilised double distilled deionised water. The chamber was placed in a humidified incubator with 5% carbon dioxide in air at 37 °C 24 h prior to use allowing the temperature of the ultrasound absorbing chamber and the water contained within to stabilise at 37 °C.

Figure 2.3 Placement of pulp tissue sections in a 25 cm^2 culture flask.

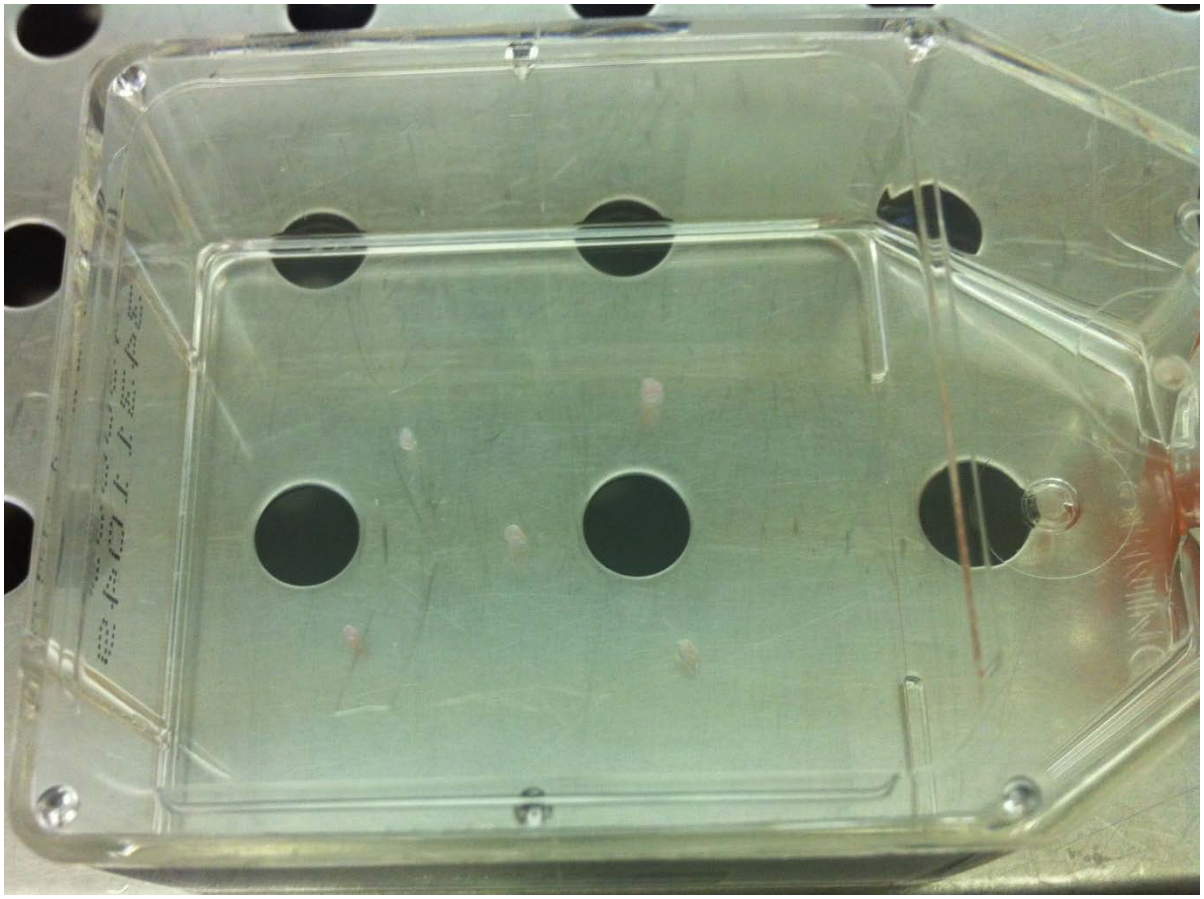

Figure 2.4 Phase-contrast microscope image showing attached HDPC outgrowth from the dental pulp explant at the top of the image.

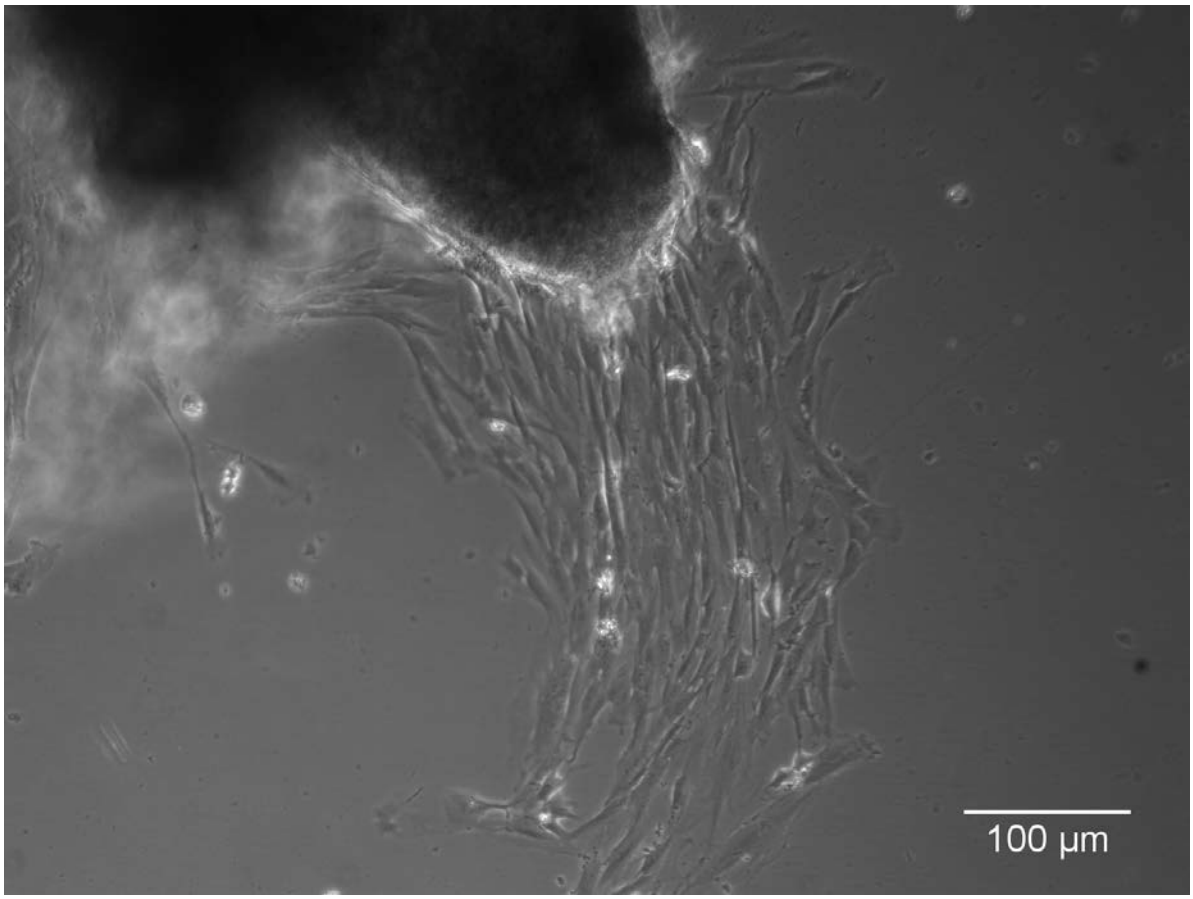

The DuoSon transducer was attached to a scissor lift (VWR, UK) using a G-clamp, clamp stand and a three pronged clamp. A thermostat controlled hotplate (Bibby, UK) was used to keep the temperature of the water in the ultrasound absorbing chamber at 37 °C (+/- 1 °C). All equipment was disinfected with a 70% solution of ethanol immediately before arranging them in a laminar flow hood to prevent infection as shown in Figure 2.6. Prior to the application of ultrasound to attached cells *in vitro*, the face and neck of the DuoSon transducer was rinsed with DMEMsup without FBS warmed to 37 °C to remove any residue of the disinfectant and to raise the surface temperature of the transducer so as not to significantly lower the temperature of the culture medium in which the cells are bathed. A six-well culture plate with wells containing culture medium and attached cells was mounted into the ultrasound absorbing chamber and placed on the hotplate. The DuoSon transducer, attached to the scissor clamp to allow for straightforward insertion and removal, was lowered into the culture well ensuring the transducer face was submerged in culture media and a space remained between the transducer shoulder and the opening of the culture well. This positioned the transducer face 5 mm from the culture surface (Figure 2.7). The required ultrasound mode was selected on the DuoSon base unit and ultrasound was applied to the cells through the transducer for the required period of time. The temperature of the water in the ultrasound absorbing chamber was monitored regularly using a thermometer to ensure the cells attached to the culture surface of each well were maintained at a temperature of 37 °C (+/- 1 °C).

Figure 2.5 The stages of construction of the ultrasound absorbing chamber. (A) Modelling wax scaffold and six-well plate in place on top of silicone rubber base inside square plastic box. (B) Silicone rubber poured into square plastic box around modelling wax scaffold. (C) Final set silicone rubber support with excess silicone and modelling wax scaffold removed. (D) Six-well culture plate in place within chamber.

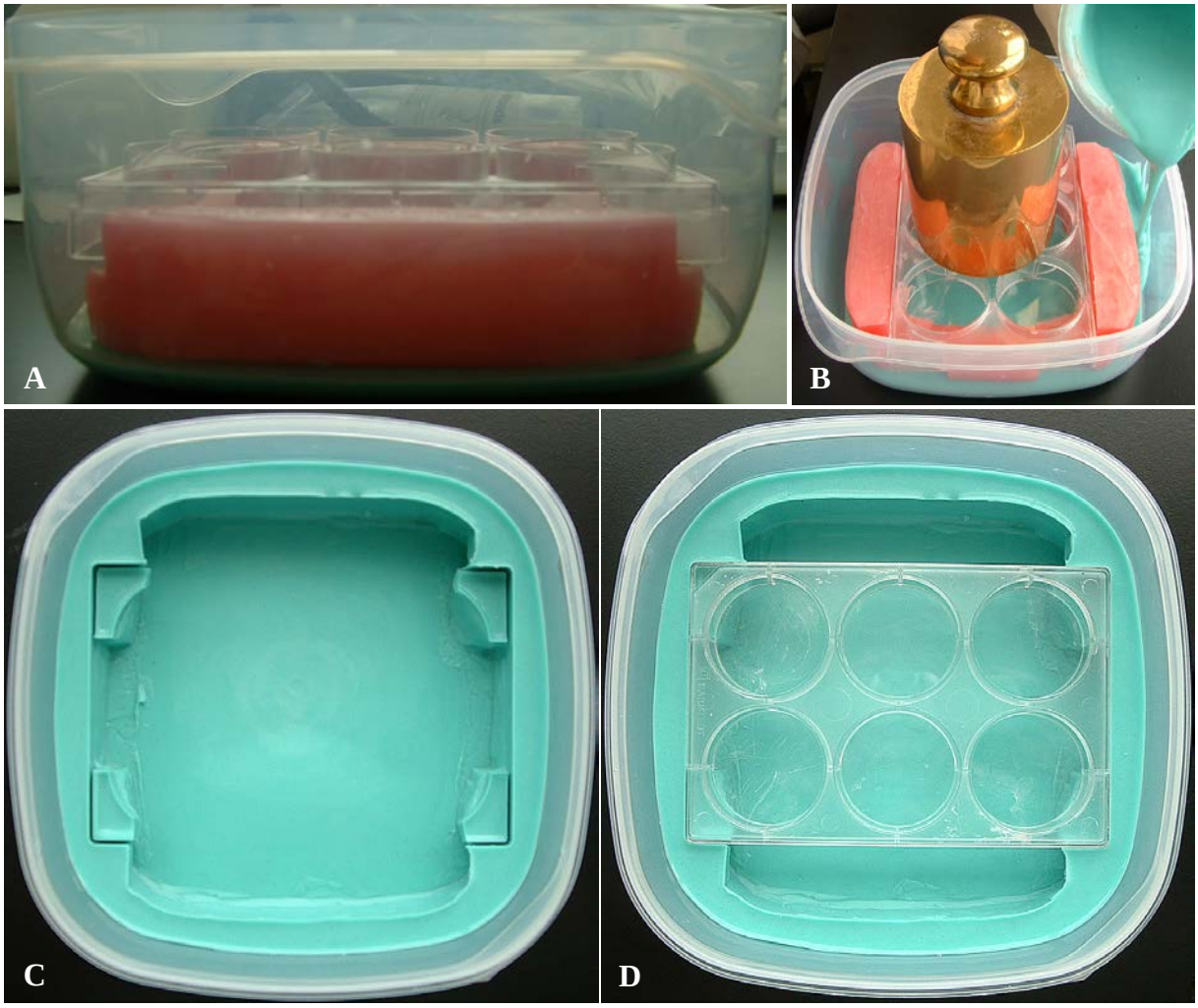

Figure 2.6 Arrangement of equipment in a laminar flow hood for treating biological cells with ultrasound in six-well culture plates with a stationary transducer. Left to right ultrasound absorbing chamber on top of a hotplate, DuoSon transducer, clamp stand, scissor lift, DuoSon base unit.

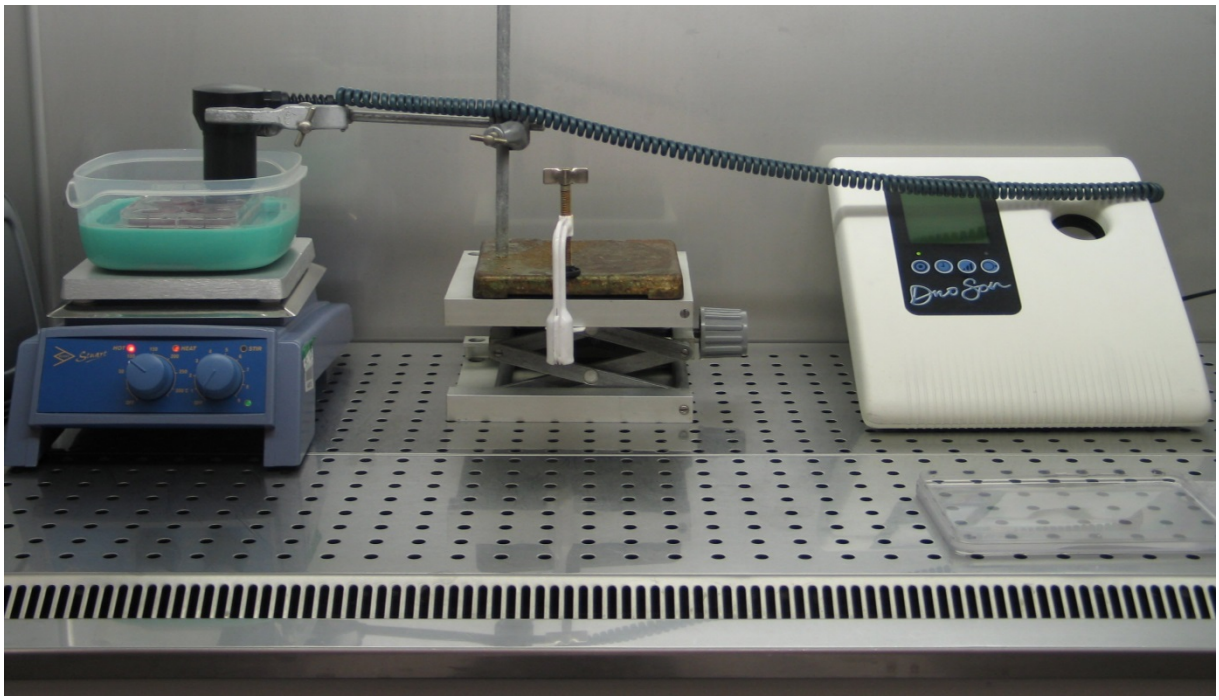

Figure 2.7 Transducer positioning in a six-well culture plate. (A) Six-well culture plate supported by silicone rubber in an ultrasound absorbing chamber containing sterilised double distilled deionised water at 37 °C (+/- 1 °C) with the transducer face submerged in culture media. (B) Annotated diagram illustrating the position of the transducer face from the base of the culture well.

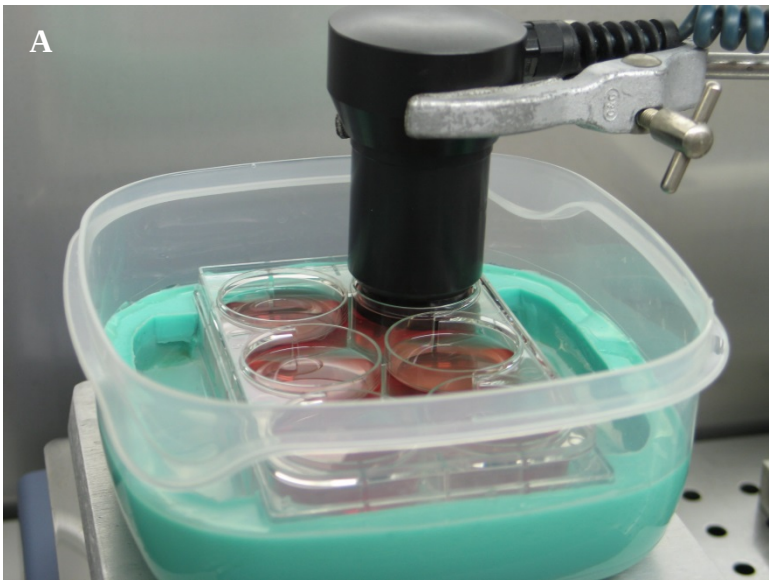

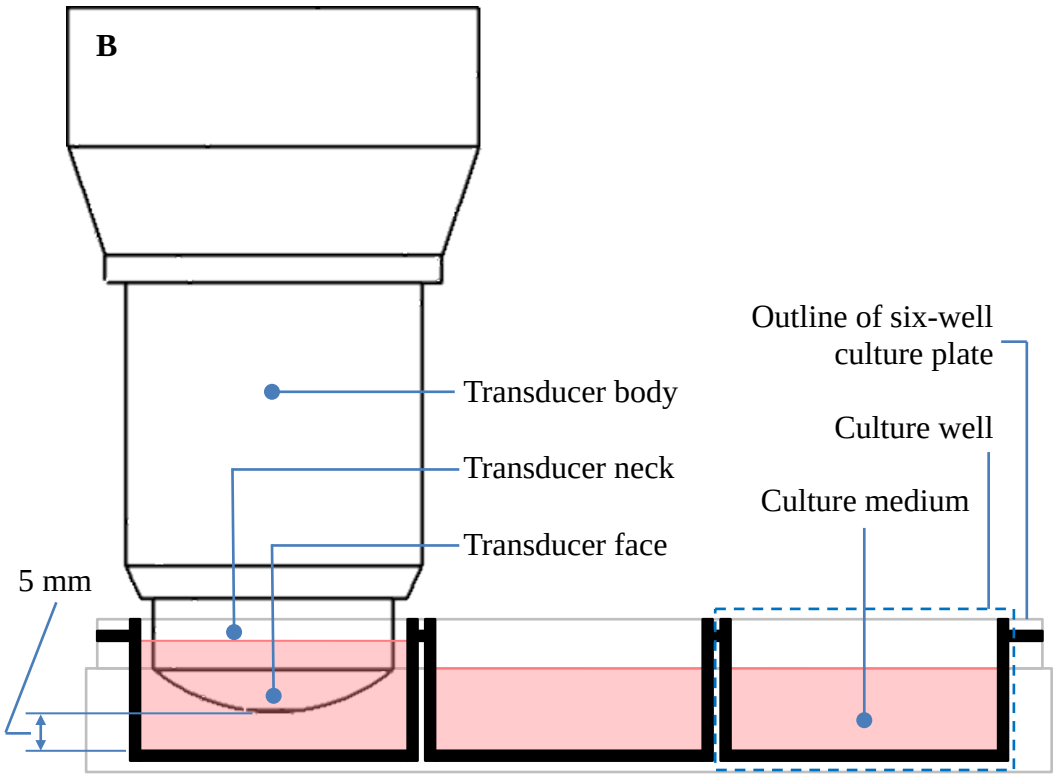

Figure 2.7 Transducer positioning in a six-well culture plate. (C) Annotated diagram illustrating the culture wells used for cell culture (pink) and ultrasound application (labels) in the experiment where ultrasound is applied to multiple wells of a six well culture plate (Section 2.5.1.2). (D) Annotated diagram illustrating the culture wells used for cell culture (pink) and ultrasound application (labels) in the experiment where ultrasound is applied to a single well of a six well culture plate (Section 2.5.1.3).

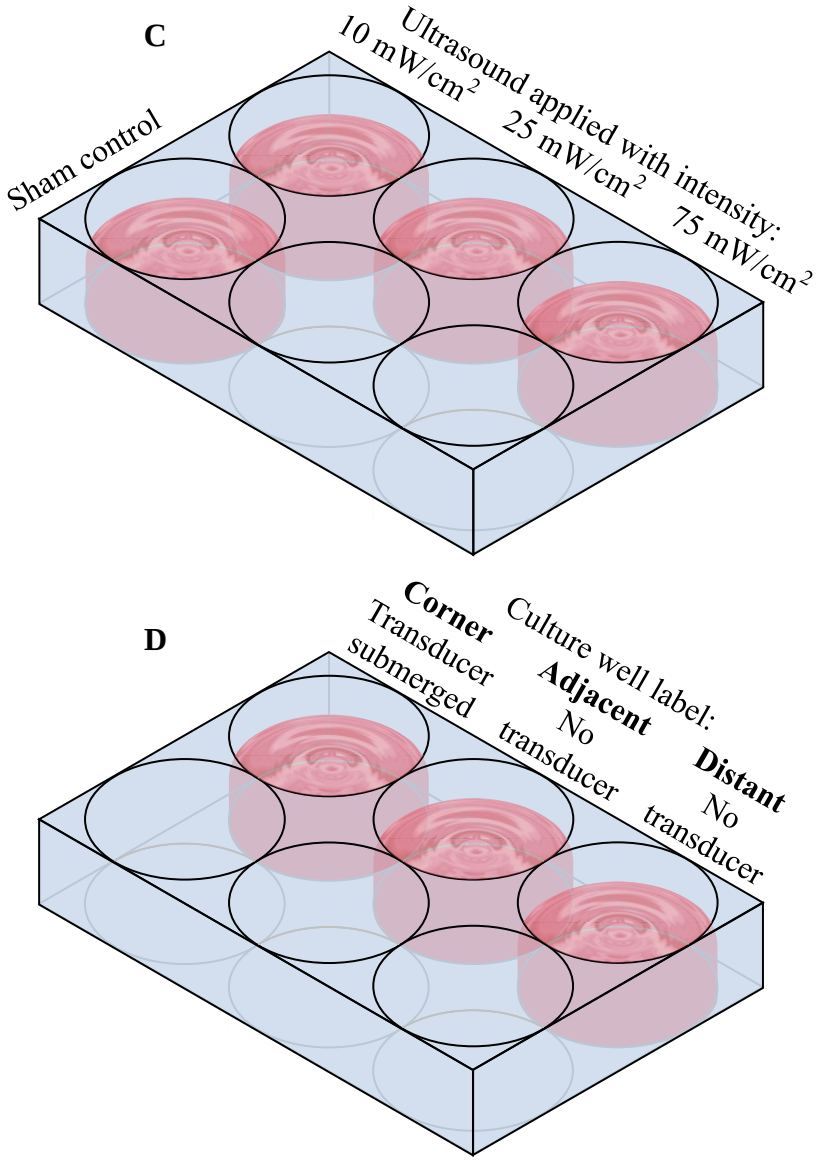

2.5.1.1 PREPARATION OF MDPC-23 CELL LINE FOR ULTRASOUND APPLICATION

Cells from the MDPC-23 cell line were detached from confluent 75 cm^2 culture flasks (Section 2.4.1) by first discarding the culture media in the culture flask and subsequently washing the attached cells in each culture flask twice with 3 ml sterile PBS with each wash. A 3 ml solution of 2.5 g/l of Trypsin in 0.38 g/l of EDTA (Invitrogen, UK) was added to the culture flask and incubated in a humidified incubator with 5% carbon dioxide in air at 37 °C for no more than 10 min. The Trypsin and cell solution was transferred to a 15 ml Falcon tube (Appleton Woods, UK) containing 3 ml of DMEMsup. The Falcon tube was centrifuged at 800 rpm for 5 min (5804R, Eppendorf, UK) forming a pellet of cells. The supernatant was discarded from the Falcon tube and the cells were re-suspended in DMEMsup. The cells were seeded in six-well culture plates (Costar® tissue-culture treated; Corning®, Tewksbury, MA, USA) at a density of 5×10^4 cells per well and were incubated in a humidified incubator with 5% carbon dioxide in air at 37 °C for 24 h prior to the start of each experiment.

2.5.1.2 APPLICATION OF ULTRASOUND TO MULTIPLE WELLS OF A SIX-WELL CULTURE PLATE

MDPC-23 cells were seeded (as described in Section 2.5.1.1) into 12 culture wells equally divided amongst 3 six-well culture plates. Four culture wells were used in each six-well culture plate (Figure 2.7C). The same culture wells in each six-well culture plate contained a monolayer of attached MDPC-23 cells. The three culture wells adjacent to each other in a row had ultrasound with a frequency of 45 kHz applied at an intensity of 10, 25 and 75 mW/cm^2

respectively for 5 min once every other day for 7 days starting on the second day of the experiment. On the first day, the culture medium in each culture well with attached MDPC-23 cells was replenished with 9 ml of DMEMsup to facilitate the approximation of the transducer face to the cells whilst the transducer was submerged within the culture media (Figure 2.7). The fourth culture well containing cells in each culture plate on a separate row was designated as the sham control (Figure 2.7C); having the face of the transducer submerged however no ultrasound was generated. The culture media was replenished in each culture well 24 h after ultrasound was applied (including control). The experiment concluded on day 7 after 3 episodes of ultrasound application had taken place; cell analysis took place on day 8. This experiment was repeated three times.

2.5.1.3 APPLICATION OF ULTRASOUND TO A SINGLE WELL OF A SIX-WELL CULTURE PLATE

MDPC-23 cells were seeded (as described in Section 2.5.1.1) into 36 culture wells equally divided amongst 12 six-well culture plates. Three culture wells were used in each six-well culture plate (Figure 2.7D). The same culture wells in each six-well culture plate contained a monolayer of attached MDPC-23 cells. Only the culture well in the corner (Figure 2.7D) of each six-well culture plate had ultrasound with a frequency of 45 kHz applied at an intensity of 10, 25 and 75 mW/cm^2 for 5 min once every other day for 7 days starting on the second day of the experiment. On the first day, the culture medium in each culture well with attached MDPC-23 cells was replenished with 9 ml of DMEMsup to facilitate the approximation of the transducer face to the cells whilst submerged within the culture media (Figure 2.7). The corner culture well containing cells in 3 of the 12 six-well culture plates was designated as the

control; having the face of the transducer submerged however no ultrasound was generated. The culture media was replenished in each culture well 24 h after ultrasound was applied (including control). The experiment concluded on day 7 after 3 episodes of ultrasound application had taken place; cell analysis took place on day 8. This experiment was repeated three times.

2.5.2 MOVING TRANSDUCER IN A CULTURE DISH

A system to apply ultrasound in motion to attached cells in a single well culture dish was devised for the following reasons.

- To minimise the time cell cultures were kept out of incubation conditions, specifically a humidified environment with 5% carbon dioxide in air.
- To prevent the divergent beam of ultrasound with a frequency of 45 kHz (Section 3) from affecting cells cultured in the adjacent and distant culture wells in the same multi-well culture plate.
- To prevent a significant rise in temperature of the culture medium in which the attached cells are bathed when ultrasound with a frequency of 45 kHz is applied for more than 5 min (Section 4.1).
- To reduce the incidence of standing waves by keeping the origin of the ultrasound beam in constant motion.

The system was designed whereby the DuoSon transducer would be mounted to an electric motor and appropriate gear head to produce a reproducible path of circular movement at a controllable speed of 0.5 to 6 rpm whilst the transducer face was submerged in the culture media of a culture dish. Whilst the transducer was in motion, the system was designed to keep

the relative position of the transducer constant to avoid the cable connecting the transducer to the base unit from becoming twisted and entangled. The transducer mount was also designed to be set at varying diameters of circular movement to allow the system to work with culture dishes of different diameters. A mechanised apparatus was constructed as per these design specifications by the Biosciences Workshop, University of Birmingham, UK (Figure 2.8). An electric motor (Oriental Motor Co Ltd, Japan) connected to a gear head (Oriental Motor Co Ltd, Japan) and control unit (Oriental Motor Co Ltd, Japan) with an on/off switch and potentiometer was mounted to a rigid frame. The control unit was secured to a water resistant enclosure (Eaton Moeller, UK) to the left side of the frame whilst the motor was mounted on a steel plate on top of the frame. The transducer mount located below the steel plate was connected to the shaft of the gear head through a hole in the steel plate. The transducer was secured to the mount of the apparatus using three grub screws and the diameter of rotation was set to 47 mm placing the transducer equidistant between the centre and the periphery of the culture dish (Corning®, NY, USA) that had an external diameter of 89 mm. The potentiometer on the control unit was set exactly half way between ‘low’ and ‘high’ which generated a rotation speed of 3.5 rpm. Thus the transducer was moving at a speed of 8.6 mm/s. A thermostat controlled water bath (Grant Instruments, UK) containing a polycarbonate base tray (Grant Instruments, UK) and a 120 mm square piece of acoustically absorbing polyurethane rubber (Apltile SF5048; Precision Acoustics, Dorchester, UK) was used to keep the temperature of the cells in the culture dish at 37 °C (+/- 1 °C) (Figure 2.9). The water bath was filled with 1.5 l of sterilised double distilled deionized water and placed on top of a scissor lift (VWR, UK) positioned directly below the transducer mount. All equipment was disinfected with a 70% solution of ethanol immediately before arranging them in a laminar flow hood to prevent infection as shown in Figure 2.8. Prior to the application of

ultrasound to attached cells *in vitro*, the face and neck of the DuoSon transducer was rinsed with DMEMsup without FBS warmed to 37 °C to remove any residue of the disinfectant and to raise the surface temperature of the transducer so as not to significantly lower the temperature of the culture medium in which the cells are bathed. A culture dish containing culture medium and attached cells was placed in an acrylic bracket (Biosciences Workshop, University of Birmingham, UK) and transferred to the water bath (Figure 2.9). The water bath was raised using the scissor lift until the transducer face was submerged in culture media. This positioned the transducer face 5 mm from the culture surface as shown in Figure 2.9. The electric motor on the apparatus was switched on using the control panel and the required ultrasound mode was selected on the DuoSon base unit. Ultrasound was applied to the cells through the transducer for the required period of time. The transducer moving at 8.6 mm/s did not generate a visible disturbance in the culture media in the culture dish. The temperature of the water in the water bath was monitored regularly using a thermometer to ensure the cells attached to the culture surface of each well were maintained at a temperature of 37 °C (+/- 1 °C).

2.5.2.1 PREPARATION OF PRIMARY HDPC FOR ULTRASOUND APPLICATION

Primary HDPC were detached from confluent 75 cm^2 culture flasks at passage 1, 2 or 3 (Section 2.4.2) as previously described in Section 2.5.1.1. HDPC at passage 2, 3 or 4 were used for experimentation. The cells were seeded in 100 mm culture dishes (Corning®, NY, USA) at a density of 5×10^5 cells per culture dish and were incubated in a humidified incubator with 5% carbon dioxide in air at 37 °C.

Figure 2.8 Arrangement of equipment in a laminar flow hood for treating biological cells with ultrasound in single well culture dishes with a transducer in motion. Mechanised apparatus with DuoSon transducer in place over scissor lift and water bath (left), DuoSon base unit (right). The control unit (inset top right) is attached to the left of the mechanised apparatus.

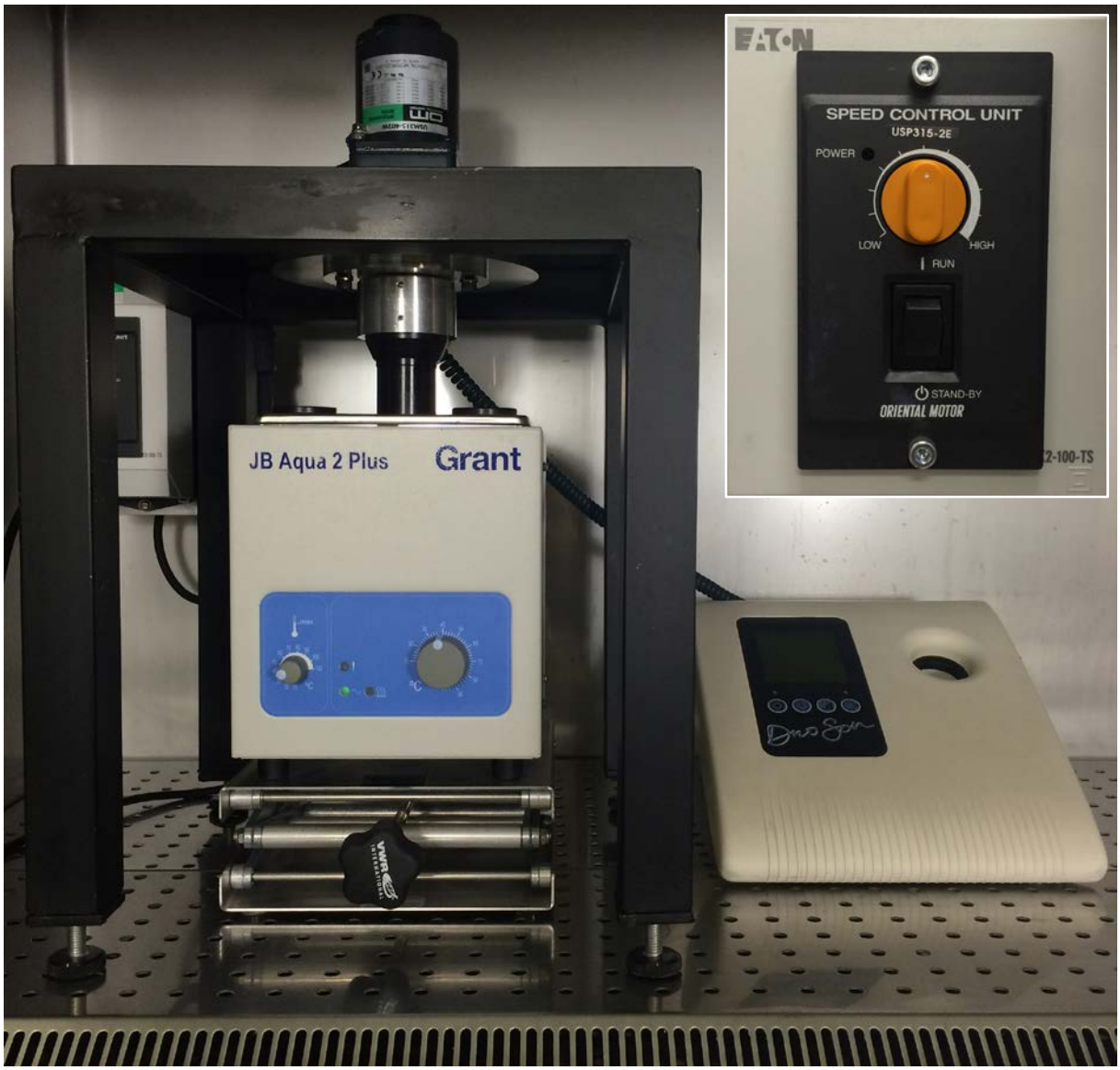

Figure 2.9 Arrangement of equipment and materials in the water bath. (A) View from above showing the opening of the water bath and in place, culture dish holder, bracket and acoustically absorbing material.

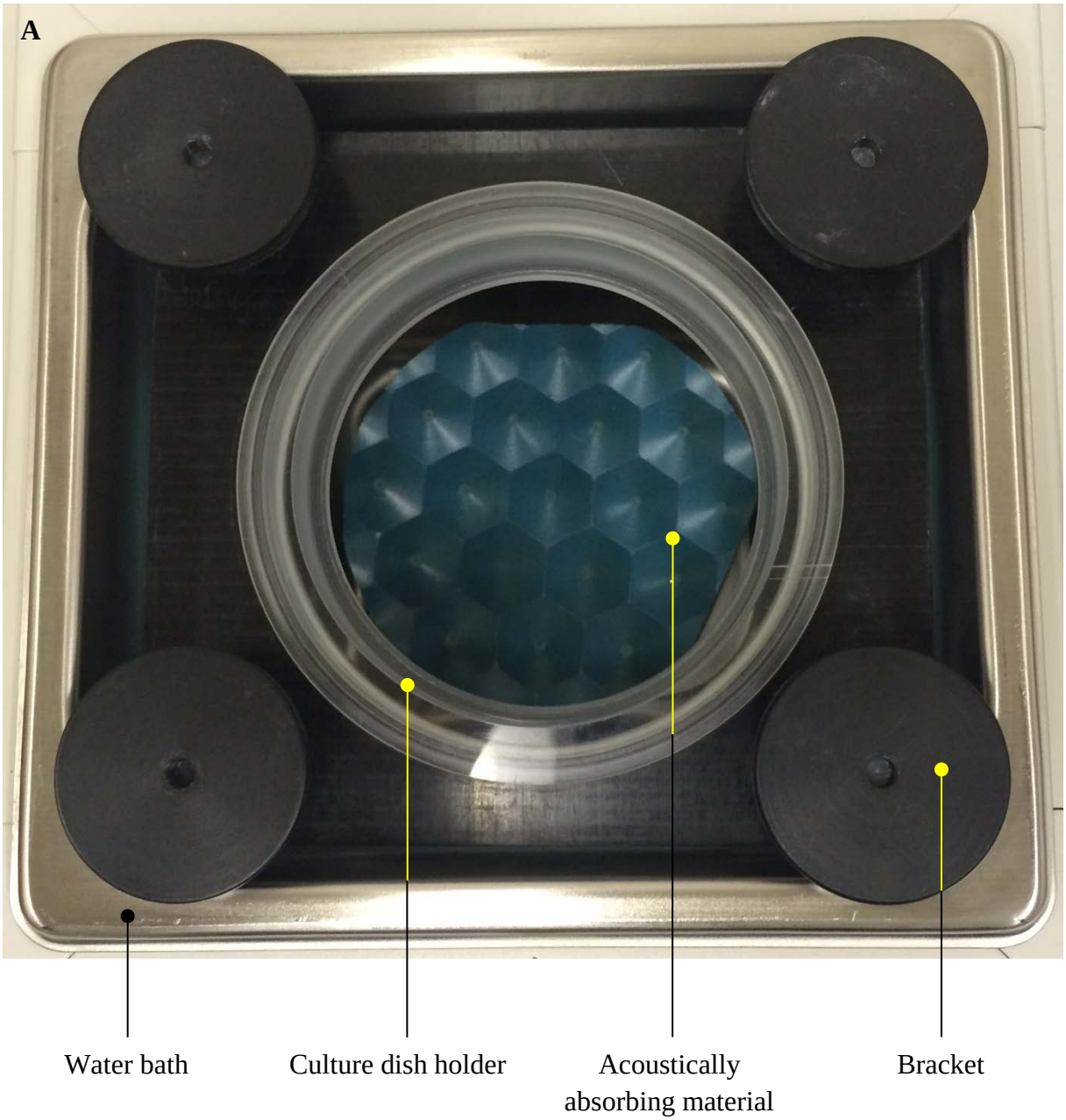

Figure 2.9 Arrangement of equipment and materials in the water bath (continued).

(B) Annotated diagram illustrating the position of equipment and materials within the water bath.

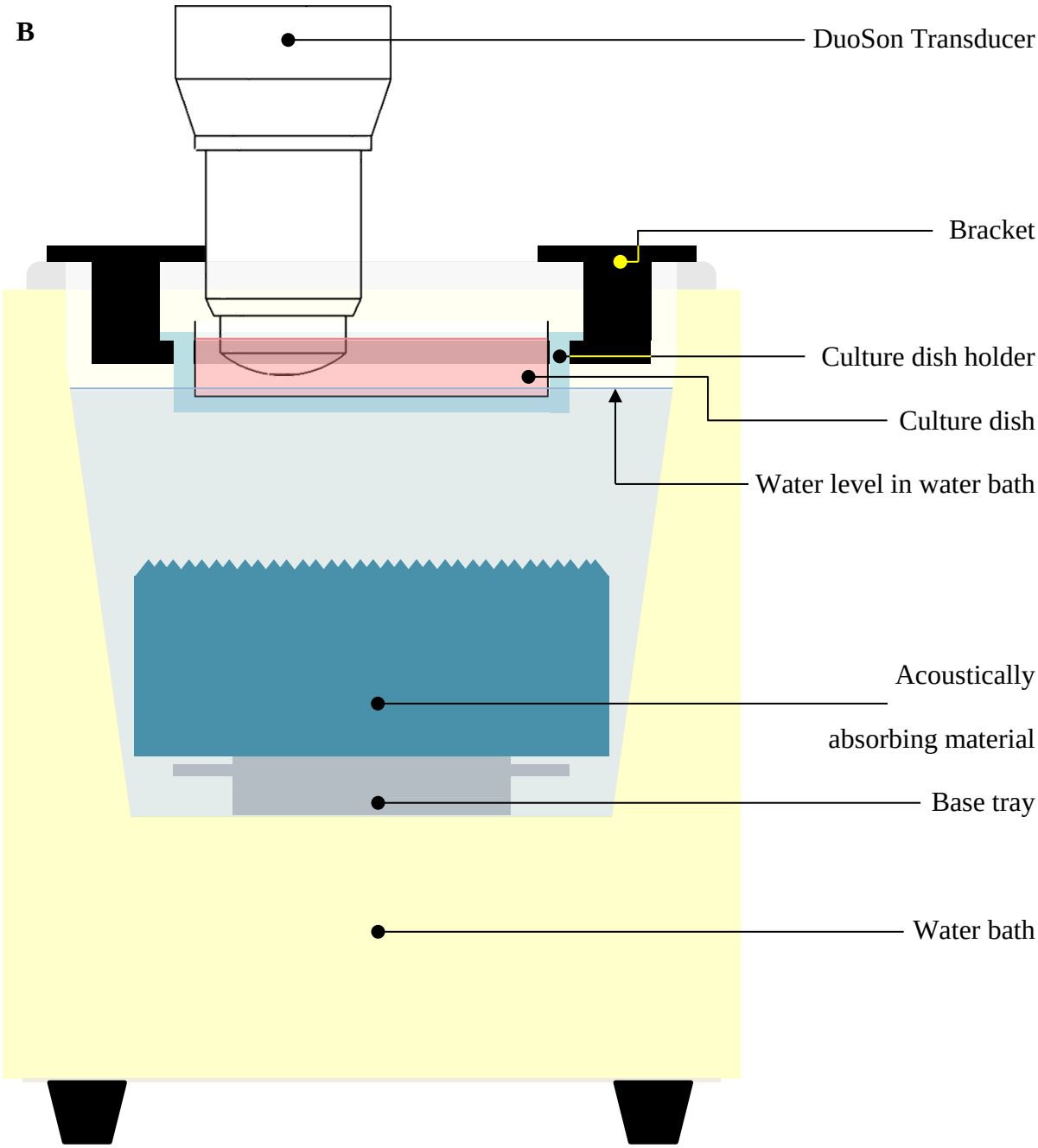

2.5.2.2 APPLICATION OF ULTRASOUND TO A CULTURE DISH

Primary HDPC were seeded (as described in Section 2.5.2.1) into culture dishes. Ultrasound with a frequency of 45 kHz was applied at intensities of 10 and 25 mW/cm^2 for 5, 10, 15 and 20 min once every other day for 7 days starting on the second day of the experiment. Primary HDPC harvested from the same tooth were seeded into nine culture dishes for each time duration experiment (5, 10, 15 and 20 min) allowing for three repeats. In total 36 culture dishes were used for this experiment. Ultrasound was applied in motion (as described in Section 2.5.2). On the first day, the culture medium in each culture dish was replenished with 50 ml of DMEMsup to facilitate the approximation of the transducer face to the cells whilst submerged within the culture media (Figure 2.9B). Control culture dishes had the face of the transducer submerged however no ultrasound was generated. The culture media was replenished in each culture dish 24 h after ultrasound was applied (including control). The experiment concluded on day 7 after 3 episodes of ultrasound application had taken place.

2.6 TEMPERATURE MEASUREMENTS

The apparatus was set up as described in Sections 2.5.1 and 2.5.2. A six-well plate containing 9 ml of DMEMsup and a culture dish containing 50 ml of DMEMsup, were taken from a humidified incubator with 5% carbon dioxide in air at 37 °C and positioned in the apparatus as described previously. Pilot studies with a sterilized fine wire thermocouple (RS Components Ltd. Corby, UK), to enable live temperature readings during ultrasound application experiments, found inaccurate temperatures were recorded due to the interaction of the ultrasound beam with the metal wire of the thermocouple. The temperature recorded by this thermocouple would rise sharply when ultrasound was emitted and then a sudden drop in temperature would be found when ultrasound application ceased. This was confirmed as an error with a separate analogue laboratory thermometer by measuring the temperature of the culture medium at the same time. A rubber insulated thermocouple (TC-PVC-T-24-180; Omega Engineering Limited, Manchester, UK) which had a larger diameter was used to measure the temperature rise of the culture medium in the culture dish or well in which the transducer was submerged. However as this thermocouple could not be sterilized, temperature measurements could not be carried out whilst cells were in culture. Temperature measurements were also taken in the adjacent and distant culture well (Figure 2.7D). The thermocouple was positioned on the culture plastic, at the center of each well. Measurements were taken every 30 s to ensure specific time points would be recorded to ascertain appropriate application durations.

2.7 ASSESSMENT OF CELL VIABILITY AND NUMBER

Cell counts and an assessment of cell viability were undertaken on day 8, 48 h following the final application of ultrasound. A cell suspension was created as previously described (Section 2.5.1.1) and 20 µl of cell suspension was added to an identical volume of a 0.4% solution of trypan blue (Sigma-Aldrich, UK) in a 2 ml Eppendorf (Appleton Woods, UK). The contents of the Eppendorf were gently vortexed (Vortex Genie-2; Scientific Industries, UK) for 3 s and 10 µl of the mixed suspension was added to each of the 2 chambers of a Neubaeur haemocytometer (Neubaeur, Germany) beneath a glass cover slip. A light microscope (Zeiss Axiovert 25) with a 10x objective was used to visualise the counting grid and the number of stained (non-viable) and unstained (viable) cells in a primary square (1 mm^2) were counted. Cell counts were repeated three times for each sample. Cell concentration (per ml) of the suspension was determined by multiplying the number of cells counted by 10^4 and the dilution factor. The percentage of viable cells in the suspension was calculated by dividing the total number of cells by the number of viable cells.

2.8 MINERALISED NODULES IN PRIMARY HDPC

2.8.1 PREPARATION OF PRIMARY HDPC

Primary HDPC were seeded in 100 mm culture dishes as previously described (Section 2.5.2.1) and 24 h later the culture media was replenished with a solution of freshly made up culture media containing additives to promote mineralisation; DMEMmin (DMEMsup supplemented with 10 mM β-glycerol phosphate disodium salt pentahydrate (β-GP; Sigma-

Aldrich, UK), 50 µg/ml ascorbic acid (AA; Sigma-Aldrich, UK) and 10 nM dexamethasone (DEX; Sigma-Aldrich, UK). Culture dishes containing HDPC were cultivated for 2 weeks prior to the application of ultrasound (Section 2.5.2.2).

2.8.2 STAINING MINERALISED NODULES WITH ALIZARIN RED S

Calcium based mineral deposits in attached cell cultures were identified using alizarin red S (ARS; BDH, UK). An ARS solution was prepared with a concentration of 40 mM adjusted to a pH of 4.2 using a 10% solution of acetic acid (Sigma-Aldrich, UK). Attached cells in culture dishes were washed with PBS three times and fixed with a 10% solution of formalin (VWR, UK) for 30 min. Cells were washed with PBS and 5 ml of the previously prepared ARS solution was added to the cells in each culture dish. The culture dishes were gently agitated for 20 min at room temperature, after which the unincorporated ARS solution was gently aspirated from each culture well. Cells were washed with distilled water twice whilst the culture dish was gently agitated and then left to air-dry at room temperature. Stained nodules were visualised using light microscopy and photomicrographs were captured.

2.8.3 MICRO-COMPUTED TOMOGRAPHY

A polychromatic SkyScan-1172 µCT scanner (Bruker, Belgium) was used to identify the radio-opacity of ARS stained nodules located in HDPC cultures (Section 2.8.2). A tapered round end diamond bur (Dentsply, UK) was used to cut a 12 mm diameter section of culture plastic around the stained nodule as the culture dish was too large for the sample area of the µCT scanner. The cut section of culture plastic was rigidly fixed to a metal stub, to reduce

unwanted movement during scanning, and then mounted to the rotating turntable within the specimen area. The samples were analysed in air. A 0.5 mm aluminium filter was used to reduce the number of low-energy photons to improve image quality and a resolution of 2000 by 1200 pixels was selected with a pixel size of 9 µm. X-rays were produced at an electrical potential of 40 kV and using an appropriate current for each sample. Each exposure took 700 ms and was undertaken with a rotation step of 0.3 degrees. The scans were reconstructed using NRecon (Bruker, Belgium) and viewed with CTvox (Bruker, Belgium).

2.8.4 SCANNING ELECTRON MICROSCOPY (SEM) AND ENERGY DISPERSIVE X-RAY SPECTROMETRY (EDX)

A Zeiss EVO MA10 scanning electron microscope (Zeiss, Germany) was used to identify surface topology and the elemental content of ARS stained nodules located in HDPC cultures (Section 2.8.2). Previously prepared samples (Section 2.8.3) were dehydrated overnight and fixed to aluminium stubs (Agar Scientific, UK). Samples were gold sputter coated under vacuum for 2 min at 25 mA (Emitech K550X; Quorum Technologies Ltd, UK) after which a conductive Acheson electrodag tape (Agar Scientific, UK) was applied to the surface of the coated sample near its periphery and extended to the base of the aluminium stub. SEM images of ARS stained nodules in each sample were obtained using the secondary and backscattered modes under vacuum at an accelerating voltage of 5-20 kV. Elemental analysis of the ARS stained nodules was acquired using energy dispersive x-ray spectrometry (INCA, Oxford Instruments, UK). The scanning electron microscope imaged the samples using the secondary electron mode with a working distance of 8.5 mm and an accelerating voltage of 20 kV.

2.9 GENE EXPRESSION ANALYSIS

2.9.1 PREPARATION OF PRIMARY HDPC

Primary HDPC were seeded in culture dishes as previously described (Section 2.5.2.1) and prepared for the application of ultrasound with DMEMmin as described in Section 2.8.1. Ultrasound was applied to primary HDPC in culture over 7 days as described in Section 2.5.2.2. The experiment concluded on day 7 after 3 episodes of ultrasound application had taken place.

2.9.2 RNA ISOLATION

RNA extraction from primary HDPC was undertaken on day 8, 48 h following the final application of ultrasound. In total, RNA extraction was carried out from 36 individual samples; 9 from each time duration experiment (5, 10, 15 and 20 min). Each experiment had 3 samples with 45 kHz ultrasound applied at an intensity of 10 mW/cm^2, a further 3 with 45 kHz ultrasound applied at an intensity of 25 mW/cm^2 and the remaining 3 were sham control samples where the transducer face was submerged into the culture media for the same length of time and conditions but no ultrasound produced (n=3 repeats). The RNeasy mini kit (Qiagen, UK) was used to isolate RNA from sample cells. The instructions provided with the kit were followed. Briefly, attached cells were washed and then lysed with 350 µl of a mixture of 1 ml buffer RLT (supplied with the kit) and 10 µl of beta-mercaptoethanol (β-ME, Sigma-Aldrich, UK) for 5 min at room temperature with gentle agitation. The resulting lysate was transferred to a 1.5 ml Eppendorf and homogenised by rapidly pipetting the mixture for 10 s. A

70% solution of ethanol was chilled on ice and an equal volume (350 µl) was added to the cell lysate. The mixture was pipetted into a spin column (supplied with the kit) and centrifuged (Eppendorf 5804R, Eppendorf, UK) at 10,000 rpm for 30 s. The flow-through liquid was discarded and RNA bound itself to the membrane within the spin column. DNA contamination was eliminated with the addition of DNase 1 (RNase-free DNase kit, Qiagen, UK). After a series of washing and centrifugation steps to reduce other contaminants, pure RNA was finally eluted in RNase-free water. The concentration of RNA was quantified using a spectrophotometer (Biophotometer Plus; Eppendorf, UK).

2.9.3 REVERSE TRANSCRIPTION

RNA collected as described previously (Section 2.9.2) was used to generate single stranded cDNA using the Tetro cDNA Synthesis Kit (Bioline, UK). The instructions provided with the kit were followed. Briefly, 4-5 µg of RNA was added to 1 µl of Oligo $(dT)_{18}$ Primer Mix, 1 µl of a 10 mM concentration of dNTP Mix, 4 µl of 5x RT Buffer, 1 µl of Ribosafe RNase Inhibitor and 1 µl of Tetro Reverse Transcriptase. All components are supplied with the kit and stored on ice during the reverse transcription process. RNA-free, molecular grade water was added to make the volume of the mixture up to 20 µl. The mixture was incubated at 45 °C for 30 min to generate the complementary nucleotide pairings with the RNA. The reaction was terminated by incubating at 85 °C for 5 min to remove the template RNA and then chilled on ice.

A Microcon centrifugal filter device (Millipore, UK) was used to concentrate cDNA. RNA-free, molecular grade water was added to the cDNA to make the volume of the mixture up to 500 µl. This was placed in the Microcon filter and centrifuged for 2 min at 10,000 rpm. The

volume of liquid in the filter was checked and if more than 50 µl, the filter was centrifuged for a further minute at 8,000 rpm. This was repeated as required. When the desired volume was achieved, the filter was inverted into a 1.5 ml collection tube (Millipore, UK) and centrifuged at 800 rpm for 1 min. The concentration of cDNA was quantified using a spectrophotometer (Biophotometer Plus; Eppendorf, UK).

2.9.4 SEMI-QUANTITATIVE REVERSE TRANSCRIPTASE POLYMERASE CHAIN REACTION (sqRT-PCR)

A BioMix Red kit (Bioline, UK) was used to prepare the primer and cDNA mix prior to thermo-cycling. Primers (Table 2.1) were initially prepared to a 25 µM concentration prior to creating the forward and reverse primer mix; 10 µl forward primer, 10 µl reverse primer, 60 µl RNA-free water. Approximately 75 ng of cDNA (less than 2 µl) was added to 12.5 µl of BioMix Red (supplied with the kit) and 2 µl of the forward and reverse primer mix in a 0.2 ml PCR tube (Appleton Woods, UK). The total volume of the mixture was made up to 25 µl with RNA-free water and then gently mixed by pipetting prior to centrifuging to collect all liquid to the bottom of the PCR tube. Samples were placed in a Mastercycler Gradient Thermal Cycler (Eppendorf, UK) for denaturation at 94 °C for 5 min. Each sample was held at this temperature for a further 20 s to continue separation of the DNA strands and make them available to bind to primers (annealing). Samples were held at the annealing temperature for each primer (Table 2.1) for 20 s and thereafter the temperature was raised and held at 68 °C for a further 20 s for primer extension. The combination of each 20 s step is considered a cycle and this was repeated specific to each primer as shown in Table 2.1. Once the final cycle had completed, the samples were held at 72 °C for 10 min prior to analysis.

Prior to this study, the annealing temperature for each primer (Table 2.1) had been optimised with human dental pulp cells by previous researchers and laboratory technicians in house (Molecular Biology Laboratory, School of Dentistry, University of Birmingham, UK). Primers had been sourced and custom designed using the National Centre for Biotechnology Information Gene database and commercially produced as specified in Table 2.1.

Table 2.1 Details of the primers used for sqRT-PCR including their corresponding annealing temperatures, cycle numbers, sequences and source / accession number.

Primer	**Annealing temperature (°C)**	**Cycle Number**	**Primer sequence (5' → 3')**	**Source / Accession Number**
Collagen type 1 alpha 1 (C1α1)	60	42	F-TGGGAGTGCAAGGATACTCTATATCG R-CCCATCCCATCTTCGACGTAC	(Levin et al. 1999, Myers et al. 1981) Thermo Hybaid OR135882-17/18
Dentine matrix protein-1 (DMP-1)	60	40	F-AGGAGAGACAGCAAGGGTGA R-GCTGAGCTGCTGTGAGACTG	Invitrogen 262560-X5539 NM004407.1
Dentine sialophosphoprotein (DSPP)	60	55	F-CCTAAAGAAAATGAAGATAATT R-TAGAAAAACTCTTCCCTCCTAC	(Buchaille et al. 2000) Thermo Hybaid OR135882-23/24 NM014208.2
Glyceraldehyde-3-phosphate dehydrogenase (GAPDH)	60	18-27	F-TCTAGACGGCAGGTCAGGTCC R-CCACCCATGGCAAATTCCATG	Invitrogen 291573-E1540
Osteocalcin (OCN)	60	34	F-GGCAGCGAGGTAGTGAAGAG R-CTGGAGAGGAGCAGAACTGG	(Al-Habib et al. 2013) Invitrogen 373095-X7617 X53698
Osteopontin (OPN)	60	42	F-TCACCAGTCTGATGAGTCTCACC R-CACCATTCAACTCCTCGCTTTCC	Sigma Genosys J04765.1 BC02284
Transforming growth factor beta 1 (TGF-β1)	60	30	F-CGCCTTAGCGCCCACTGCTCCTGT R-GGGGCGGGACCTCAGCTGCAC	(McLachlan et al. 2003) Invitrogen 262560-X5543

2.9.5 GEL ELECTROPHORESIS

A 1.5% agarose gel was created by adding 0.9 g of agarose (Web Scientific, UK) to 60 ml of a 1x solution of tris-acetate-EDTA (TAE) buffer and heating in a microwave (Sanyo, UK). The heated solution was cooled whilst mixing under running water prior to the addition of 3 µl of a 0.5 µg/ml ethidium bromide solution (Helena Biosciences, UK) to aid visualisation. The agarose-TAE solution was poured into a gel casting tray and combs were added to create loading wells. The solution was left at room temperature for 30 mins to set into a gel around the combs. Gels were placed in an electrophoresis tank containing a 1x solution of TAE buffer prior to the removal of the combs to ensure bubbles of air did not become trapped within the wells. The wells were positioned over coloured strips to aid in the loading of 3 µl of the amplified cDNA (Section 2.9.4) to each well. A 3 µl solution of Hyperladder^{TM} IV (Bioline, UK) was loaded alongside the samples as a reference for size determination of the target genes. An electrical current was applied at 120 V for approximately 30 to 40 min to allow for the separation of nucleic acids. The gel was carefully removed from the tank ensuring it did not tear and was transferred to the G:BOX (Syngene, UK) for visualisation under ultra-violet light. Images were recorded and subsequently the band intensities for each target gene were analysed using GeneSnap (Syngene, UK) software. The volume density of the amplified targets was determined by comparing and normalising the intensity value against the reference gene (GAPDH) and the volume density was thus expressed as a percentage of the normalised values.

2.10 STATISTICAL ANALYSIS

Microsoft Excel (Microsoft Corporation, USA) was used to perform statistical analyses on all data in this study. Values in this study are expressed as mean ± standard deviation, unless otherwise stated. Statistical significance was determined with the use of the one way and two way analysis of variance (ANOVA) test. P values are stated in figures and tables; * ($P<0.05$), ** ($P<0.01$), *** ($P<0.001$).

CHAPTER 3

ANALYSIS OF THE DUOSON 45 KILOHERTZ ULTRASOUND FIELD

Data presented in this chapter has been published in part in the Journal of Therapeutic Ultrasound (Patel et al. 2015). This work is of an interdisciplinary nature where the ultrasound output measurements were undertaken by the author and the findings were forwarded to colleagues in the USA for further mathematical interpretation.

Therapeutic instruments, such as the DuoSon, must be regularly calibrated to ensure their ultrasonic output complies with that expected from the device (IEC 60601-2-5:2009). Failure to comply with this standard may potentially result in an unexpected ultrasound exposure leading to unreliable results and in cases used for therapy, damage to biological tissues or resulting in the therapy being ineffective. The manufacturer of the therapeutic instrument used in this study states that the power of the ultrasound generated by the DuoSon has an accuracy of 20% compared to the measured value. Whilst this complies with IEC 60601-2-5:2009, confirmation of both the beam profile and accurate ultrasonic output is needed to guide the design of the experiment set-up in order to relate the ultrasound dose to biological effects.

An objective of this study is to develop a system which was capable of characterising the ultrasonic output of the DuoSon and quantify the dose exposure of the ultrasound generated. A custom designed water tank capable of degassing large quantities of water whilst housing a hydrophone was developed and used to measure the maximum pressure displacement created by ultrasound with a frequency of 45 kHz at various pre-set levels of intensity. These values were analysed by an oscilloscope and SP intensities were calculated with post-hoc analysis of the data.

Maximum voltage and frequency measurements were recorded with the hydrophone at 60 specified positions (Section 2.2) for each of the three pre-set intensity settings (10, 25 and 75 mW/cm^2) of ultrasound with a frequency of 45 kHz produced by the DuoSon (Table 3.1). Whilst no statistical difference was found between the frequencies recorded when ultrasound with an intensity of 10 and 25 mW/cm^2 was generated, a statistical difference ($P<0.001$) was found when comparing these groups with the ultrasound produced with an intensity of 75

mW/cm^2. The frequencies recorded using the highest intensity were only marginally higher compared to those frequencies recorded with the two lower intensities (Table 3.1). This indicates that the highest intensity output does statistically ($P<0.001$) affect the frequency of the ultrasound produced however the affect is of the magnitude of 0.1 kHz or less. It should be noted that whilst a relatively constant frequency was recorded from the DuoSon transducer, the frequency was approximately 2 kHz higher than the 45 kHz quoted by the manufacturer.

Maximum voltage and frequency measurements (Table 3.1) were used to calculate spatial peak (SP) intensities as described in Section 2.3. Beam plots of calculated intensities are shown in Figures 3.1A – 3.1C. The data indicate that the measurements recorded where the transducer and hydrophone were centrally aligned were only marginally higher compared to the expected manufacturer pre-set intensity; 10.56, 25.70 and 76.04 mW/cm^2 calculated intensities for 10, 25 and 75 mW/cm^2 pre-set intensities respectively. Measurements made horizontally away from the long axis of the transducer showed a gradual reduction of the average intensity. Figures 3.1A – 3.1C also display the size of the transducer and positioning of culture wells in a six-well culture plate which are a 1:1 scale with the horizontal axis. Horizontal measurements show that at 20 and 25 mm from the central axis of the transducer, the calculated intensities without Fourier analysis were 7.75 and 5.2 mW/cm^2 respectively when an ultrasound beam using the pre-set 10 mW/cm^2 mode is selected. An ultrasound beam produced using the pre-set 25 mW/cm^2 mode recorded an average intensity of 19 and 12.5 mW/cm^2, and when using the 75 mW/cm^2 mode, 61.5 and 58.5 mW/cm^2 was recorded at 20 and 25 mm respectively from the central axis of the transducer. The beam plots of the 10 and 25 mW/cm^2 modes (Figures 3.1A and 3.1B) are similar in form, as opposed to that of the 75

mW/cm^2 mode (Figure 3.1C). The 75 mW/cm^2 mode produces an ultrasound beam which has a flatter peak. These data imply that when biological cells cultured in dishes of a six-well culture plate are treated with ultrasound, adjacent culture wells will also be exposed to an ultrasound field. This finding is based on measurements recorded in 'free-field' conditions and not in the presence of cell culture plates. Biological data from further investigation carried out with six-well culture plates (Section 4.3) supports this finding.

Table 3.1 The recorded maximum voltage and frequency of ultrasound produced from the DuoSon in 'free-field' conditions when a 10, 25 and 75 mW/cm^2 ultrasound beam is produced from the transducer. Measurements were taken at 1 mm distances up to 10 mm vertically from the transducer face at 0, 5, 10, 15, 20 and 25 mm horizontally from the long axis of the transducer.

Measurement position		DuoSon pre-set intensity (mW/cm^2)					
		10		25		75	
Vertical (mm)	Horizontal (mm)	Maximum voltage (mV)	Frequency (kHz)	Maximum voltage (mV)	Frequency (kHz)	Maximum voltage (mV)	Frequency (kHz)
1	0	2.43	47.55	3.75	47.4	6.56	47.52
2	0	2.41	47.57	3.76	47.43	6.50	47.51
3	0	2.43	47.55	3.74	47.43	6.38	47.52
4	0	2.38	47.53	3.76	47.42	6.40	47.52
5	0	2.39	47.52	3.75	47.43	6.43	47.52
6	0	2.49	47.53	3.74	47.42	6.45	47.51
7	0	2.36	47.5	3.74	47.41	6.46	47.5
8	0	2.39	47.47	3.72	47.41	6.47	47.5
9	0	2.36	47.46	3.72	47.4	6.41	47.49
10	0	2.38	47.43	3.70	47.41	6.41	47.47
1	5	2.38	47.58	3.71	47.45	6.50	47.49
2	5	2.37	47.57	3.70	47.43	6.46	47.5
3	5	2.36	47.56	3.70	47.43	6.45	47.5
4	5	2.36	47.55	3.71	47.44	6.43	47.51
5	5	2.36	47.54	3.71	47.43	6.43	47.52
6	5	2.36	47.53	3.70	47.42	6.43	47.52
7	5	2.36	47.52	3.68	47.4	6.44	47.53

Measurement position		DuoSon pre-set intensity (mW/cm^2)					
		10		25		75	
Vertical (mm)	Horizontal (mm)	Maximum voltage (mV)	Frequency (kHz)	Maximum voltage (mV)	Frequency (kHz)	Maximum voltage (mV)	Frequency (kHz)
8	5	2.34	47.5	3.64	47.37	6.35	47.51
9	5	2.32	47.48	3.64	47.36	6.29	47.5
10	5	2.32	47.47	3.63	47.35	6.26	47.5
1	10	2.36	47.54	3.61	47.43	6.48	47.46
2	10	2.36	47.53	3.69	47.42	6.49	47.47
3	10	2.33	47.52	3.65	47.42	6.51	47.48
4	10	2.30	47.53	3.63	47.41	6.49	47.49
5	10	2.29	47.53	3.61	47.4	6.44	47.5
6	10	2.28	47.5	3.59	47.4	6.42	47.5
7	10	2.27	47.45	3.57	47.38	6.37	47.5
8	10	2.26	47.44	3.57	47.36	6.31	47.54
9	10	2.25	47.43	3.54	47.35	6.27	47.51
10	10	2.23	47.43	3.52	47.34	6.24	47.5
1	15	1.93	46.74	3.26	46.82	6.04	47.44
2	15	1.92	46.89	3.17	46.89	6.07	47.44
3	15	1.91	47.08	3.21	46.95	6.07	47.47
4	15	1.99	47.35	3.24	47.3	6.09	47.49
5	15	2.14	47.45	3.30	47.43	6.15	47.49
6	15	2.19	47.46	3.36	47.42	6.24	47.52
7	15	2.26	47.46	3.38	47.42	6.23	47.51
8	15	2.27	47.43	3.47	47.35	6.22	47.53
9	15	2.31	47.41	3.42	47.34	6.20	47.55
10	15	2.25	47.41	3.39	47.31	5.99	47.53

Measurement position		DuoSon pre-set intensity (mW/cm^2)					
		10		25		75	
Vertical (mm)	Horizontal (mm)	Maximum voltage (mV)	Frequency (kHz)	Maximum voltage (mV)	Frequency (kHz)	Maximum voltage (mV)	Frequency (kHz)
1	20	2.09	47.36	3.02	47.16	5.75	47.32
2	20	2.17	47.38	3.16	47.36	5.79	47.39
3	20	2.22	47.37	3.17	47.37	5.80	47.42
4	20	2.21	47.36	3.20	47.41	5.83	47.42
5	20	2.10	47.36	3.26	47.42	5.86	47.45
6	20	2.06	47.35	3.29	47.41	5.88	47.47
7	20	2.01	47.34	3.29	47.42	5.89	47.48
8	20	1.95	47.33	3.30	47.43	5.88	47.5
9	20	1.84	47.3	3.22	47.43	5.62	47.5
10	20	1.81	47.31	3.15	47.44	5.59	47.52
1	25	1.60	47.2	2.54	47.32	5.62	47.3
2	25	1.68	47.22	2.48	47.31	5.66	47.31
3	25	1.70	47.24	2.65	47.31	5.64	47.32
4	25	1.69	47.26	2.69	47.3	5.66	47.38
5	25	1.66	47.29	2.73	47.29	5.71	47.41
6	25	1.69	47.31	2.77	47.3	5.65	47.41
7	25	1.69	47.3	2.73	47.3	5.69	47.42
8	25	1.66	47.3	2.58	47.29	5.58	47.46
9	25	1.65	47.29	2.45	47.28	5.61	47.49
10	25	1.66	47.32	2.37	47.27	5.56	47.53

Figure 3.1 Spatial-peak intensity calculated when a 10 (A), 25 (B) and 75 mW/cm^2 (C) ultrasound beam with a frequency of 45 kHz is produced from the DuoSon transducer. Dimensions of the transducer and culture wells are to a 1:1 scale with the horizontal axis. A diagrammatic representation of the culture wells in a six-well culture plate have been superimposed to demonstrate proximity of the culture wells to each other and their spatial relationship to the ultrasound beam and average intensities. Intensity without Fourier analysis is shown as mean ± SD (continued on next page).

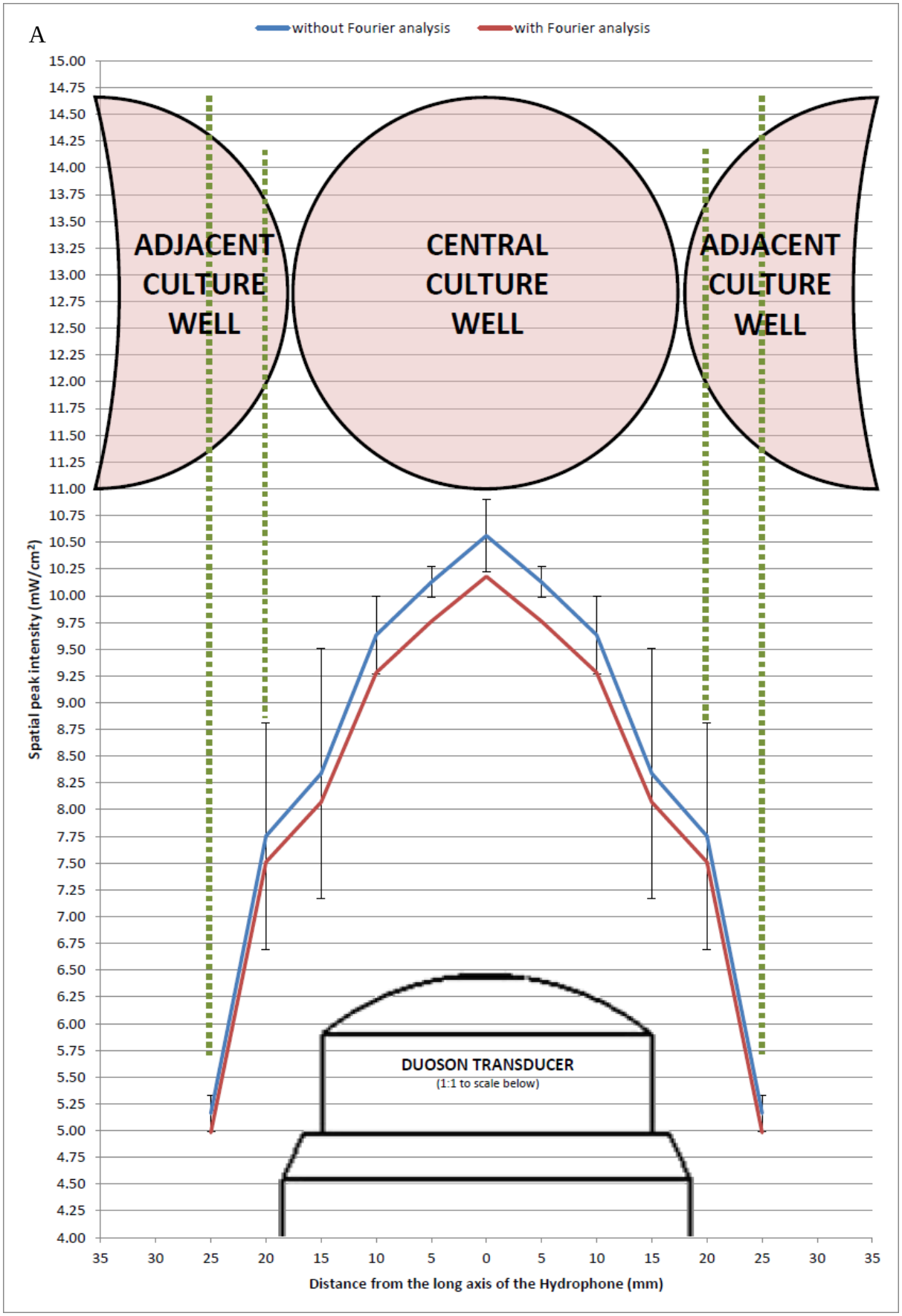
A
without Fourier analysis
with Fourier analysis
ADJACENT CULTURE WELL
CENTRAL CULTURE WELL
ADJACENT CULTURE WELL
Spatial peak intensity (mW/cm²)
DUOSON TRANSDUCER
(1:1 to scale below)
Distance from the long axis of the Hydrophone (mm)

B

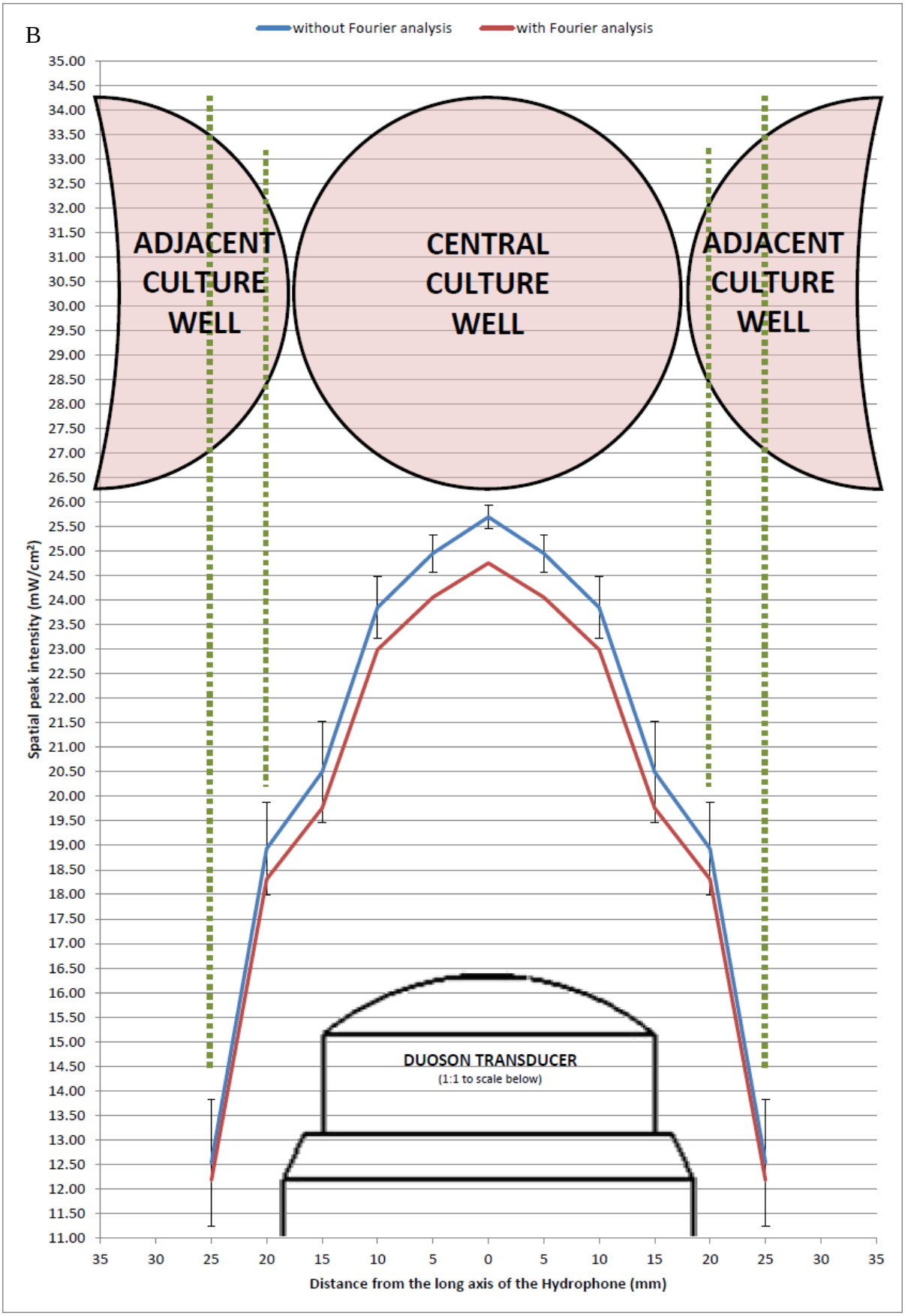
without Fourier analysis
with Fourier analysis
ADJACENT CULTURE WELL
CENTRAL CULTURE WELL
ADJACENT CULTURE WELL
Spatial peak intensity (mW/cm²)
DUOSON TRANSDUCER
(1:1 to scale below)
Distance from the long axis of the Hydrophone (mm)

C

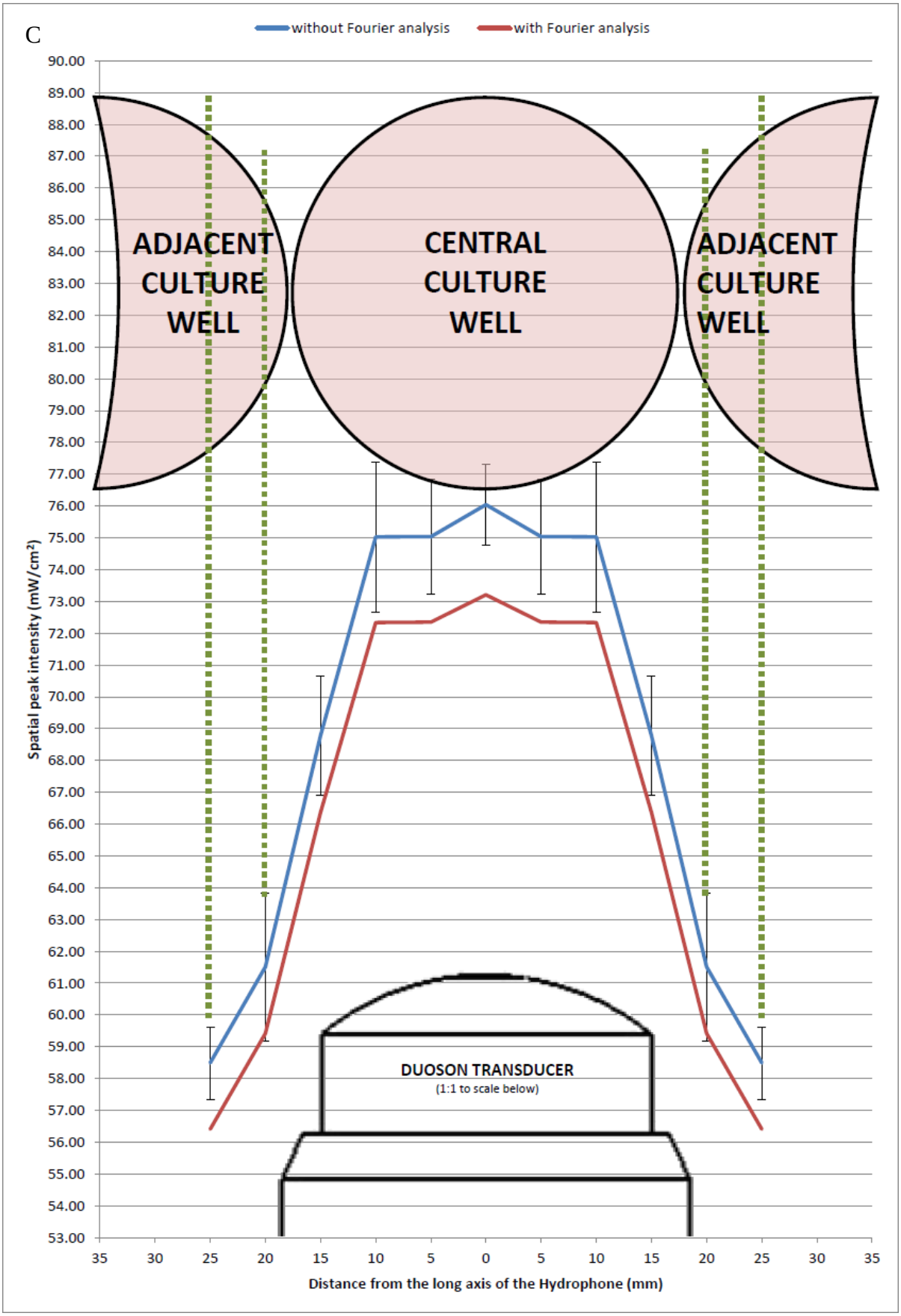
without Fourier analysis
with Fourier analysis
ADJACENT CULTURE WELL
CENTRAL CULTURE WELL
ADJACENT CULTURE WELL
DUOSON TRANSDUCER
(1:1 to scale below)
Spatial peak intensity (mW/cm²)
Distance from the long axis of the Hydrophone (mm)
90.00
89.00
88.00
87.00
86.00
85.00
84.00
83.00
82.00
81.00
80.00
79.00
78.00
77.00
76.00
75.00
74.00
73.00
72.00
71.00
70.00
69.00
68.00
67.00
66.00
65.00
64.00
63.00
62.00
61.00
60.00
59.00
58.00
57.00
56.00
55.00
54.00
53.00
35 30 25 20 15 10 5 0 5 10 15 20 25 30 35

CHAPTER 4

THE EFFECT OF A STATIONARY TRANSDUCER IN A MULTI-WELL CULTURE PLATE ON AN ODONTOBLAST-LIKE CELL LINE

Data presented in this chapter has been published in part in the Journal of Therapeutic Ultrasound (Ghorayeb et al. 2013, Patel et al. 2015). The author of the present study carried out the laboratory-based investigations including cell culture, ultrasound application, data collection from cell culture and temperature measurements, analysis and interpretation of data.

The application of ultrasound to *in vitro* cell culture provides a good opportunity to study the effects of ultrasound on specific cell types however there is little consensus in the literature regarding the most optimal strategy for ultrasound application (Hensel et al. 2011, Padilla et al. 2014). The majority of studies investigating *in vitro* ultrasound bio-effects in the literature apply LIPUS ultrasound (Padilla et al. 2014) which utilises a frequency in the megahertz range however kilohertz ultrasound is known to better penetrate hard dental tissues (Ghorayeb et al. 2013) and may be more appropriate for investigating ultrasound mediated dental repair. This present study initially investigated the effects of kilohertz ultrasound on the proliferation and cell viability of an odontoblast-like cell line (MDPC-23) cultured in six-well culture plates.

An objective of this study is to develop a system to deliver 45 kHz ultrasound in a controlled and reproducible manner to cells *in vitro* culture. Thermal variation and biological effects in adjacent and distant culture wells were also analysed to determine if this was the most appropriate set-up to investigate the effects of kilohertz ultrasound on biological cells *in vitro* culture. The analysis of temperature changes in culture media determines the ability of the set-up apparatus to control the temperature of the culture media whilst providing an indication of the type of bio-effects which may be taking place (thermal or mechanical). Data from two experiments are presented in this section. The first experiment (Section 4.2) applied 45 kHz ultrasound to multiple culture wells of the same six-well culture plate and included the sham control culture well on the same culture plate (Figure 2.7C). The aim of the second experiment (Section 4.3) was to determine whether 45 kHz ultrasound applied to one culture well of a six-well culture plate would affect MDPC-23 cells cultured in the adjacent and distant culture wells of the same culture plate (Figure 2.7D).

Pilot studies and previous research treating MDPC-23 with 45 kHz ultrasound indicated that whilst a single dose of ultrasound with a short duration does not significantly increase MDPC-23 cell numbers compared to sham control, multiple treatments separated by at least 24 hours had a more positive effect (Man et al. 2012). Ultrasound application experiments were carried out as follows:

Day 0: MDPC-23 cells were seeded in six-well culture plates as described in Section 2.5.1.1

Day 1: culture media replenished

Day 2: ultrasound applied

Day 3: culture media replenished

Day 4: ultrasound applied

Day 5: culture media replenished

Day 6: ultrasound applied

Day 7: culture media replenished

Day 8: experiment halted for analysis.

4.1 TEMPERATURE OF CULTURE MEDIA

Temperature measurements were recorded to assess the capability of the experimental setup (described in Section 2.5.1) to maintain the temperature of the culture medium bathing cells in a six-well culture plate at 37 °C whilst in a laminar flow hood and to record any changes in temperature during the application of ultrasound. The recorded temperatures indicated that ultrasound with a frequency of 45 kHz, and at the three specified intensities (10, 25 and 75 mW/cm^2), did not significantly affect the temperature of the culture medium in culture wells adjacent to (Figure 4.2A) and distant from (Figure 4.2B) the culture well being treated with

ultrasound (Figure 2.7D). Figure 4.1 shows the gradual temperature rise in the culture medium of the culture well with the transducer face submerged. Initially, the temperature of the culture media dropped by 0.5 °C when the transducer face was submerged into the culture well. However, as shown by the sham control temperature measurements in Figure 4.1, the water bath set-up (Section 2.5.1 and Figure 2.7) was able to keep the temperature of the culture medium stable at 37 °C (±1 °C). The highest of the three intensities, 75 mW/cm^2, produced a temperature rise of 15.9 °C to 52.3 °C after 30 min of ultrasound exposure. Intensities of 10 and 25 mW/cm^2 increased the temperature of the culture medium resulting in maximum temperatures of 40.7 °C and 43.4 °C respectively over 30 min of ultrasound exposure. It was observed for the lower two intensities, the temperature rise reached a plateau before the maximum treatment time of the device was reached. This did not occur at the highest intensity. After 5 min of ultrasound application, the temperature of the culture media had risen to 38.3 °C, 39.6 °C and 42 °C with 10, 25 and 75 mW/cm^2 respectively. These data indicate that the application of ultrasound using this method increases the ambient temperature of the culture medium, and longer times up to 30 min, can generate a significant temperature rise.

Figure 4.1 Changes in the temperature of culture media in the corner culture well of a six-well culture plate in which the transducer face was submerged (n=3, mean ± SD). Temperatures were recorded over 30 min whilst ultrasound with a frequency of 45 kHz was generated at an intensity of 0 (sham control), 10, 25 and 75 mW/cm^2.

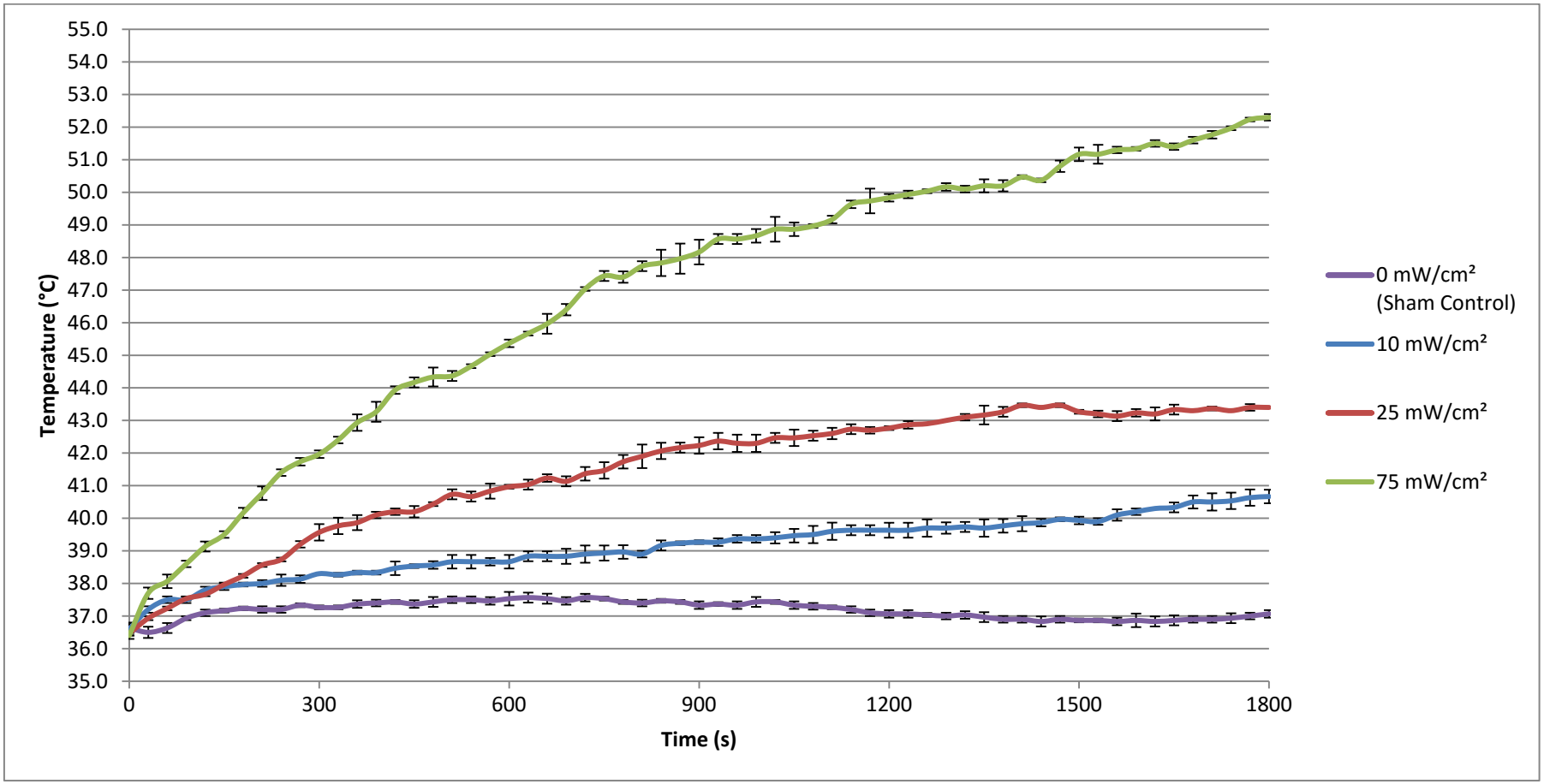

Figure 4.2 Changes in the temperature of culture media in the adjacent (A) and distant (B) culture well (n=3, mean ± SD). Temperatures were recorded over 30 min whilst ultrasound with a frequency of 45 kHz was generated at an intensity of 0 (sham control), 10, 25 and 75 mW/cm^2.

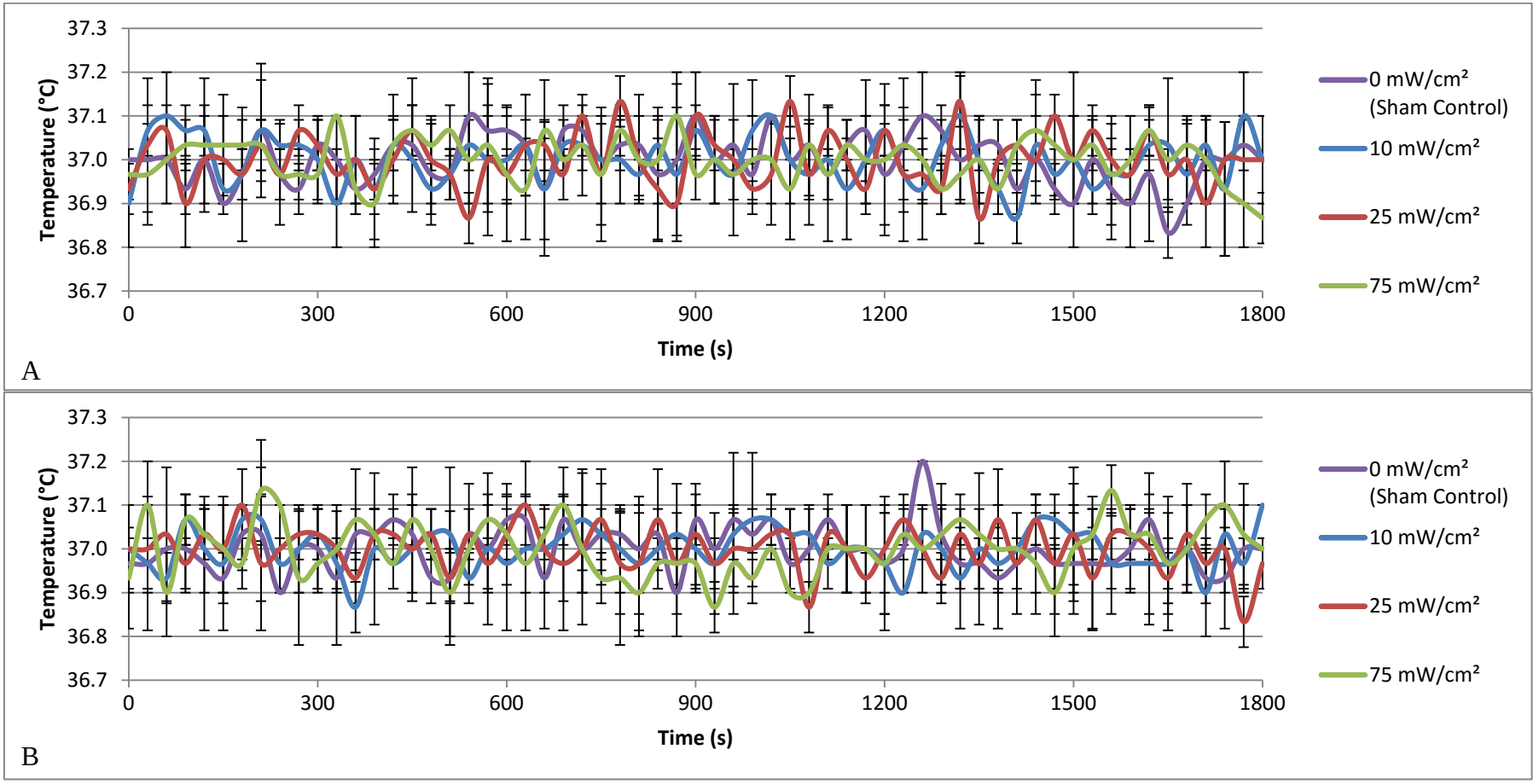

4.2 APPLICATION OF ULTRASOUND TO MULTIPLE WELLS OF A SIX-WELL CULTURE PLATE

4.2.1 CELL VIABILITY

The application of ultrasound with a frequency of 45 kHz for 5 min at an intensity of 10 mW/cm^2 at three time points (day 2, 4 and 6) over a 7 day period did not significantly affect the viability of odontoblast-like MDPC-23 cells when compared to the sham control (Figure 4.3), however, there was a significant ($P<0.05$) albeit marginal reduction when 25 mW/cm^2 intensity was applied. The highest intensity resulted in the most significant ($P<0.01$) and greatest reduction in cell viability when compared to the sham control, however cell viability was greater than 90%. A significant difference ($P<0.01$) was also found when comparing the cell viability of odontoblast-like MDPC-23 cells when exposed to 25 and 75 mW/cm^2 compared to 10 mW/cm^2. These findings indicate that ultrasound with a frequency of 45 kHz has an intensity dependent effect on the viability of odontoblast-like MDPC-23 cells *in vitro* culture. Post application of ultrasound, cell viability was higher than 90% indicating that ultrasound with a frequency of 45 kHz did not adversely affect *in vitro* cultures however higher intensities are not as well tolerated by MDPC-23 cells compared to the lower intensities used in this study when applied three times for 5 min over 7 days.

Figure 4.3 Percentage change in the number of odontoblast-like MDPC-23 cells and viability after the application of three episodes of 5 min duration of ultrasound with a frequency of 45 kHz at an intensity of 0 (sham control), 10, 25 and 75 mW/cm^2, separated by 48 h over seven days (n=3, mean ± SD) (* P<0.05, ** P<0.01, *** P<0.001).

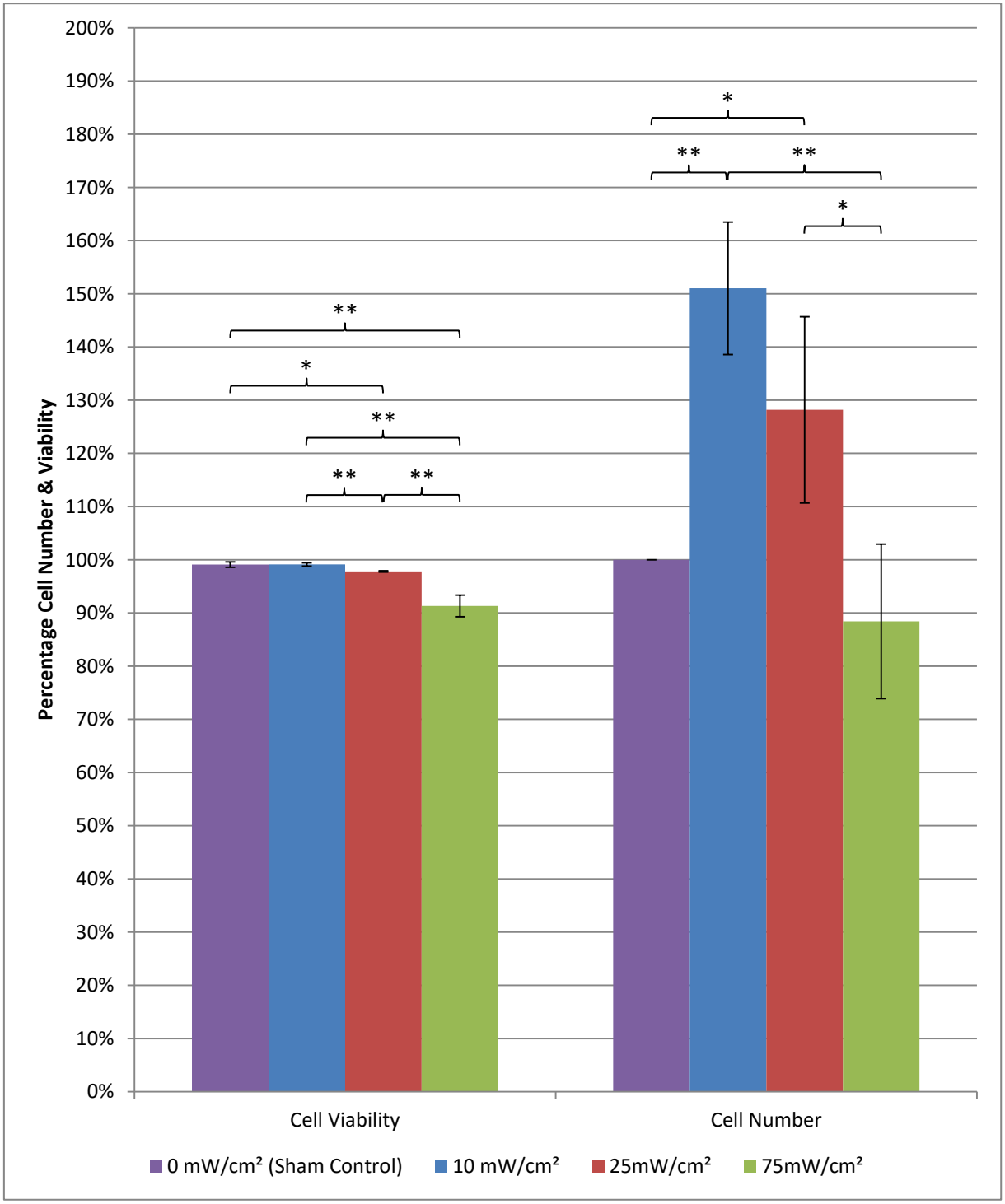

4.2.2 CELL NUMBER

The results demonstrated that odontoblast-like MDPC-23 cell numbers were significantly increased following three ultrasound treatments with an intensity of 10 ($P<0.01$) and 25 mW/cm^2 ($P<0.05$) over a 7 day culture period as compared with the sham control (Figure 4.3). The number of cells remaining, when compared to sham control, was reduced by less than 12% when ultrasound with an intensity of 75 mW/cm^2 was applied. This was not a statistically significant reduction. However the difference in cell number after the application of ultrasound with an intensity of 10 and 25 mW/cm^2 compared to 75 mW/cm^2 is statistically significant; $P<0.01$ and $P<0.05$ respectively. These findings indicate that ultrasound affected cell proliferation at low-intensity therapeutic intensities in a dose-dependent manner with an upper threshold where higher intensities adversely affect cell viability and proliferation.

4.3 APPLICATION OF ULTRASOUND TO A SINGLE WELL OF A SIX-WELL CULTURE PLATE

In this experiment, 45 kHz ultrasound with an intensity of 10, 25 and 75 mW/cm^2 was applied to the corner culture well of a six-well culture plate as described in Section 2.5.1.3. Ultrasound was not applied to the other culture wells in the same six-well culture plate. An assessment of cell viability and the number of cells present after the application of three episodes of ultrasound in three of the culture wells of the six-well culture plates was made. The culture well in which the transducer face was submerged (corner), the adjacent culture well (adjacent) and the distant culture well (distant) on the opposite side. The aim of this experiment was to assess the ability of ultrasound with a frequency of 45 kHz to affect cells

cultured in culture wells of the same six-well culture plate where ultrasound is applied to only one of the culture wells.

4.3.1 CELL VIABILITY

Analysis of cell viability from the culture well in which the transducer was submerged has demonstrated similar results to that found in a previous experiment (Section 4.2.1) in this research study where ultrasound was applied to multiple culture wells in the same six-well culture plate. This experiment showed that the highest ultrasound intensity significantly reduced cell viability compared to the two lower intensities and sham control ($P<0.001$) (Figure 4.4). However, with the highest intensity, cell viability was higher than 90% indicating that 45 kHz ultrasound did not instigate a substantial drop in viable cells. Cell viability was not significantly affected in the adjacent and distant culture wells compared to sham control for the two lower intensities however the highest intensity demonstrated a significant ($P<0.05$) decrease in the cell viability of MDPC-23 cells compared to sham control. This indicates that ultrasound with a frequency of 45 kHz at an intensity of 75 mW/cm^2 had an effect on MDPC-23 cells cultured in the non-exposed culture wells of the same six-well culture plate. This effect was more pronounced in the adjacent culture well compared to the distant culture well, 93.44% and 97.11% respectively, indicating that the proximity of the culture well to the transducer influenced cell viability.

Figure 4.4 Percentage change in the number of odontoblast-like MDPC-23 cells and viability after the application of three episodes of 5 min duration of ultrasound with a frequency of 45 kHz at an intensity of 0 (sham control), 10, 25 and 75 mW/cm^2, separated by 48 h over seven days to the corner culture well of a six-well culture plate. Cell viability and number in adjacent and distant wells are also shown (n=3, mean ± SD) (* P<0.05, ** P<0.01, *** P<0.001).

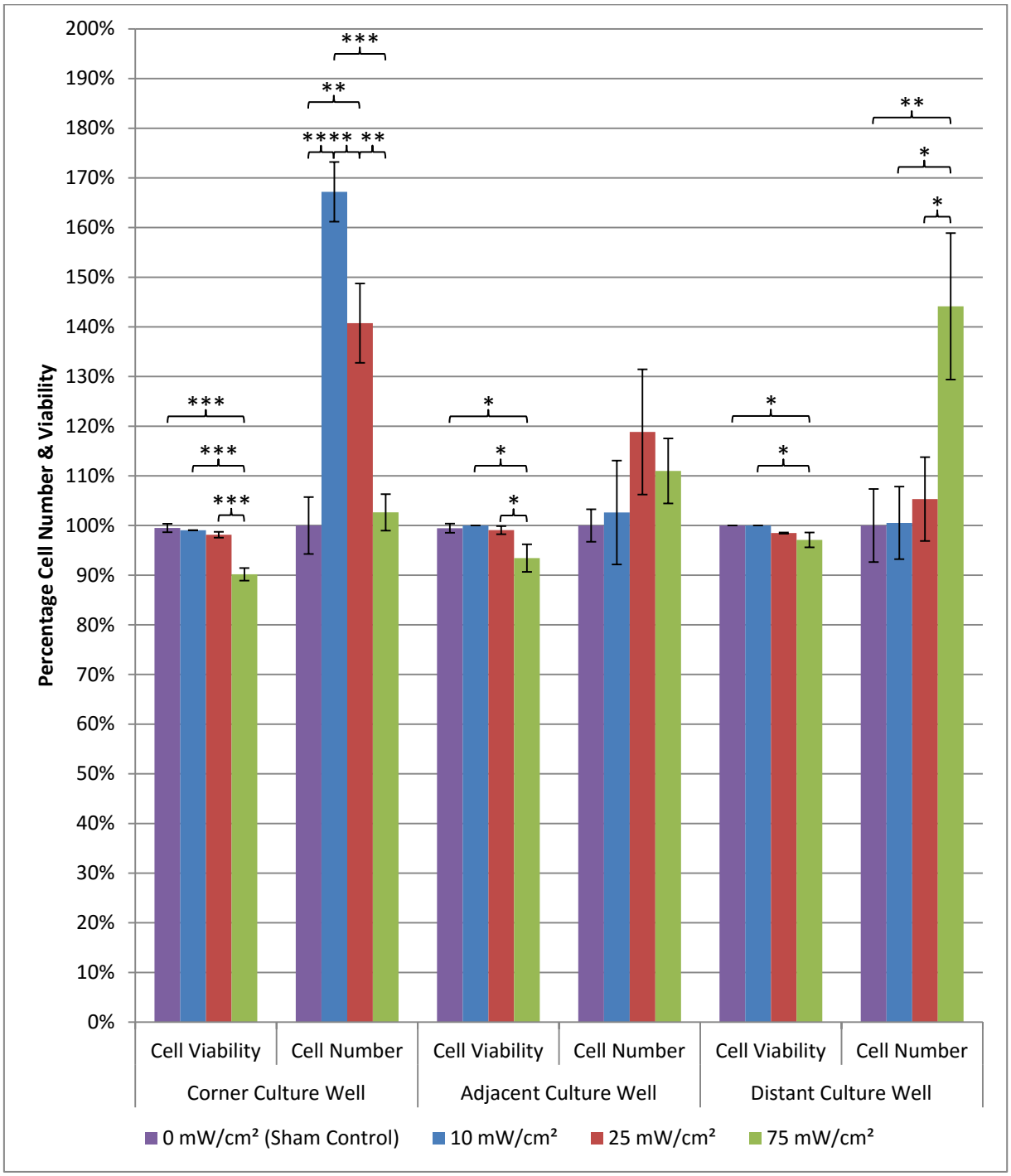

4.3.2 CELL NUMBER

Application of 45 kHz ultrasound at the two lower pre-set intensity levels of 10 and 25 mW/cm^2 resulted in cell counts from the culture well in which the transducer face was submerged to be significantly higher than the sham control group ($P<0.001$ and $p<0.01$ respectively) suggesting ultrasound-stimulated cell proliferation. The pattern of response to ultrasound in the culture well in which the transducer face was submerged is similar to the previous experiment (Section 4.2.2). However in the current experiment the difference in cell number compared to sham control for the 10 and 25 mW/cm^2 intensities was higher (167.2% and 140.74% respectively) and more significant ($P<0.001$ and $P<0.01$ respectively) compared to the previous experiment ($P<0.05$). Whereas in the previous experiment, the highest intensity resulted in a drop in cell number (11.58% compared to sham control), in the current experiment, the highest intensity resulted in an increase in cell number (2.65% compared to sham control). These data indicated that applying ultrasound to a single culture well in a six-well culture plate may result in data that is more precise and reflects the true effect of a specific intensity and time duration. Applying ultrasound to multiple culture wells of the same six-well culture plate may reduce the observed effect. No significant findings were reported from cell counts from the immediately adjacent culture wells, although cell numbers were marginally increased by approximately 20% and 10% with the two pre-set intensity levels of 25 and 75 mW/cm^2 respectively, compared to the sham control (Figure 4.4). Cell numbers in the distant culture well, were found to be significantly ($p<0.01$) increased when 75 mW/cm^2 intensity ultrasound was used compared to the sham control (Figure 4.4). However, the lower intensities did not significantly increase cell numbers in the distant culture well as shown in Figure 4.4. The increase in cell numbers in distant culture wells of six-well plates where 75

mW/cm^2 intensity ultrasound is used, indicates that ultrasound at this intensity has a positive effect on cell number when the cells are not directly exposed. This suggests that there is potential for ultrasound with higher intensities to affect other culture wells in the same six-well plate, with lower intensities, this effect is not significant.

CHAPTER 5

THE EFFECT OF A MOVING TRANSDUCER IN A CULTURE DISH ON PRIMARY HDPC

The data from the previous two sections (Sections 3 and 4) indicate that applying 45 kHz ultrasound to multi-well culture plates is not appropriate for evaluating dose specific effects of ultrasound. Furthermore, to enable the application of ultrasound for longer than 5 minutes without significantly increasing the temperature of the culture media, the apparatus set-up would need to be re-developed. An objective of this study is to develop a system to deliver 45 kHz ultrasound in a controlled and reproducible manner to cells *in vitro* culture. The results presented in this section are based on the use of a mechanised apparatus that provides a controlled movement of the ultrasound transducer whilst the transducer face is submerged within the culture media. A larger, single well culture dish is used to enable movement of the transducer within the culture dish and prevent ultrasound contamination of sample cell cultures. A further objective of this study is to ascertain the cellular and molecular effects of low intensity 45 kHz ultrasound on cells harvested from the dental pulp of a human tooth. Cell proliferation, viability and gene expression of primary HDPC were investigated with the application of 10 and 25 mW/cm^2 intensities of 45 kHz ultrasound. Pilot studies and previous research treating MDPC-23 with 45 kHz ultrasound indicated that the application of ultrasound for 30 minutes significantly improved cell proliferation (Man et al. 2012). Ultrasound was applied to primary HDPC in culture as with MDPC-23 (see time points for ultrasound application at the beginning of Section 4).

The markers selected for gene expression study from primary HDPC were C1α1, DMP-1, DSPP, OCN, OPN and TGF-1. Their roles in dentinogenesis and dentine repair as nucleating factors and signalling molecules have been discussed previously (Section 1.2.2.1) and adapting their expression in primary HDPC with ultrasound treatment may indicate a potential dental treatment modality for ultrasound. The expression of C1α1 in primary HDPC is

investigated as collagen type 1, which is known to be predominant in the dentine matrix and can be mineralised by hydroxyapatite crystals (Smith et al. 2012a). Increased production of type 1 collagen may enhance the speed and quality of mineralisation.

5.1 TEMPERATURE OF CULTURE MEDIA

The temperature of the culture media in a culture dish with the transducer face submerged and in motion was found to be stable at 37 °C (± 1 °C) with the sham control group over the 30 min application period. This shows that the set-up described in Section 2.5.2 could maintain the temperature of the cells cultured in the culture dish at 37 °C (± 1 °C) whilst in a laminar flow hood. When ultrasound was produced from the transducer at the three different intensities, the overall temperature rise was proportional to the intensity of the ultrasound (Figure 5.1). This pattern is similar to that seen with a stationary transducer submerged in culture media (Figure 4.1). The highest intensity generated the largest recorded temperature of 39.8 °C after 23 min, whereas the two lower intensities did not record a temperature higher than 38.2 °C. The highest recorded temperature of the mid-level intensity, 25 mW/cm^2, was reached at a similar time as the strongest intensity, 22 and 23 min respectively, and thereafter plateaued. The lowest intensity recorded its highest temperature after 16 min 30 s, 37.9 °C, however conversely to the higher two intensities, the temperature of the culture media steadily declined to 37.3 °C at 28 min before again rising. The explanation for this difference compared to the temperature plots of the higher two intensities may be as a result of the small amount of energy produced by a 10 mW/cm^2 intensity being insufficient to warm up the culture media whilst the thermostat controlled water-bath disengaged its heating element. In comparison to the experiment with a stationary transducer (Section 4.1) where there was a

steady increase in temperature right up to the end of the 30 min application period when the 10 mW/cm^2 intensity was applied. Whilst the temperature rise for the two lower intensities was no more than 1.2 °C, the highest intensity resulted in a temperature rise of 2.6 °C over the 30 min application period. The temperature of the culture media can affect the behaviour of the cells in which they are cultured and this experiment has demonstrated that whilst at lower intensities, the temperature of the culture media can be kept stable, at higher intensities the temperature rise is difficult to control. This is also demonstrated with a stationary transducer (Section 4.1).

5.2 CELL VIABILITY

The application of three 5 min episodes of ultrasound with a frequency of 45 kHz to primary HDPC *in vitro* culture did not significantly affect cell viability compared to sham control (Figure 5.2). Longer application periods demonstrated a significant difference between the cell viability of the sham control group versus the ultrasound group and the longest periods, 15 and 20 min, showed a significant difference between the two intensities of 45 kHz ultrasound applied to primary HDPC. The cell viability of the sham control group remained higher than 98% across all four time period groups. This indicates that the duration of ultrasound application alone does not affect cell viability *in vitro* conditions. Cell viability is affected by a combination of the duration and the application of ultrasound with the longest duration and highest intensity used in this experiment reducing the cell viability of primary HDPC to 95.23%. This is statistically significant ($P<0.01$) however a cell viability of 95% is considered typical especially as the primary HDPC were kept in atmospheric conditions for 20 mins compared to ideal culture conditions (humidified atmosphere with 5% CO_2 in air).

Figure 5.1 Changes in the temperature of culture media in the culture dish in which the transducer face is submerged (n=3, mean ± SD). Temperatures were recorded over 30 min whilst ultrasound with a frequency of 45 kHz was generated at an intensity of 0 (sham control), 10, 25 and 75 mW/cm^2. The transducer was moving at a speed of 8.6 mm/s in a circular motion.

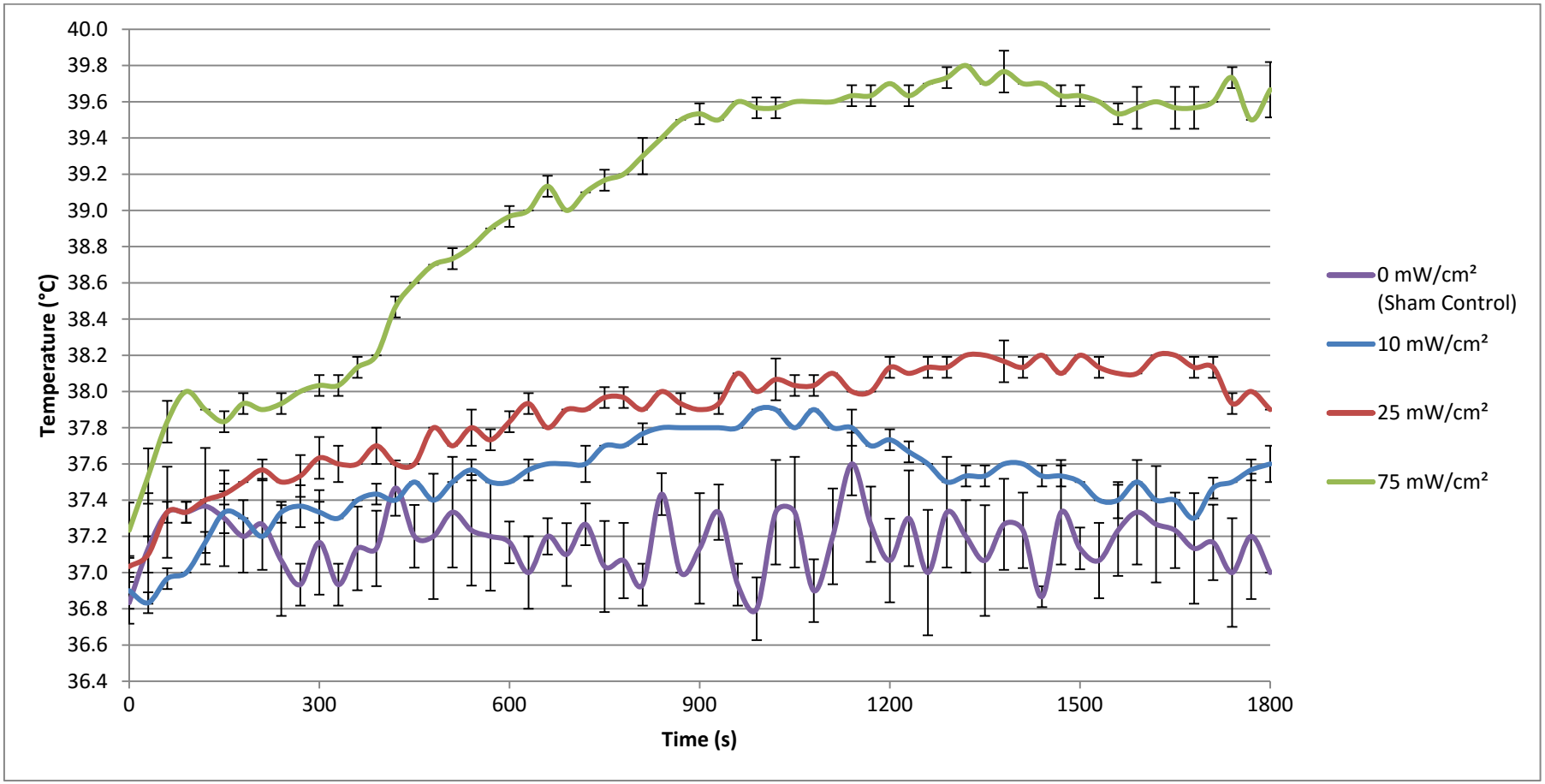

Figure 5.2 Percentage change in the number of primary HDPC and viability after the application of three episodes of 5, 10, 15 & 20 min duration of ultrasound with a frequency of 45 kHz at an intensity of 0 (sham control), 10 and 25 mW/cm^2, separated by 48 h over seven days (n=3, mean ± SD) (* P<0.05, ** P<0.01, *** P<0.001).

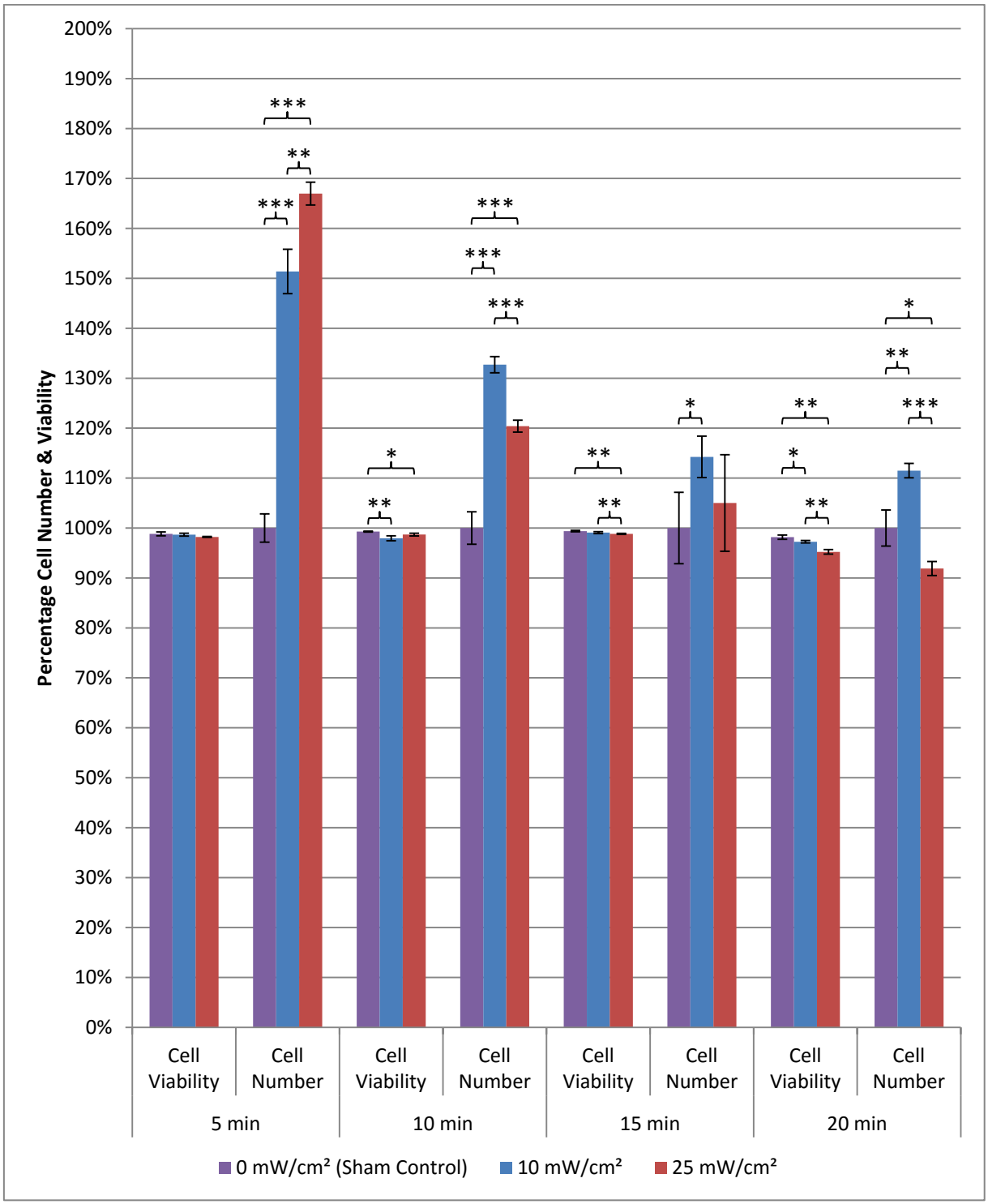

5.3 CELL NUMBER

Cell number data (Figure 5.2) from primary HDPC in culture indicates that the application of 45 kHz ultrasound at an intensity of 10 and 25 mW/cm^2 promoted cell proliferation when applied at three time points with a 5 or 10 min duration. This was a significant effect compared to sham control with both intensities ($P<0.001$) and whereas the higher intensity produced the greater increase in cell number compared to sham control (167%) in the 5 min group, the lower intensity produced the higher result (133%) in the 10 min group. This trend continued with the 15 and 20 min groups with the lower intensity ultrasound enhancing cell proliferation (114% and 112% respectively) compared to the higher intensity (105% and 92% respectively). The difference in cell number between the two intensities was significant in the 5, 10 and 20 min groups ($P<0.01$, $P<0.001$, $P<0.001$ respectively) whereas the 15 min group did not demonstrate a significant difference. This indicates a dose-dependent effect of 45 kHz ultrasound on cell proliferation of primary HDPC. Whilst the highest intensity demonstrated the greatest difference in cell number compared to sham control (167%), this effect reduced with increasing duration of ultrasound application, and in the longest (20 min) group, the cell number percentage compared to sham control was reduced by 8% ($P<0.05$). This result coupled with the reduction in cell viability (Section 5.2) demonstrates a negative effect of the higher intensity ultrasound coupled with a 20 min duration time for primary HDPC *in vitro* culture. Conversely the lower intensity promoted cell proliferation ($P<0.01$) compared to sham control in the same 20 min group indicating that this effect is dependent on the dose of ultrasound. The duration of treatment has also been shown to have an effect on the cell proliferation of primary HDPC with the shorter application groups producing a greater difference in cell number compared to sham control (Figure 5.2). This indicates that primary

HDPC *in vitro* culture produce a greater proliferative response to shorter periods (5 and 10 min) of 45 kHz ultrasound application compared to longer durations (15 and 20 min). The shortest duration (5 min) of 45 kHz ultrasound application with an intensity of 25 mW/cm^2 has been shown to be more effective at enhancing cell proliferation compared to the lower intensity ($P<0.01$).

5.4 GENE EXPRESSION BY PRIMARY HDPC

The application of multiple episodes of 45 kHz ultrasound to primary HDPC resulted in the increased expression of the DMP-1 gene. This result was statistically significant compared to sham control in all four time groups and with both the 10 and 25 mW/cm^2 intensities (Figure 5.3). Application of 45 kHz ultrasound with the lower intensity resulted in a greater statistical significance in the 5 ($P<0.01$), 10 ($P<0.001$) and 20 ($P<0.01$) min groups compared to the higher intensity, whereas the 15 min group demonstrated the same significance ($P<0.01$). The highest mean increase of DMP-1 expression was found in the 15 min group compared to sham control. This was the highest increase for both intensity groups and whereas in the other time groups where there is a statistical significance between the two intensities, favouring the lower intensity, there is none in the 15 min group. This indicated that 15 min is the optimal time duration for the repeated application of 45 kHz for the expression of DMP-1 irrespective of intensity. However, within the 15 min group there were no significant increases in the expression of the other genes investigated in this experiment. The two lower duration groups (5 and 10 min) had the most number of genes that significantly increased their expression as a response to 45 kHz ultrasound. In the 10 min group, DMP-1 and TGF-β1 expression was increased by both intensities compared to sham control (statistically significant) however whilst there was a statistically significant difference between the two intensities for the expression of DMP-1 ($P<0.01$), there was none for

Figure 5.3 Gene expression (normalised to GAPDH) as a percentage of sham control (100%) found in primary HDPC after the application of three episodes of 5, 10, 15 & 20 min duration of ultrasound with a frequency of 45 kHz at an intensity of 10 and 25 mW/cm^2, separated by 48 h over seven days (n=3 culture well cell samples, mean ± SD) (* P<0.05, ** P<0.01, *** P<0.001).

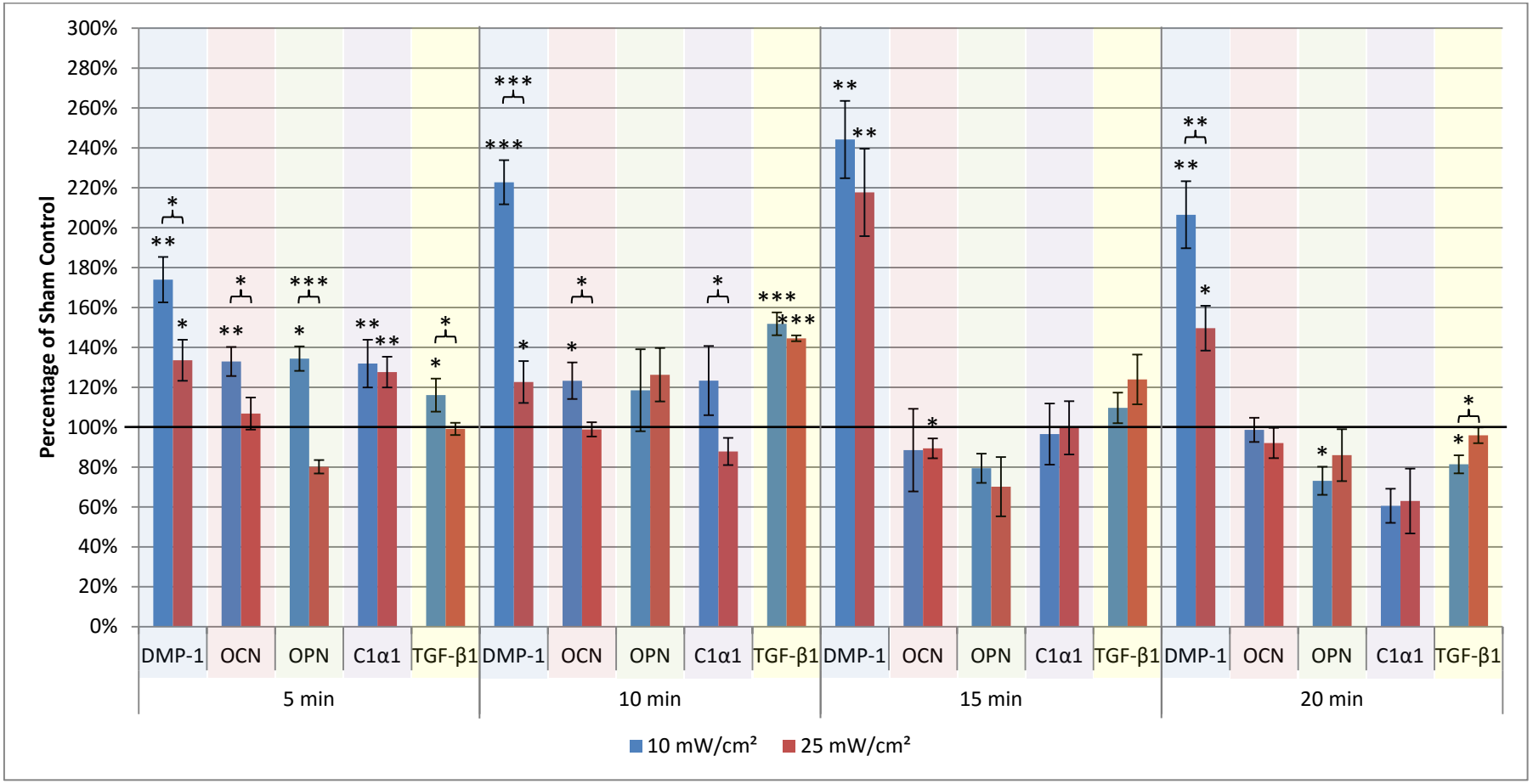

Figure 5.4 Representative gel images showing relative gene expression found in primary HDPC after the application of three episodes of 5, 10, 15 & 20 min duration of ultrasound with a frequency of 45 kHz at an intensity of 10 and 25 mW/cm^2, separated by 48 h over seven days.

	5 min			10 min			15 min			20 min		
	Sham Control	10 mW/cm^2	25 mW/cm^2	Sham Control	10 mW/cm^2	25 mW/cm^2	Sham Control	10 mW/cm^2	25 mW/cm^2	Sham Control	10 mW/cm^2	25 mW/cm^2
GAPDH	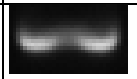	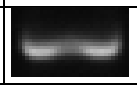	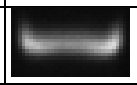	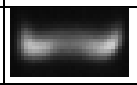	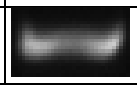	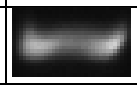	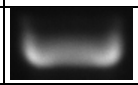	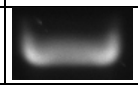	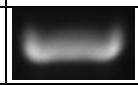	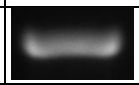	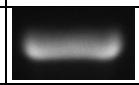	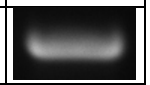
DMP-1		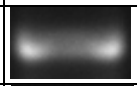	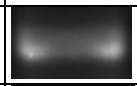		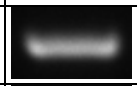	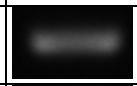		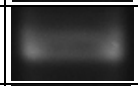	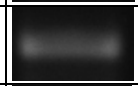			
OCN	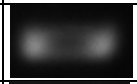	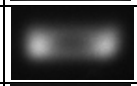	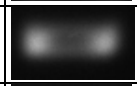		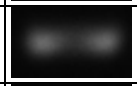			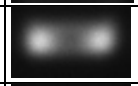	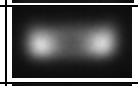	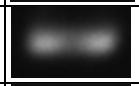	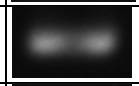	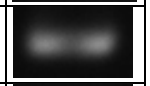
OPN		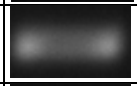										
C1α1												
TGF-β1												

TGF-β1 indicating that genes expressed in primary HDPC may not respond in the same way to different ultrasound intensities. In the same time group, OCN and C1α1 demonstrated a statistically significant ($P<0.05$) difference between the two intensities however OP did not. Whereas only four of the five genes studied in this experiment demonstrated a statistically significant increase in expression in the 10 min group responding to 10 mW/cm^2 intensity ultrasound, all five of the genes in the 5 min group demonstrated a statistically significant increase compared to sham control with the same intensity (Figure 5.3). Only DMP-1 and C1α1 showed a statistically significant increase compared to sham control with the higher intensity. The difference in gene expression was statistically significant for the DMP-1, OCN, OPN and TGF-β1 genes between the two intensities for the 5 min group ($P<0.05$, $P<0.05$, $P<0.001$, $P<0.05$). These data indicated that the lower of the two 45 kHz ultrasound intensities studied in this experiment produced a greater increase in gene expression from primary HDPC *in vitro* culture when applied for 5 or 10 min compared to longer 15 and 20 min durations. Longer durations of ultrasound application have demonstrated a negative or negligible effect on the expression of the genes studied except for DMP-1. This may indicate that DMP-1 is expressed by a greater proportion of the cells in the primary HDPC culture that are more resilient to the mechanical stimulation of 45 kHz ultrasound, such as differentiated odontoblast-like cells, compared to less robust cells, such as precursors, which may be more inclined to increase the expression of the other genes studied. Whilst the expression of DMP-1, OCN, OPN, C1α1 and TGF-β1 was detected from primary HDPC in this experiment, DSPP expression was not detected.

CHAPTER 6

MINERALISED NODULES FROM PRIMARY HDPC

It has been demonstrated that the dental pulp has the ability to repair and regenerate dentine (Smith et al. 1995). The final step of this innate process is the mineralisation of an extracellular matrix to form hard tissue which can maintain continuity of the pulp chamber to protect the pulp tissues, enabling the tooth to respond to future threats and prevent the need for complex dental treatment (Simon et al. 2014). Kilohertz ultrasound has been shown to enhance the production of mineralised calcium deposits from MDPC-23 cells *in vitro* culture and with a more pronounced effect with longer treatment times (Man et al. 2012). However, LIPUS treatment of human tooth slice organ culture *in vitro* did not show a significant effect on predentine layer thickness or gene expression of DSPP (Al-Daghreer et al. 2012, 2013). One of the research questions for the present study was to investigate whether ultrasound with a frequency of 45 kHz was able to stimulate dental pulp cells to express markers to stimulate tertiary dentinogenesis and to see if dental pulp cells responded differently to changes in the duration and intensity of ultrasound. The data reported in this section demonstrates the methods used to analyse mineralised nodules found in primary HDPC *in vitro* culture. Primary HDPCs were cultured with osteogenic media (DMEMmin) for two weeks prior to the application of three episodes of ultrasound (Section 2.5.2.2).

Day 0: HDPCs were seeded in 100 mm culture dishes as described in Section 2.5.2.1

Day 1: culture media replenished with DMEMmin

Day 3: culture media replenished

Day 5: culture media replenished

Day 7: culture media replenished

Day 9: culture media replenished

Day 11: culture media replenished

Day 13: culture media replenished

Day 14: ultrasound applied

Day 15: culture media replenished

Day 16: ultrasound applied

Day 17: culture media replenished

Day 18: ultrasound applied

Day 19: culture media replenished

Day 21: culture media replenished

Day 23: culture media replenished

Day 25: culture media replenished

Day 27: culture media replenished

Day 28: experiment halted for analysis

6.1 ALIZARIN RED S STAINING

Primary HDPC were stained with ARS dye to identify calcium rich deposits (Figure 6.1). Stained deposits visualised with phase contrast microscopy show a darker central area surrounded by a circular and well demarcated ARS stained area which appears to sit on top of the attached primary HDPC (Figure 6.2). The image at the top left of Figure 6.2 appears to show two circular areas with an obvious cleaving point at polar opposite ends. This may indicate the fusion of two mineral nodules forming in close proximity to each other, or the division of a nodule. These deposits were not detected in those cultures where ultrasound was applied (Figure 6.1B) however sham control culture dishes (Figure 6.1A) demonstrated deposits stained with ARS dye (Figure 6.1). No discernible correlation could be made between the numbers of stained nodules, which ranged from 1 to 20 per culture dish, and the

length of time for sham application of ultrasound. This indicates that 45 kHz ultrasound prevented the formation of mineral deposits irrespective of the intensity of the ultrasound beam. Whilst it has been demonstrated in this experiment that primary HDPC cultured with DMEMmin can generate calcium rich deposits *in vitro*, the amount of mineral detected with ARS dye has been nominal.

Figure 6.1 Representative ARS stained primary HDPC in culture dishes (culture surface diameter 85 mm) for sham control (A) and ultrasound (B) groups.

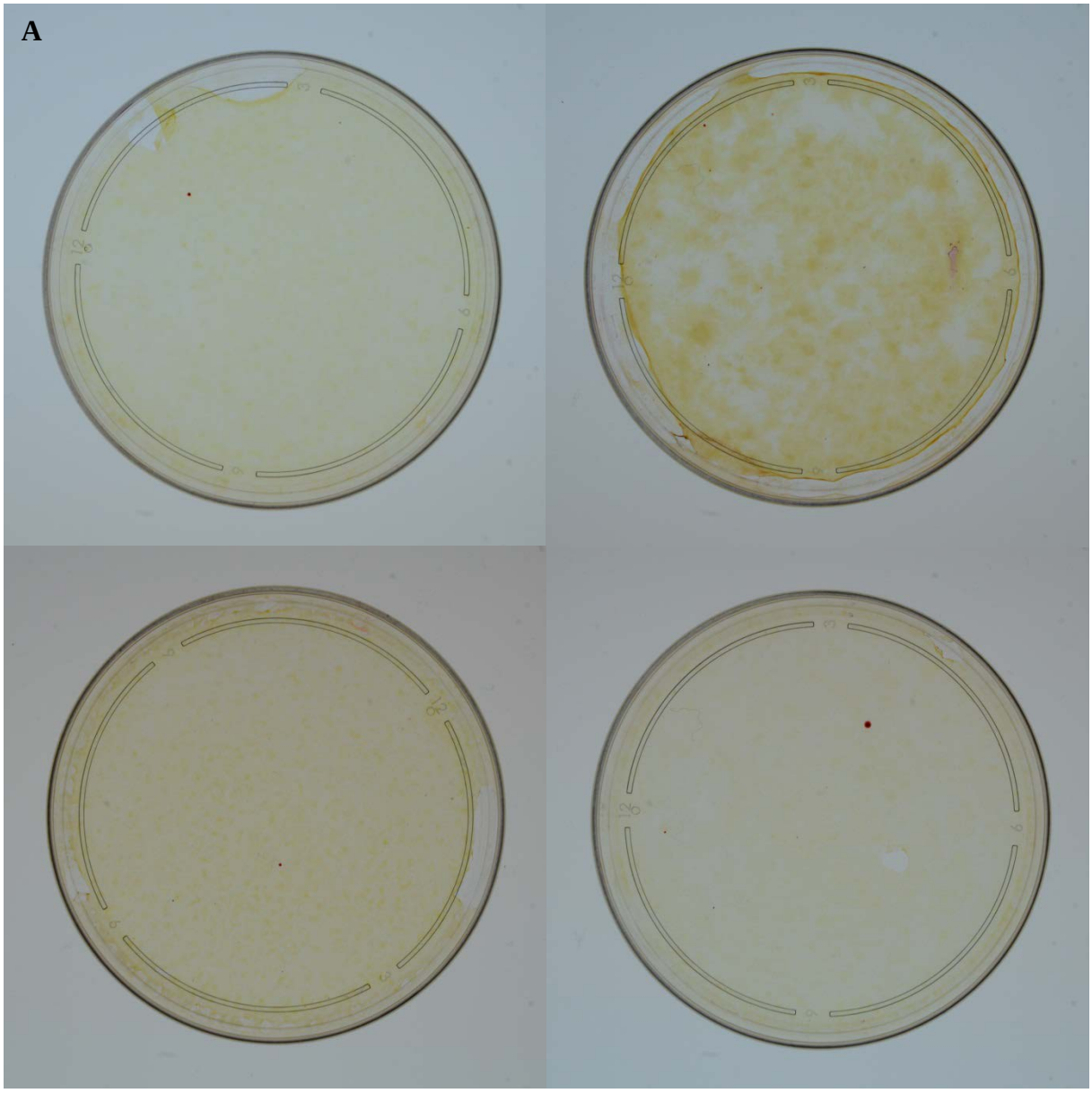

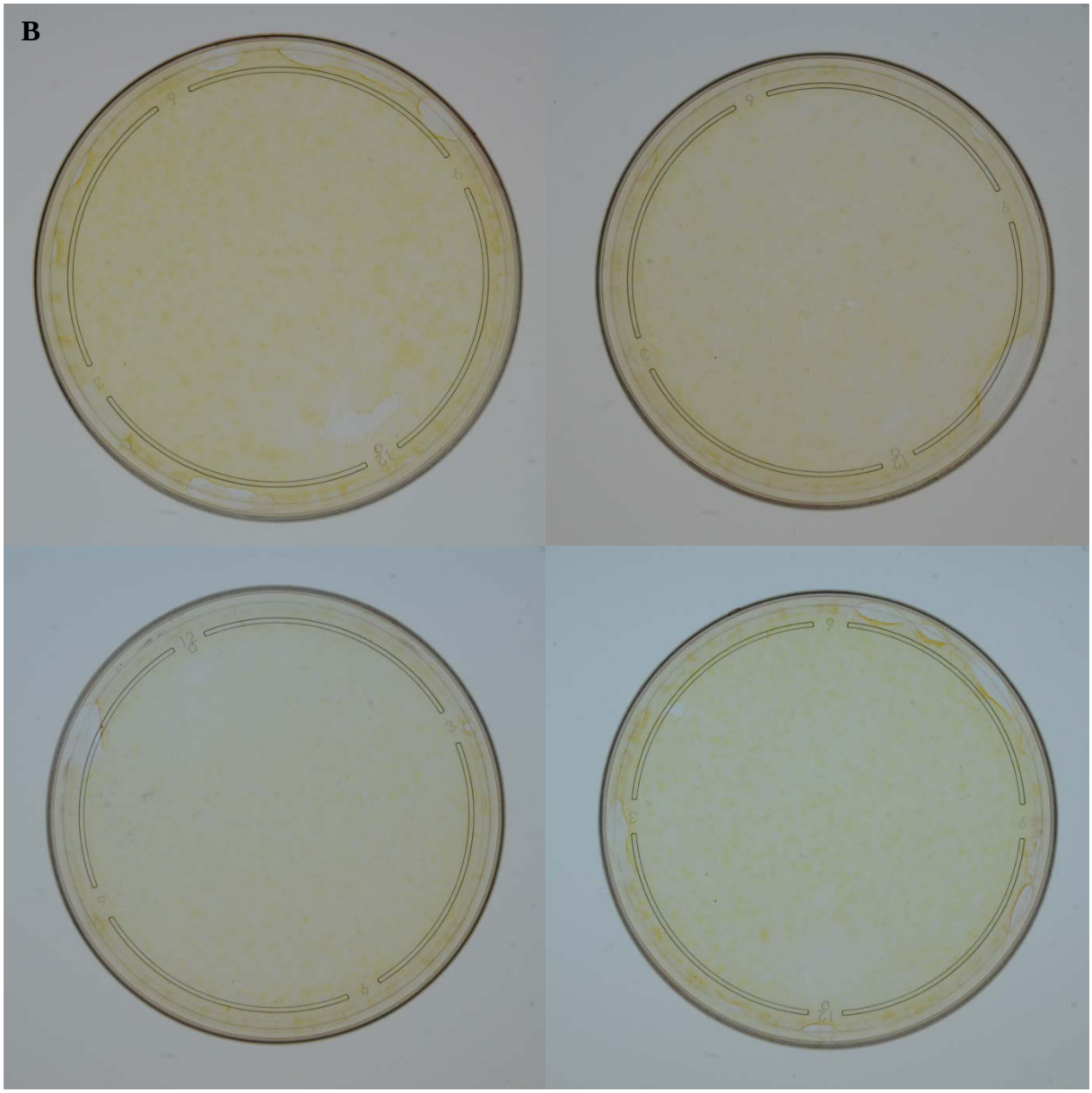
B

Figure 6.2 Phase contrast microscope images of representative ARS stained nodules in primary HDPC culture.

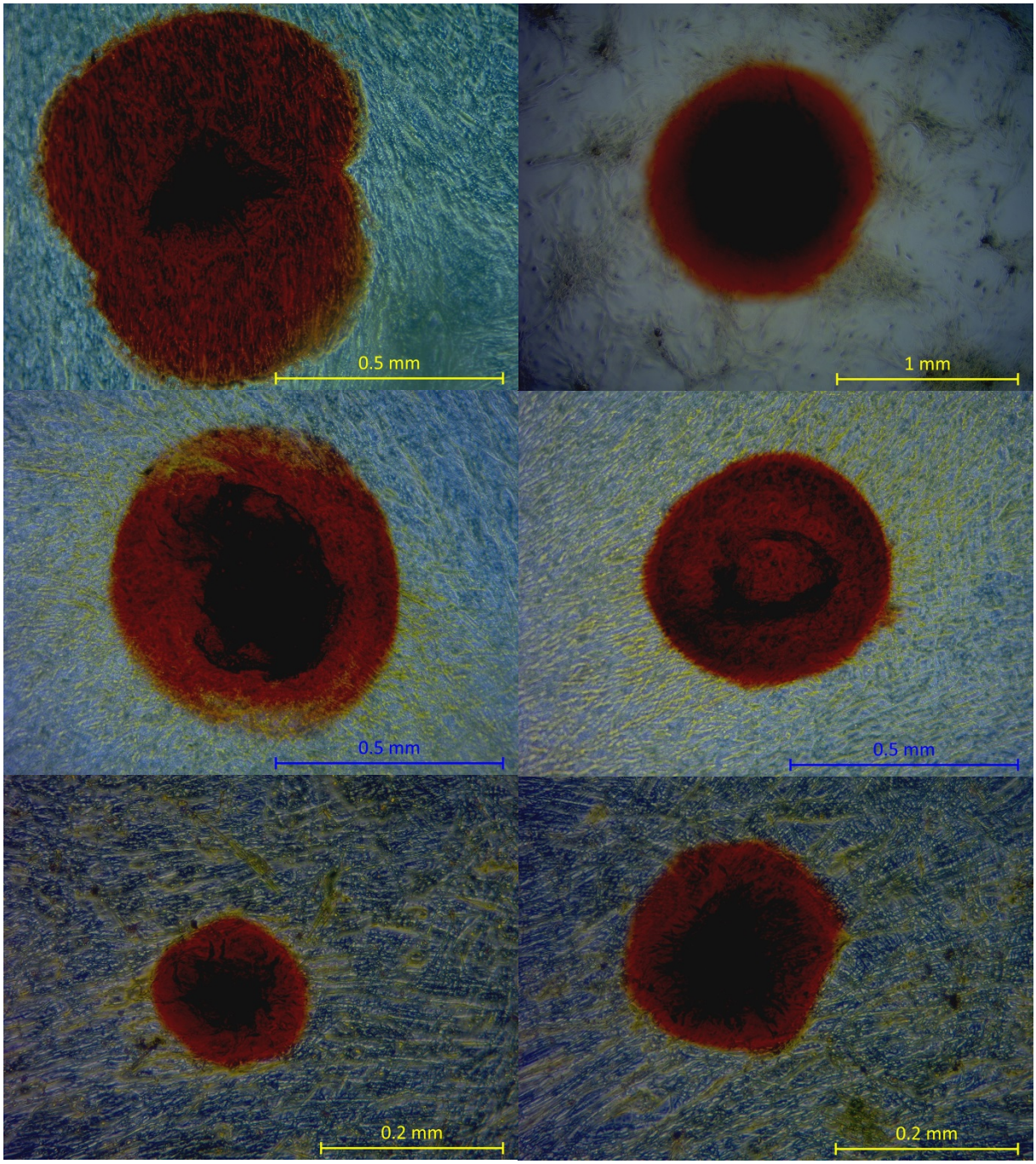

6.2 MICRO-COMPUTED TOMOGRAPHY

The radio-opacity of calcium deposits identified by ARS dye staining was investigated with µCT scanning of sections of the culture dish on which primary HDPC were cultured. Mineral deposits shown in Figure 6.3 are radio-opaque to varying degrees compared to the surrounding attached primary HDPC indicating the presence of material that attenuates x-rays. The brightness of the radio-opacity in the µCT image mirrors the darker staining found in the core of ARS stained areas. This may indicate an area of denser radio-opaque material compared to the rest of the nodule. This is demonstrated in both µCT scans shown in Figure 6.3. Nodules showing a large and darkly stained core compared to the rest of the nodule, as in Figure 6.4, may indicate a mature nodule with denser material. This can be seen in the lateral µCT view (inset Figure 6.4) showing a bright and well defined shape that is wider at the base and is raised to a plateau in the centre. The raised area in the centre of this nodule indicates that the material in the nodule accumulates on top of itself in layers and this thickness of material could obscure the light needed in a phase contrast microscope making the core of the nodule appear darker as in Figure 6.2, 6.3 and 6.4.

Figure 6.3 Micro-computed tomogram of representative ARS stained nodules in primary HDPC culture. Inset phase contrast microscope images of same nodules.

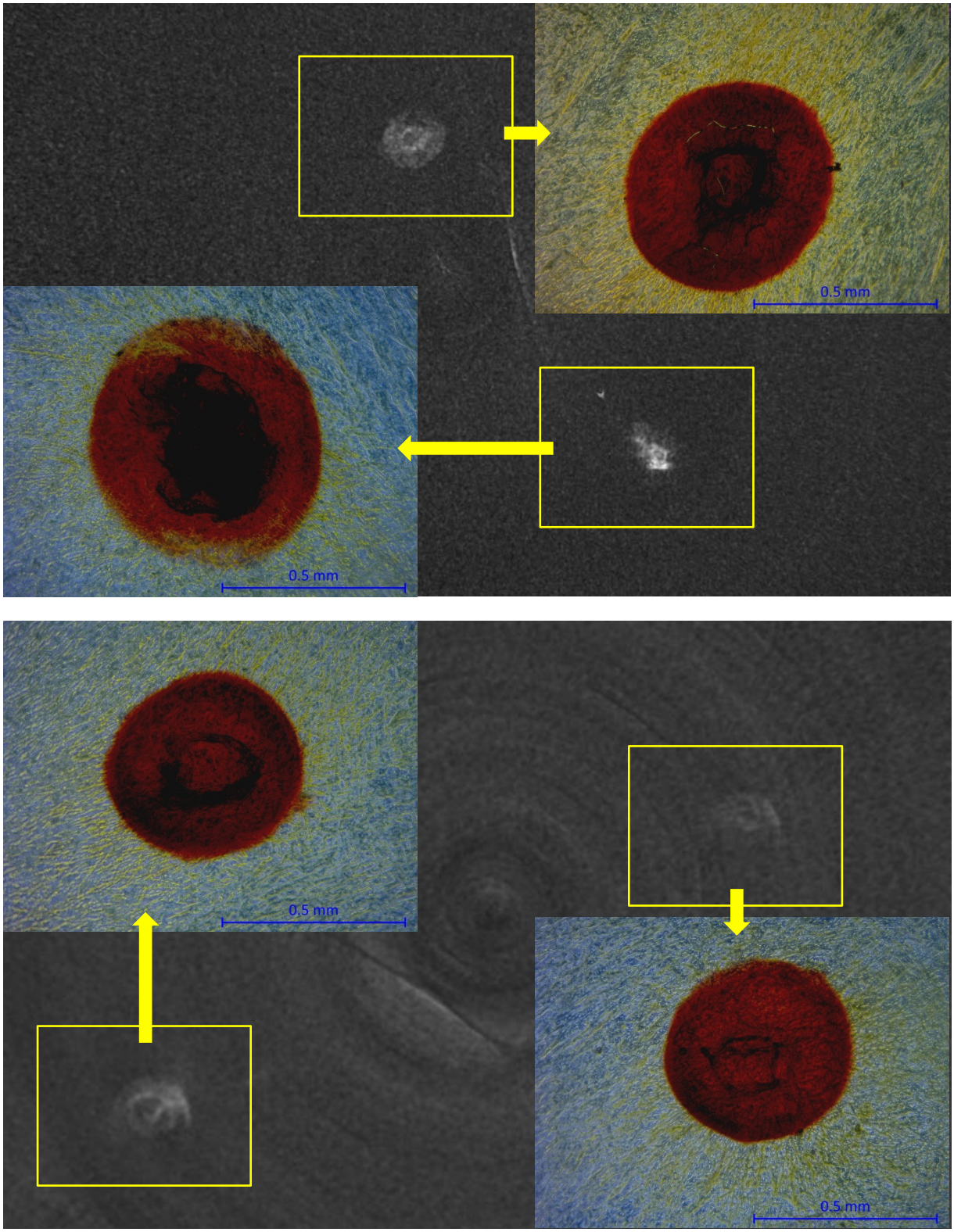

Figure 6.4 Micro-computed tomogram of ARS stained nodule in primary HDPC culture (central in image). Inset phase contrast microscope image of same nodule and µCT lateral view of radio-opacity (found centrally in large µCT image).

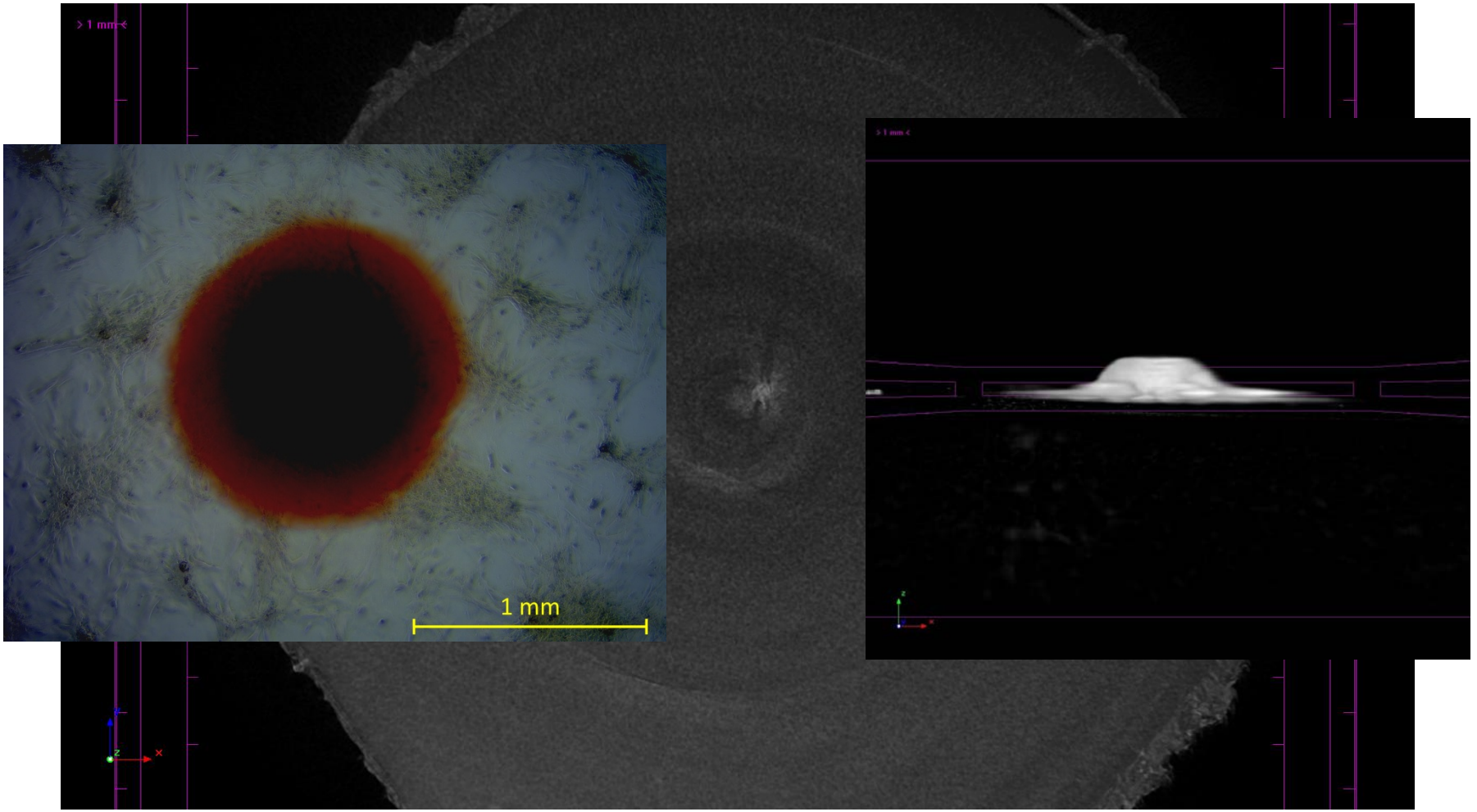

6.3 SURFACE TOPOLOGY AND ELEMENTAL ANALYSIS

Scanning electron micrographs of ARS dye stained nodules in primary HDPC culture (Figure 6.5) demonstrate a non-uniform surface topology, however, in general each nodule has a centrally raised area. In some scans, these central areas have been captured ‘intact’ as in the images top right and bottom right of Figure 6.5. However in some images (middle left of Figure 6.5) the central area of the nodule has appeared to ‘burst’ leaving a rolled margin around this area and exposing the culture plastic below. The inset phase contrast microscope images in Figure 6.5 correlate the shape of the darkly ARS dye stained central areas with the centrally raised areas found in the SEM images. These images also indicate that the lightly ARS dye stained areas are also raised compared to the attached primary HDPC grown on the culture plastic. Processing defects (‘cracking’) can also be seen, such as in images top right and bottom left of Figure 6.5, as a result of the dehydration process and vacuum generated during the SEM scan removing any moisture from within the nodule. This may indicate that the nodule requires moisture to maintain its three-dimensional shape.

Elemental analysis of different aspects of an ARS dye stained nodule in primary HDPC culture has shown that both the light and dark stained areas of a nodule demonstrate the presence of calcium whereas the area outside the ARS dye stained nodule does not show calcium (Figure 6.6 and 6.7). The identification of calcium indicates that the *in vitro* culture of primary HDPC is able to undertake the process of mineralisation. Sulphur was detected as it is included in the chemical composition of the ARS dye used in this experiment. Gold was shown to be present due to the coating placed prior to scanning and can be seen in SEM images as bright specks that can be mistaken for debris (Figure 6.8 Spectrum 3 and 5). In a

Figure 6.5 SEM images of representative ARS stained nodules in primary HDPC culture. Inset phase contrast microscope images of the same nodules.

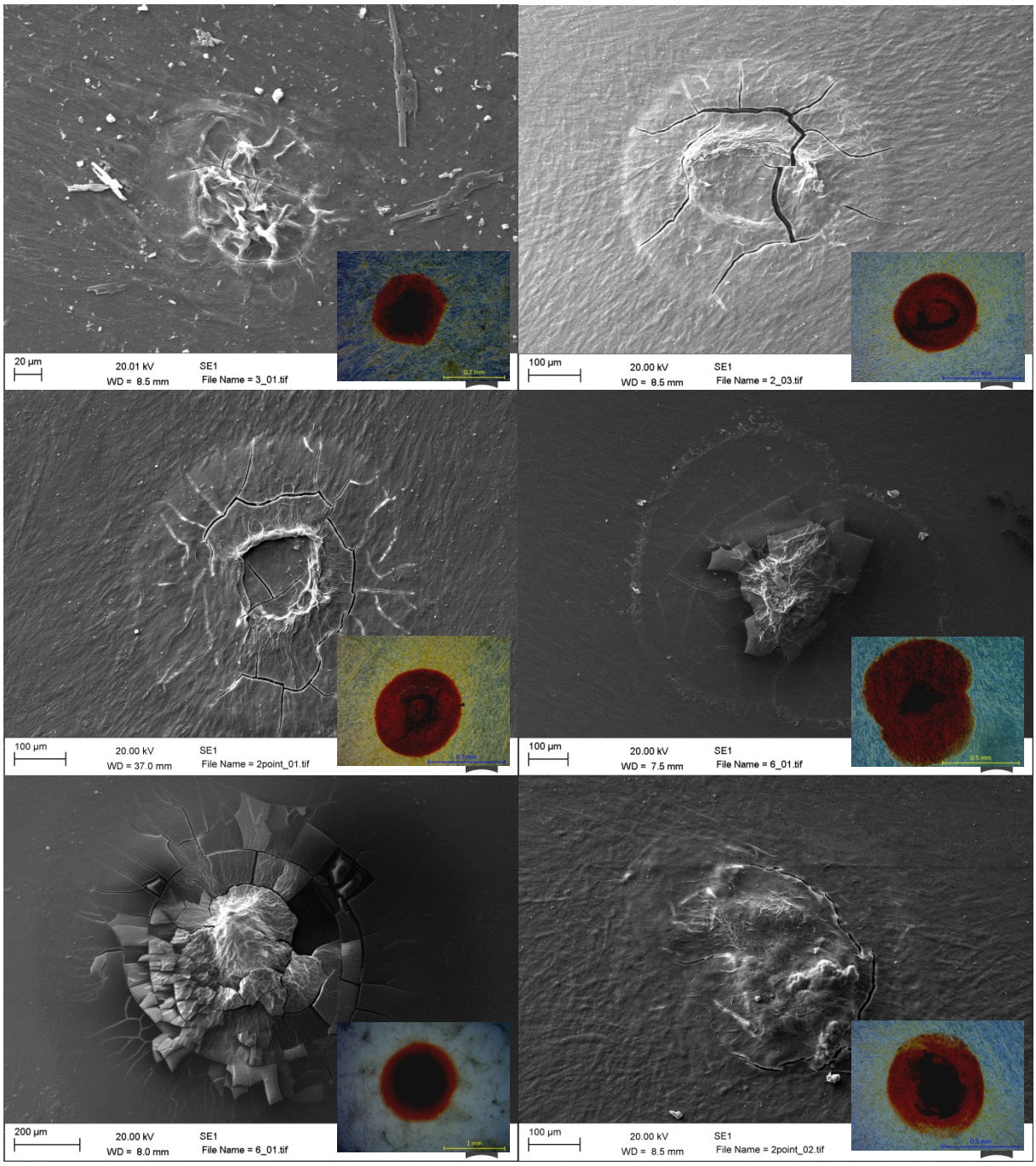

Figure 6.6 SEM images of a ‘burst’ ARS stained nodule in primary HDPC culture indicating the area of elemental analysis. Element percentage breakdown by weight is shown below each SEM image.

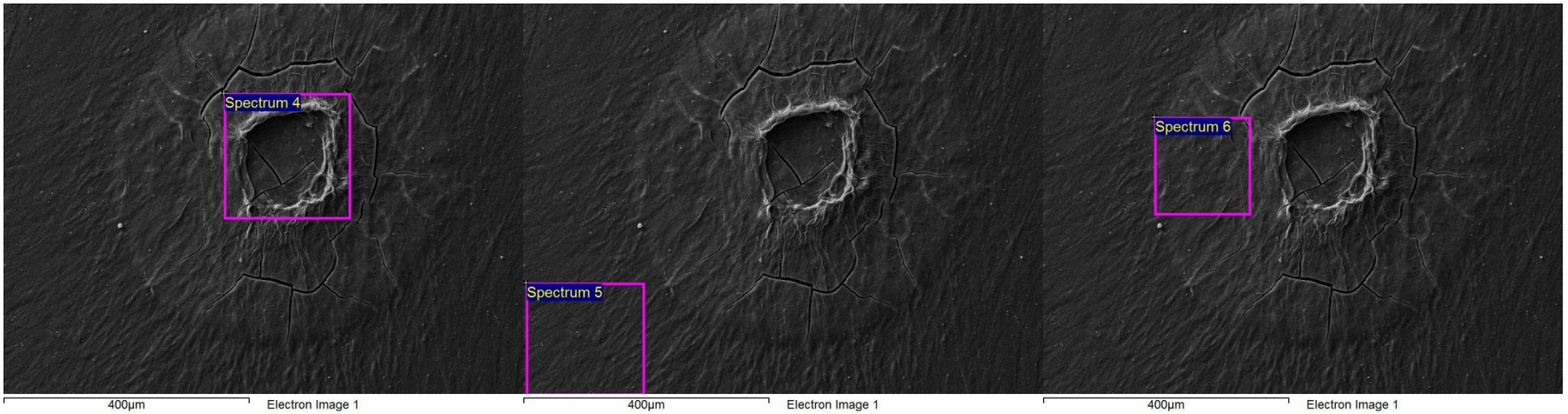

Spectrum 4

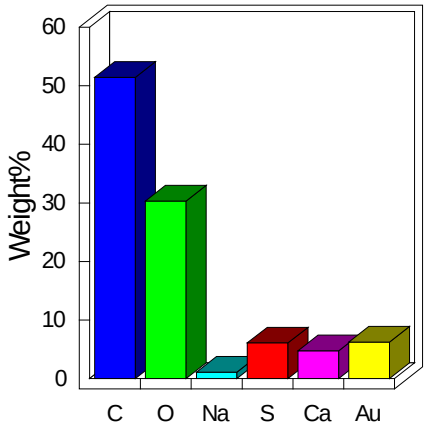

Spectrum 5

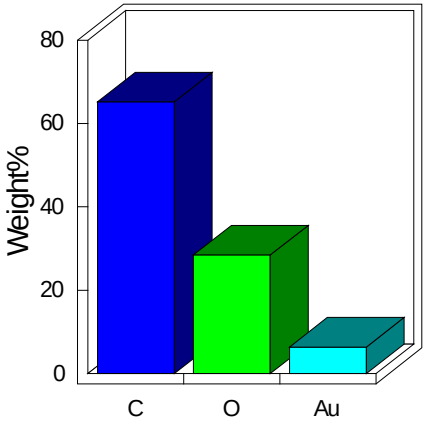

Spectrum 6

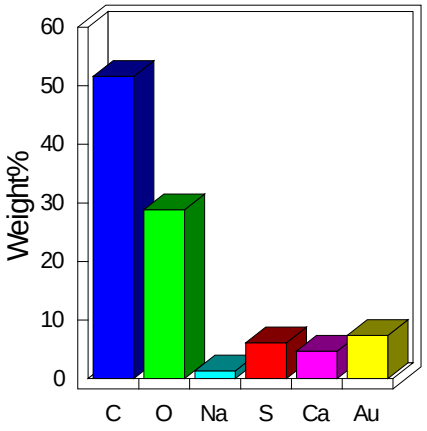

Figure 6.7 SEM images of an ‘intact’ ARS stained nodule in primary HDPC culture indicating the area of elemental analysis. Element percentage breakdown by weight is shown below each SEM image.

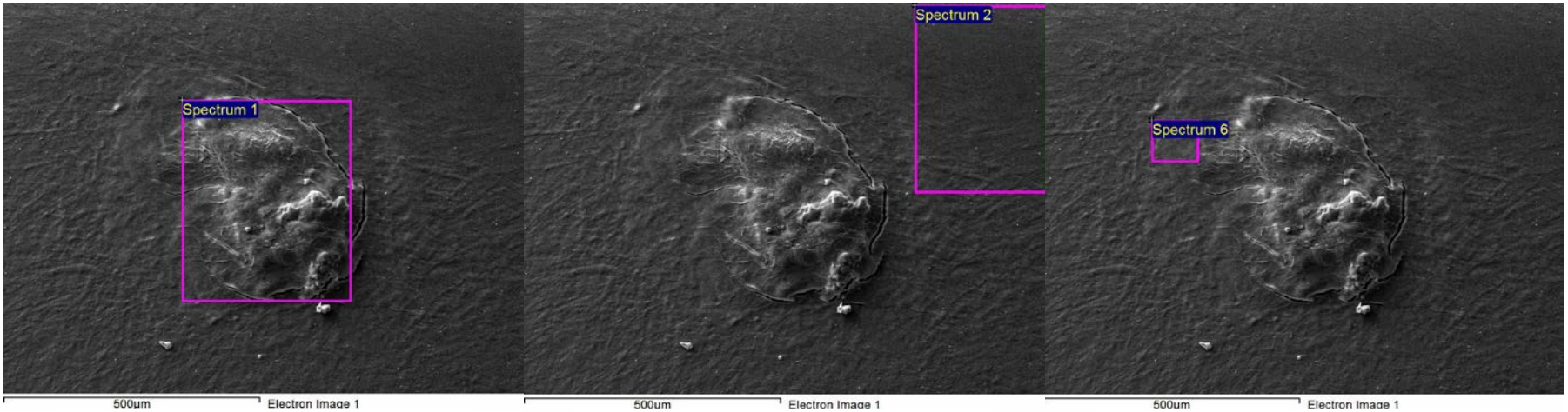

Spectrum 1 Spectrum 2 Spectrum 6

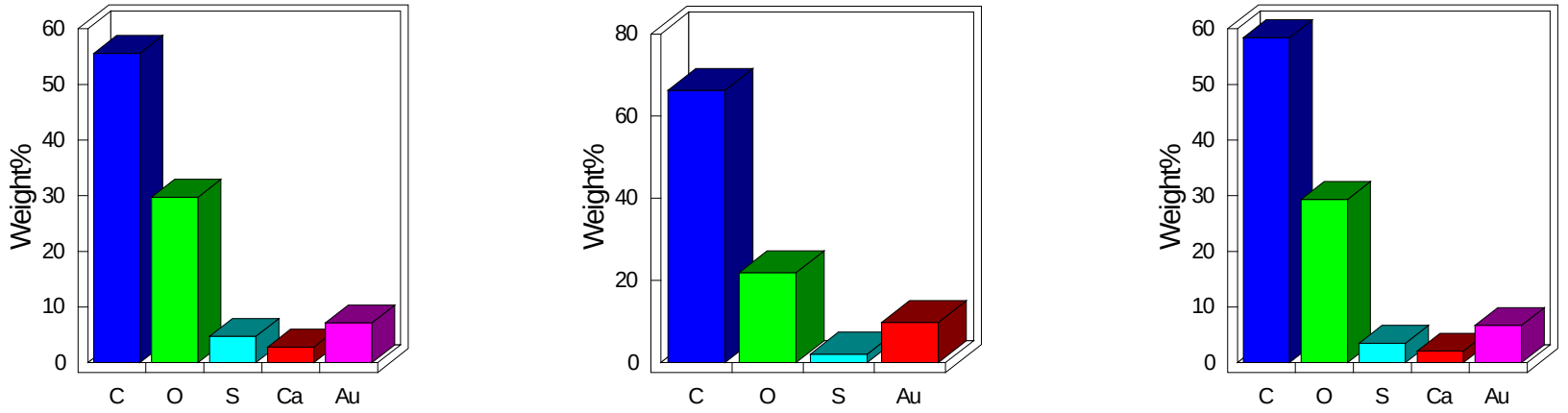

Figure 6.8 SEM images of an ‘intact’ ARS stained nodule in primary HDPC culture indicating the specific points of elemental analysis. Element percentage breakdown by weight is shown below each SEM image.

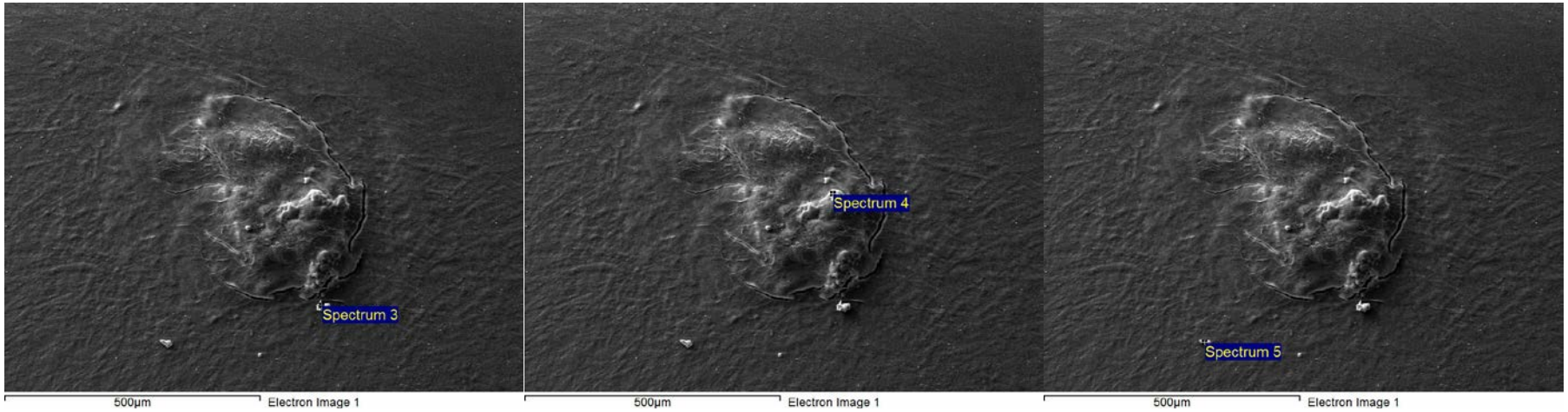

Spectrum 3

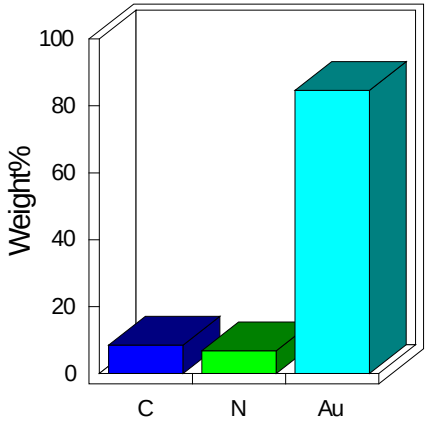

Spectrum 4

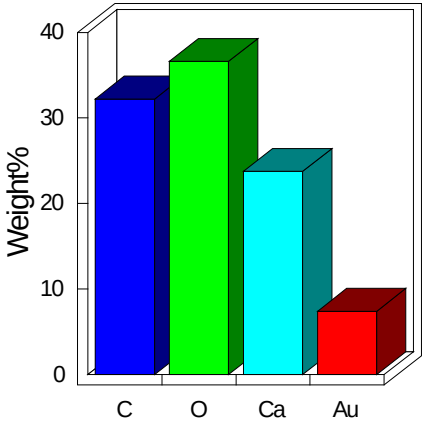

Spectrum 5

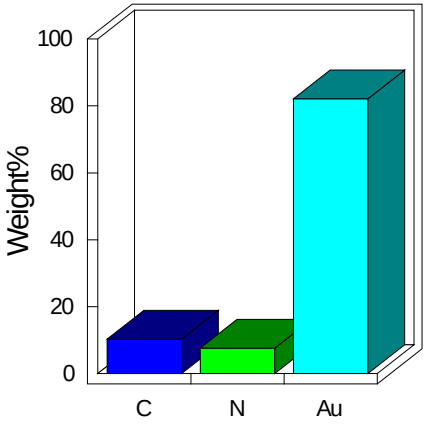

burst nodule the levels of calcium are similar in the core (Figure 6.6 Spectrum 4) as in the outer region (Figure 6.6 Spectrum 6) of the nodule whereas in an intact nodule the percentage weight of calcium is slightly higher in the core (Figure 6.7 Spectrum 1) compared to the outer region (Figure 6.7 Spectrum 6). Point analysis of specific features of an SEM scan found that certain regions within the core of a nodule demonstrated higher levels of calcium as shown by Figure 6.8 (Spectrum 4).

CHAPTER 7

DISCUSSION

7.1 APPARATUS SET UP FOR THE APPLICATION OF ULTRASOUND

The early use of kilohertz ultrasound for the treatment of disease in dentistry had been limited to the removal of plaque and calculus from the tooth surface using an oscillating scaler tip (Walmsley 1988). Later, endodontic files and cutting tips where driven ultrasonically to improve locating and cleaning root canals during endodontic treatments (Plotino et al. 2007, Walmsley et al. 1992). The novel approach of utilising kilohertz ultrasound to promote dental repair is currently in its infancy, however, early work with dental scalers has demonstrated biological effects on dental pulp cells (Scheven et al. 2009a, Scheven et al. 2007) and further work employing an ultrasound therapy transducer, designed for the treatment of soft tissue and bone fracture injuries, has reported positive biological results (Gao et al. 2016, Man et al. 2012, Patel et al. 2015). Kilohertz ultrasound has been demonstrated to transfer efficiently through the multi-layered structure of a tooth to the pulp chamber (Ghorayeb et al. 2013). This is in contrast to higher (megahertz) frequency ultrasound, such as that used in LIPUS, which is more attenuated by the hard tissues of a tooth (Section 1.1.2). The aim of this study was to investigate the potential of kilohertz ultrasound as a treatment modality for the repair of the dental pulp. This study has demonstrated that the application of kilohertz ultrasound to dental cells *in vitro* culture results in both duration and intensity dependent biological effects. Whilst it is acknowledged that the heat generated from the application of therapeutic ultrasound may provide a beneficial effect at a tissue level (Hayes et al. 2004, Robertson 2002, Speed 2001), it is difficult to separate the thermal from the non-thermal (mechanical) mechanism as the cause of these effects, hence it is largely unclear how cells respond to ultrasound generated mechanical stimulation (Baker et al. 2001, Feril and Kondo 2004, Johns 2002, Scheven et al. 2009b) albeit the therapeutic effects of pulsing megahertz ultrasound are

well documented in the literature (Claes and Willie 2007, Griffin et al. 2014, Heckman et al. 1994, Rubin et al. 2001). Eliminating significant thermal variation, as a result of ultrasound application, allows us to investigate the biological effects which arise as a result of mechanical stimulation. Controlling the conditions under which ultrasound is applied to *in vitro* cell cultures and characterising the ultrasound field is important to ensure that the experiments are reproducible and the findings are correctly reported. This study identified that six-well culture plates are not the ideal set-up to study kilohertz ultrasound treatment of cells *in vitro* culture because of the divergent nature of the ultrasound beam reaching adjacent culture wells and the attenuation of the culture plate transmitting ultrasound to distant culture wells. The study also concluded that the cell proliferation of dental cells is affected by ultrasound through non-thermal mechanical stimulation only.

The DuoSon transducer produced an ultrasound beam of ultrasound waves vibrating at a frequency between 46.74 and 47.58 kHz (Table 3.1). The resulting beam was found to have a wide pattern of dispersion inherent to the nature of kilohertz ultrasound (Figure 3.1) and as a result of the concave shape of the face of the transducer and the frequency of the ultrasound waves in the kilohertz range (Drury 2005). This specification of transducer head and frequency is reported in the manufacturer's documentation to produce a diverging beam such that ultrasound can be applied to a large area of the skin in a circular motion and thus reduce treatment times when used in the therapy for soft tissue injuries. Due to limitations with the equipment used to measure the ultrasound field from the DuoSon transducer, maximum voltage and frequency measurements further than 25 mm lateral to the central axis of the transducer could not be made. However the data and theoretical knowledge of ultrasound propagation suggests that there could be further lateral propagation. It is important to consider

that the ultrasound characterisation measurements reported in this study are in ‘free-field’ conditions and thus different to the experiment set-up where ultrasound is applied to attached cells *in vitro* culture. Analysis of the effect of ultrasound on MDPC-23 proliferation and viability in adjacent culture wells of six-well culture plates (Section 4.3 and 7.2.1) provided biological evidence to support the ultrasound characterisation measurements recorded in ‘free-field’ conditions. These findings have a major influence on future *in vitro* cell culture study designs where kilohertz ultrasound is applied to multi-well culture plates. The clinical implications of a diverging ultrasound field are also relevant in the oral cavity due to the close proximity of adjacent teeth including the root cementum and surrounding tissues such as the periodontal ligament and bone. The degree to which an ultrasound beam, with a kilohertz frequency, diverges could be controlled by the design of the transducer; however, a convex face on the ultrasound emitting surface has the potential to focus the ultrasound beam, potentially creating high intensity points within the ultrasound field (Canney et al. 2008). This technique is utilised in high-power ultrasound applications such as ablation therapy (HIFU) and lithotripsy where the goal is to necrotise tissue, however this would not be suitable for tissue repair and regeneration (Mason 2011, ter Haar 2007). A flat faced transducer would provide the least divergence. Regardless, the application of kilohertz ultrasound to individual teeth would need to be carefully modelled and optimal conditions to control and limit this field may be required. A potential innovation for the delivery of ultrasound to specific dental tissues would involve the miniaturisation of the transducer and implanting it on the tooth surface or within the tooth after caries removal. This could potentially limit the ultrasound field however the reduction in size of the transducer prevents the use of kilohertz ultrasound which requires transducers to have a diameter of a few centimetres to generate the required wavelength of ultrasound. In this case, megahertz frequency ultrasound, such as that used in

LIPUS technology, may be more appropriate however more research and development is needed in this area.

Thermal variation in cell culture medium with ultrasound treatment is a concern since a temperature rise greater than 5 °C above 37 °C may adversely affect cell viability (Blay and Price 2010) which may be a confounding factor in the interpretation of data. The observed rise in the temperature of the culture media following ultrasound application for longer than 5 mins (Figure 4.1) may be due to constructive and destructive interference (standing waves) that occur as a result of the reflection of the ultrasound beam against the culture plastic. Moreover, the increase in temperature could be due to the submerged transducer itself. Utilising a more energy efficient transducer would help to reduce the heat generated during the application of ultrasound (Richard et al. 2004, Saunders et al. 2004), however such equipment was not available for this study. Thus to avoid these pitfalls, the initial apparatus set-up was re-designed to use a single culture dish, with a larger surface area, and with the transducer in motion. The culture dish set up with the transducer in motion may have reduced the occurrence of standing waves and thus reduce heat production (Hykes et al. 1985, O'Brien 2007, Reher et al. 1999). The larger volume and increased surface area of the culture media to the continuously circulating air in the laminar flow hood may have improved the ability of this set-up to better regulate the temperature of the culture media. Indeed, this new ‘individual culture dish’ set-up with a moving transducer maintained the cultures at 37 °C (±1 °C) allowing us to analyse the mechanical effects of kilohertz ultrasound.

The method of ultrasound application used in this study, where the transducer face is submerged in the culture media of the culture well, is an acceptable method for the

application of ultrasound to cells *in vitro* culture (Hensel et al. 2011). Whilst this method of application has been described in the literature (Doan et al. 1999, Hayton et al. 2005, Ikeda et al. 2006, Man et al. 2012, Reher et al. 1997, Su et al. 2010, Takayama et al. 2007), attempts have been made to keep the transducer or culture dish in motion, as in the present study, during the application of ultrasound (Gao et al. 2016, Maddi et al. 2006). In contrast to these attempts, where existing laboratory equipment such as a rotating platform or shaker has been used, the set up described in the present study utilised a custom designed apparatus to provide a strictly controlled and reproducible movement of the transducer. Whilst the previously reported attempts may inadvertently mechanically stimulate the cells by moving the culture dish or plate in which cells are cultured, the set-up described in the present study only moves the transducer in a pre-determined circular motion within the culture dish, ensuring the transducer does not touch the culture well periphery, and moves at a speed which ensures visible waves are not generated within the culture medium which may mechanically stimulate the attached cells *in vitro* culture. The moving transducer apparatus described in this study for the application of ultrasound is the first set-up to demonstrate such a controlled movement of the transducer in a culture dish meeting the objective of this study to investigate the effects of mechanical stimulation on attached cells *in vitro* culture through ultrasound application without confounding interference of changes in culture medium temperature.

In studies where ultrasound is applied directly to cells *in vitro* culture, the distance between the transducer face and the culture surface has been reported to be between 3 and 6 mm (Chiu et al. 2008, Ikeda et al. 2006, Reher et al. 1998, Reher et al. 1997, Reher et al. 2002). In the present study, the intention was to ensure ultrasound from the far field of the ultrasound beam (Section 1.1.3) was applied to the attached cells resulting in these cells being exposed to a

more homogenous ultrasound intensity compared to that found in the near field (Section 1.1.3.1). The distance of the boundary between the near and far fields from the transducer face for the DuoSon transducer was calculated (Equation 3) to be between 7.11 and 7.23 mm using measured frequencies (Table 3.1). The maximum distance that could be achieved in the present study was 5 mm thus the attached cells were still exposed to ultrasound in the near field of the ultrasound beam. Pilot studies were carried out to increase the distance between the transducer face and the culture surface. These involved increasing the amount of culture media in each culture well such that the transducer face did not need to be lowered further into the culture well. However, this increased the risk of infection as a result of spillage when transferring the culture dishes and plates from the humidified incubator to the laminar flow hood and when placing the culture plate into the supporting apparatus.

The intensity measured and calculated directly over the central axis of the transducer can be considered the central or core intensity of the ultrasound beam. It is frequently this intensity figure that is quoted by manufacturers in their documentation or displayed on the device when in use. To ensure robustness of the data collected, ultrasonic output must be characterised prior to use for *in vitro* study (ter Haar et al. 2011b). In the present study, the manufacturer's quoted intensities aligned well with the intensities calculated without Fourier analysis (Figure 3.1); however the intensities calculated with Fourier analysis were lower. This may partially be due to the fact that the Fourier Transform calculation determines the intensity over multiple frequencies. Furthermore, as the hydrophone sensitivity is rarely constant as a function of frequency, interpolation was used to determine the correct calibration factor which caused the marginal discrepancy seen between calculated intensities with and without Fourier analysis. Another source for this discrepancy could be due to the use of null values when

completing the data set in order to obtain 2^n (n = 1, 2, …) data points which could introduce marginal errors in the Fourier coefficients, which in turn may have hindered the outcome of the original signal. Whilst the calculated intensities correlated well with the intensities quoted by the manufacturer, there is a degree of variation that can be seen by the error bars in Figure 3.1. This variation in the calculated intensity plot is as a result of the values measured in the near field of the ultrasound beam. This will result in the attached cells being affected by a non-homogenous ultrasound beam with an intensity which may be higher or lower than expected (Figure 1.2). An ultrasound transducer with a reduced BNR would result in a more homogenous ultrasound beam, reducing variation in the intensity of the field. Whilst this is a theoretical limitation of the present set-up, the variation in the measured intensity is small (Figure 3.1) and will not cause significant overlap between the three intensities used in this study. Thus based on the measurements and calculations in this study, it can be concluded with some certainty that the manufacturer's three pre-set intensities are within the parameters specified by IEC 60601-2-5:2009 and there is a distinct dosage for each of the three pre-set ultrasound intensities.

7.2 NON-THERMAL EFFECTS OF KILOHERTZ ULTRASOUND

The experiments conducted with MDPC-23 cultures in adjacent and distant culture wells of multi-well culture plates and primary HDPC cultures in the redesigned apparatus allowed the author to investigate the non-thermal effects of kilohertz ultrasound. These effects will be discussed in this section.

7.2.1 MDPC-23 IN MULTI-WELL CULTURE PLATES

It was postulated that the application of ultrasound to a culture well in a multi-well culture plate may result in the mechanical stimulation of cells in adjacent and distant culture wells of the same multi-well culture plate. This is a result of the attenuation of ultrasound waves (Section 1.1.2) by the polystyrene culture plastic of the culture plate. Whilst a significant temperature rise was recorded in the culture media of the culture well where the transducer face was submerged (corner culture well) (Figure 4.1), no thermal variation was found in adjacent and distant culture wells during the application of ultrasound (Figure 4.2). The transducer face was not submerged in these culture wells and therefore heating of the culture media from the transducer face and standing waves (Section 7.1) was not present. Furthermore, the six-well culture plate was partially submerged in an ultrasound absorbing chamber containing water which was temperature controlled by a hotplate (Section 2.5.1 and Figure 2.6) ensuring the culture media was kept at a stable temperature.

The cell viability of MDPC-23 cultured in the corner culture well was reduced compared to the adjacent and distant culture wells (Figure 4.4). This is most notable with the highest

intensity setting and coincidently resulted in the recording of a significant temperature rise (5 °C) in the culture media after 5 min of ultrasound application (Figure 4.1). This indicates that the significant increase in temperature will have played a role, possibly together with the intensity, to decrease the cell viability of MDPC-23 cultured in this culture well. Cell culture studies have reported the production of heat shock proteins with temperature rises of at least 42 °C (5 °C higher than physiological temperature) (Amano et al. 2006, Wagner et al. 1996). Heat shock proteins are an early indicator of cell damage (Nussbaum and Locke 2007) and have also been shown to increase expression under mild heat stress (less than 5 °C) to improve survival by regulating apoptosis pathways (Garrido et al. 2001, Takayama et al. 2003). This emphasises the need to keep the temperature of the culture media close to baseline to prevent cell death by apoptosis so as not to mask a positive mechanical effect of ultrasound. Since a temperature rise was not detected in the culture media of adjacent and distant culture wells, the observed biological effects to MDPC-23 cells cultured in those culture wells implied that the mechanism of action in this case is mechanical stimulation, possibly via microstreaming effects on the cell membrane transmitted through the cytoskeleton and ultimately leading to increased mitosis (Baker et al. 2001, Feril and Kondo 2004). Data collected in this study also indicates that higher intensities of kilohertz ultrasound may prove detrimental for the cell and result in irreversible cell damage and death. This has also been demonstrated with earlier dental scaler studies (Scheven et al. 2009a, Scheven et al. 2007). The data also indicates that the proximity of the cultured cells to the source of ultrasound transmission in a multi-well culture plate has an intensity dependent effect. This correlates with the theory of ultrasound transmission where vibrational energy is lost the further the ultrasound wave travels through a medium (Hykes et al. 1985). However in the case of the highest intensity setting, the distant culture well demonstrated the least reduction

in cell viability and the most significant increase in cell number ($P<0.01$) compared to the other culture wells. This finding indicates that the multi-well culture plate may have attenuated the intensity of the ultrasound beam sufficiently to a level whereby the ultrasound energy experienced by these cells in the distant culture well was in the stimulatory range for dental cells.

The biological dose-dependent response to ultrasound has not been fully established as yet but this effect has been highlighted with the MDPC-23 cell line in previous studies, initially with ultrasonic dental scalers (Scheven et al. 2009a, Scheven et al. 2007) and more recently with a calibrated ultrasound transducer (Ghorayeb et al. 2013, Man et al. 2012). The cellular effects seen in the corner culture well were much greater with the 10 and 25 mW/cm^2 intensity setting compared with the adjacent and distant culture wells. As the temperature rise with these two intensities was marginal (1.3 °C and 2.6 °C respectively), it is highly plausible that the cellular effects were brought about by non-thermal (mechanical) mechanisms. Investigating the effects of ultrasound affecting cell cultures in other (non-treated) culture wells of the same culture plate had not been reported in the literature previously to the publication of this data (Patel et al. 2015), and whilst this is a significant finding, a disadvantage of this method of investigation is the difficulty in measuring the intensity of ultrasound that affects the cells cultured in adjacent and distant culture wells. The discussion so far has focussed on work with a cell line and whilst it is acknowledged that the investigation of established and immortalised cell lines, such as MDPC-23 used in the present study, provides both a reproducible and reportable experimental basis for research, the MDPC-23 cell line is derived from murine cells and further work with primary human cells is required to better reflect human physiology.

7.2.2 PRIMARY HDPC IN CULTURE DISHES

To improve the physiological and human relevance of *in vitro* biological data, primary human dental pulp cell cultures were established enabling the author to better evaluate the response of the dental cell population of interest to ultrasound. It has been shown that the mechanical movement of teeth using orthodontic forces stimulates cell proliferation and the enhancement of gene expression, in particular angiogenic growth factors, from human dental pulp cells (Derringer et al. 1996, Dhopatkar et al. 2005). Biomechanical stimulation of cells within the dental pulp has been postulated to affect dental pulp cells and promote tooth repair and regeneration (Scheven et al. 2009b). The *in vitro* investigation of this hypothesis relied on the successful culture of HDPC from healthy human third molar teeth (Section 2.4.2). Cultures of HDPC were established via explant culture and similar observations in cell morphology and characterisation through sqRT-PCR (Section 5.4) and mineralisation studies (Section 6.1) were found to those previously reported in the literature (Couble et al. 2000, Spath et al. 2010, Stanislawski et al. 1997). Whilst it is envisaged that undifferentiated mesenchymal stem cells are present in the heterogeneous primary HDPC population, the major cell type observed in culture is of a fibroblast type. Figure 2.4 shows the outgrowth of cells from the explanted pulp tissue to be of fibroblast morphology. Also shown in Figure 2.4 are small spherical cells which have also been found previously with human dental pulp tissue explant culture (Spath et al. 2010, Stanislawski et al. 1997). Spath et al (2010) were able to separate these cells from the explant culture and found that whilst these spherical cells attached to a collagen coated surface, there was delayed attachment to a conventional culture surface. It can be postulated that these cells may be pre-odontoblastic or undifferentiated and may be identified by specific

surface antigens, as defined by the International Society for Cellular Therapy to be mesenchymal stem cells (Dominici et al. 2006).

The objective to investigate the non-thermal effects of kilohertz ultrasound on primary HDPC was achieved by culturing the cells using a moving ultrasound transducer (2.5.2). This set-up kept the culture media at a stable temperature of 37 °C (± 1 °C) (Figure 5.1). The results obtained underscored that dental pulp cell proliferation is dependent on the intensity of kilohertz ultrasound, with an adverse effect on cell number as the duration of application increased to 20 min (Figure 5.2). This extended period of time may have resulted in reduction of culture medium pH due to the ambient low carbon dioxide environment, as observed by a colour change in the culture media and this may have affected the integrity and permeability of cell membranes (Eagle 1973, Rubin 1971, Taylor 1962). As it has been postulated that ultrasound may mechanically stimulate cell membranes through acoustic microstreaming (Section 1.1.4.2.2) whereby stimulation of the cell membrane could activate intracellular signalling pathways and gene expression (Dinno et al. 1989, Johns 2002), a weakened or incapacitated cell membrane may adversely have affected the cells' response to higher levels of ultrasound, whilst a weaker intensity may result in a positive effect. This theory can explain the observation in the 20 min duration group whereby the lower intensity has increased cell proliferation whilst the higher intensity shows a reduction. It can be postulated that damaged or injured dental pulp cells, such as those exposed to dental caries *in vivo* (Section 1.2.2.1), may respond therapeutically better from a lower intensity of ultrasound compared to a higher intensity. Considering this theory when referring to *in vivo* conditions, the interplay between inflammation and regeneration in the dental pulp during healing would have a greater role than ultrasound on weaker cells. The initial inflammatory response from a threat to the pulp

may impede healing due to low grade inflammation and molecular signalling however the inflamed environment may give rise angiogenic, proliferative, chemotactic and stem cell differentiation events (Cooper et al. 2010, Goldberg et al. 2008).

Whilst pH is carefully controlled *in vivo* and the conditions experienced in this study are not transferrable, this finding demonstrates the need to control all environmental variables to ensure experiment data is accurate and relevant. The addition of the chemical buffering agent HEPES (Williamson and Cox 1968) to culture media was tested in pilot studies with primary HDPC culture however these resulted in reducing the proliferation rate of HDPCs (data not shown). Studies have demonstrated the ability to apply ultrasound to cells *in vitro* whilst inside a humidified incubator with 5% carbon dioxide in air (Al-Daghreer et al. 2012, Angle et al. 2011, Marvel et al. 2010). However, studies which have exposed cell lines to prolonged durations outside of an incubator have not reported a problem (Fung et al. 2014, Lu et al. 2009, Man et al. 2012). Indeed, cell lines may be more robust and can withstand minor changes in the acid-base balance of the culture media compared to primary cells.

The results suggested that kilohertz ultrasound has the greatest therapeutic benefit when applied for shorter periods. This is also demonstrated by the lower intensity outperforming the higher in the longer duration groups. Overall, it can be concluded that HDPC *in vitro* cultures are sensitive to the dose of kilohertz ultrasound applied and the data suggested that a shorter duration provides the most therapeutic benefit. In contrast to experiments carried out on the cell line MDPC-23, this study showed that the lower intensity enhanced proliferation more compared to the higher intensity when kilohertz ultrasound was applied for 5 min (Figure 4.3 and 4.4). Albeit the apparatus set-ups used for these experiments were different, this finding

suggests that cell lines may respond differently to kilohertz ultrasound compared with primary cell cultures.

Investigating the effects of kilohertz ultrasound on the gene expression of primary HDPC allowed us to analyse a variety of bioactive molecules involved in dental repair following ultrasound stimulation (Table 1.3). This study showed that, in particular, DMP-1 expression was significantly enhanced in all experimental ultrasound groups (Figure 5.3), whereas C1α1, OCN, OPN and TGF- β1 demonstrated significant upregulation following short term application (5 and 10 min) but not after the longer ultrasound duration of 15 and 20 min. This concurs with previous results indicating a greater effect on cell proliferation of HDPC after multiple episodes of kilohertz ultrasound with a shorter duration. The outlier in this theory is the expression of DMP-1 which peaked with both intensities in the 15 min group. DMP-1 plays a role in the mineralisation of dentine (He et al. 2003, Ye et al. 2008) and is involved in dental pulp cell differentiation into odontoblast-like cells (Chaussain et al. 2009). Studies have also shown DMP-1 expression to be enhanced in response to biomechanical loading during bone fracture healing (Gluhak-Heinrich et al. 2003, Harris et al. 2007). DSPP is expressed by differentiating odontoblasts (Sreenath et al. 2003) and together with DMP-1 is a positive regulator of mineralisation (Deshpande et al. 2011). A reduction in DSPP expression may be explained by the presence of TGF-β1 which has been shown to downregulate DSPP (Thyagarajan et al. 2001, Unterbrink et al. 2002). A lack of DSPP expression, even by sham control groups, can be expected in this study due to primary HDPCs only being in culture for one week prior to RNA extraction. HDPCs were also cultured in DMEM without osteogenic supplementation. Couble et al (2000) found that prior to mineralisation of an extracellular matrix, DSPP was weakly expressed in human dental pulp explant cultures and only enhanced

during the mineralisation process and when osteogenic supplements were added to the culture media. A second study also shows that the addition of an osteogenic supplement (dexamethasone) to the culture media gives rise to DSPP expression (Alliot-Licht et al. 2005) and a further study showed DSPP expression from HDPCs when they were cultured for 6-8 weeks in culture media with osteogenic supplementation (Buchaille et al. 2000). Indeed, the accuracy of gene expression data from current analysis methods has been questioned due to post-transcription, translation and protein degradation processes occurring after mRNA is formed (Vogel and Marcotte 2012). It is now thought that only 30% - 40% of the mRNA present in the cell may ultimately be translated into protein and protein analysis is needed to support PCR data. In conclusion, the data from this study indicates that kilohertz ultrasound is able to modify dental-repair related genes and the upregulation of DMP-1 underlines the biomechanical action of low intensity kilohertz ultrasound treatment.

The ability to form mineralised tissues *in vitro* with primary HDPC cultures reflects osteogenic differentiation from dental pulp precursor cells, reminiscent of the repair processes that occur in teeth (Section 1.2.2). Reparative dentinogenesis relies on undifferentiated ectomesenchymal pulp cells to respond to injuries to the dentine-pulp complex (Fitzgerald et al. 1990, Gronthos et al. 2002, Tziafas et al. 2000) and differentiate into odontoblast-like cells which secrete dentine (Smith et al. 1990). This study postulated that kilohertz ultrasound would stimulate the precursor cells within the dental pulp cell population, triggering the differentiation cascade, and ultimately resulting in odontoblast-like cells secreting dentine mineral.

This study demonstrated that long-term *in vitro* cultures of primary HDPC in osteogenic media are capable of producing calcium-rich (Figure 6.6, 6.7, 6.8) mineralised deposits (Figure 6.3 and 6.4) which are organised into nodules (Figure 6.1). However, in cell cultures with ultrasound application, no mineral nodules were observed. This finding is contrary to gene expression data, specifically DMP-1 (discussed earlier). Indeed, kilohertz ultrasound may trigger the differentiation of precursor cells in primary HDPC cultures, hence the enhanced gene expression findings, however, multiple episodes of mechanical stimulation delivered *in vitro* (as in the present study) may not provide the correct environment for mineral formation. This is in contrast to mineralisation studies with the MDPC-23 cell line where kilohertz ultrasound has demonstrated a positive effect on the mineralisation process (Man et al. 2012). As previously concluded, this may also be an indication that primary HDPC may be less robust than the MDPC-23 immortalised cell line. In the present study, whilst primary HDPCs were cultured for 28 days, 3 episodes of ultrasound application were delivered during the third week of culture. After the last episode of ultrasound, cultures were left for only 10 days before analysis. It has been shown that mineral production rapidly increases in primary cell cultures with osteogenic medium between day 10 and day 20 of culture (Gregory et al. 2004) and with the application of ultrasound, at least 2 weeks of culture is required before mineral is detected (Kang et al. 2013, Macione et al. 2015, Nagasaki et al. 2015, Wei et al. 2014, Yang et al. 2005). In the present study, an initial period of cell culture was required, prior to ultrasound application, to achieve confluency in the 100 mm culture dishes. Cell numbers were limited due to persistent cell culture infections during the study resulting in the loss of batches of primary HDPCs. Additionally, the limited proliferation rate of primary HDPC's when cultured in osteogenic media (pilot studies) required the initial 2 week culture period to achieve confluency. The intention of the study

was to keep primary HDPCs in culture for 5 weeks after ultrasound application however due to cell culture infection developing after the first week of ultrasound application, in total 4 weeks of culture in a 100 mm culture dish, further experiments were halted and mineral production analysed at that point. Due to the loss of primary HDPCs, multiple time points, whilst planned, could not be analysed to determine the effect of one or multiple applications of ultrasound. Cryopreservation was considered as a method to store primary HDPCs and make available sufficient numbers of these cells when required. However a study from our centre identified that cryopreservation incorporating 10% dimethyl sulfoxide (DMSO), whilst a recognised method (Chin et al. 2010, Thirumala et al. 2010), reduced cell viability and altered the expression of cell surface markers of primary cell cultures, indicating a reduction in the presence of pluripotent stem cells (Davies et al. 2014). Additionally, a reduction in the survival and number of colonies of porcine mesenchymal stem cells has been shown by cryopreservation and linked to the concentration of DMSO used (Ock and Rho 2011).

Further investigation of the ARS dye stained areas revealed insights into the mineralisation nodules formed *in vitro* cultures. A centrally raised area was detected in the majority of nodules and this is where the highest concentration of calcium could be found. Some nodules appeared to have a “burst” appearance where the central area of the nodule appeared to be fragmented or completely removed revealing the culture surface below, however this may be due to the processing of the sample prior to imaging. The imaging techniques used in the present study have demonstrated a new dimension to mineralised nodules not previously reported in the literature and future analysis with these techniques may be useful to determine the three-dimensional nature and complete quantification of mineralised nodules *in vitro* culture.

7.3 SUMMARY AND CONCLUSION

We are in an era of tissue-engineering where the concept of biotechnology is not seen as the future, it is the present. Ultrasound mediated dental repair has the potential to be the next advance in dental care. A non-invasive treatment modality that exploits the innate repair processes within the dental pulp can support the tooth to fight dental decay and infection, thus preventing the need for complex and potentially painful dental therapies. Maintaining the vitality of teeth ensures that the tooth is able to respond to future challenges and maintain a healthy mouth and patient. “Before we run, we must learn to walk” and data from this thesis demonstrates the necessity of a robust experimental set-up prior to undertaking *in vitro* investigations. The application of kilohertz ultrasound to multiple culture wells of the same multi-well culture plate has the potential to increase the amount of mechanical stimulation each culture well receives. A major finding is that investigating the effects of kilohertz ultrasound on cells cultured in multi-well culture plates is not appropriate. Furthermore, heating of the culture media may introduce a confounding factor in the overall results due to a decrease in cell viability. This study developed a method for the application of ultrasound directly to cells *in vitro* culture without registering a temperature rise in the culture medium. This allowed us to investigate the non-thermal effect of ultrasound on primary pulp cells from a human tooth. The data indicated that cell proliferation and viability were affected by the intensity of kilohertz ultrasound in a dose-dependent manner. The duration of ultrasound treatment was also shown to be related to cell viability and cell proliferation. Further work is still needed to optimise the delivery of ultrasound for *in vitro* culture and ultimately for *in vivo* application. The exact regime to best enhance dental repair still needs to be found however the novel application of kilohertz ultrasound is a step forward.

7.4 FURTHER WORK

Whilst the data collected in this study has demonstrated the effect of kilohertz ultrasound on dental pulp cells, further studies are required to establish the appropriate ultrasound treatment regime needed to stimulate ectomesenchymal stem cell differentiation to odontoblast-like cells in situ. Studies involving detailed analysis of primary HDPC *in vitro* cultures would be required to determine 'stem-ness' and would also help us to investigate conditions that may lead to any negative effect that kilohertz ultrasound may have on mineral production *in vitro*, a key indicator of the presence of odontoblast-like cells in *in vitro* cultures (Gronthos et al. 2002). Establishing organ culture of human teeth using the tooth slice model, which is a 3D-model, may better reflect the physiology of the dentine-pulp complex (Sakai et al. 2011, Sloan et al. 1998) and should be the *in vitro* method of culture for ultrasound experimentation moving forward. This method supports the interaction of different types of dental tissues and can also demonstrate the effects on periodontal and alveolar bone tissues peripheral to the tooth (El-Bialy et al. 2011).

The present study demonstrated the importance of apparatus design, equipment selection and ultrasound characterisation when undertaking *in vitro* studies involving kilohertz ultrasound, and in particular, the dosage (intensity) validation and control of temperature ensuring the data collected can be interpreted correctly. Long-term *in vitro* studies of kilohertz ultrasound are important to define effects and mechanisms which can be better conducted inside a cell culture incubator ensuring the cells are kept at their optimal conditions throughout the exposure. An ultrasound transducer with an improved efficiency in the conversion of electrical to mechanical energy would reduce the heating effect (Richard et al. 2004, Saunders

et al. 2004) allowing for the *in vitro* investigation of kilohertz ultrasound with higher intensities. A transducer with a reduced BNR would result in a more homogenous ultrasound beam with reduced 'hot spots' that would ensure more relevant data capture and reduce confounding factors.

Whilst it has been reported that kilohertz ultrasound can penetrate through hard dental tissues (Ghorayeb et al. 2013), further *in vitro* and laboratory based studies are needed to establish the intensity of the ultrasound beam once it has propagated through the anisotropic multi-layered structures of dentine and enamel (Ghorayeb et al. 2008, Hall and Girkin 2004, Singh et al. 2008). It must also be determined whether the intensity of kilohertz ultrasound transmitted to the pulp chamber is reproducible or if the quality and thickness of the dentine and enamel, which is unique to each tooth, affects the dosage of ultrasound received by the dental pulp cells.

Ultimately the aim of this work is to develop a transducer that is appropriate for the oral cavity. This new ultrasound device could be part of daily treatment in the dental clinic but may also be adapted so that it can be implanted on the tooth surface or within a shallow cavity. Further work is needed to consider miniaturisation of the transducer head that can be wirelessly controlled and supported by an equally small, but powerful, power source to drive the transducer.

LIST OF REFERENCES

About I, Murray PE, Franquin JC, Remusat M and Smith AJ (2001). The effect of cavity restoration variables on odontoblast cell numbers and dental repair. **J Dent** 29(2): 109-117

Aeinehchi M, Eslami B, Ghanbariha M and Saffar AS (2003). Mineral trioxide aggregate (MTA) and calcium hydroxide as pulp-capping agents in human teeth: a preliminary report. **Int Endod J** 36(3): 225-231

Advisory Group of Non-ionising Radiation (2010). Health effects of exposure to ultrasound and infrasound: report of the independent Advisory Group of Non-ionising Radiation. **Health Protection Agency** (RCE-14)

Ahmadi F, McLoughlin IV, Chauhan S and ter-Haar G (2012). Bio-effects and safety of low-intensity, low-frequency ultrasonic exposure. **Prog Biophys Mol Biol** 108(3): 119-138

Al-Daghreer S, Doschak M, Sloan AJ, Major PW, Heo G, Scurtescu C, Tsui YY and El-Bialy T (2012). Long term effect of low intensity pulsed ultrasound on a human tooth slice organ culture. **Arch Oral Biol** 57(6): 760-768

Al-Daghreer S, Doschak M, Sloan AJ, Major PW, Heo G, Scurtescu C, Tsui YY and El-Bialy T (2013). Short-term effect of low-intensity pulsed ultrasound on an ex-vivo 3-d tooth culture. **Ultrasound Med Biol** 39(6): 1066-1074

Al-Daghreer S, Doschak M, Sloan AJ, Major PW, Heo G, Scurtescu C, Tsui YY and El-Bialy T (2014). Effect of low-intensity pulsed ultrasound on orthodontically induced root resorption in beagle dogs. **Ultrasound Med Biol** 40(6): 1187-1196

Al-Habib M, Yu Z and Huang GT (2013). Small molecules affect human dental pulp stem cell properties via multiple signaling pathways. **Stem Cells Dev** 22(17): 2402-2413

Al-Mahrouki AA, Karshafian R, Giles A and Czarnota GJ (2012). Bioeffects of ultrasound-stimulated microbubbles on endothelial cells: gene expression changes associated with radiation enhancement in vitro. **Ultrasound Med Biol** 38(11): 1958-1969

Alliot-Licht B, Bluteau G, Magne D, Lopez-Cazaux S, Lieubeau B, Daculsi G and Guicheux J (2005). Dexamethasone stimulates differentiation of odontoblast-like cells in human dental pulp cultures. **Cell Tissue Res** 321(3): 391-400

Almushayt A, Narayanan K, Zaki AE and George A (2006). Dentin matrix protein 1 induces cytodifferentiation of dental pulp stem cells into odontoblasts. **Gene Ther** 13(7): 611-620

Amano T, Muramatsu T, Amemiya K, Kubo K and Shimono M (2006). Responses of rat pulp cells to heat stress in vitro. **J Dent Res** 85(5): 432-435

Angle SR, Sena K, Sumner DR and Virdi AS (2011). Osteogenic differentiation of rat bone marrow stromal cells by various intensities of low-intensity pulsed ultrasound. **Ultrasonics** 51(3): 281-288

Appleford MR, Oh S, Cole JA, Protivinsky J and Ong JL (2007). Ultrasound effect on osteoblast precursor cells in trabecular calcium phosphate scaffolds. **Biomaterials** 28(32): 4788-4794

Arai T, Busby W, Jr. and Clemmons DR (1996). Binding of insulin-like growth factor (IGF) I or II to IGF-binding protein-2 enables it to bind to heparin and extracellular matrix. **Endocrinology** 137(11): 4571-4575

Arany S, Koyota S and Sugiyama T (2009). Nerve growth factor promotes differentiation of odontoblast-like cells. **J Cell Biochem** 106(4): 539-545

Argadine HM, Bolander ME and Greenleaf JF (2006). Stimulation of Proteoglycan Synthesis with Low-Intensity 1 kHz Vibration. **2006 Ieee Ultrasonics Symposium, Vols 1-5, Proceedings**: 849-851

Baker KG, Robertson VJ and Duck FA (2001). A review of therapeutic ultrasound: biophysical effects. **Phys Ther** 81(7): 1351-1358

Bandow K, Nishikawa Y, Ohnishi T, Kakimoto K, Soejima K, Iwabuchi S, Kuroe K and Matsuguchi T (2007). Low-intensity pulsed ultrasound (LIPUS) induces RANKL, MCP-1, and MIP-1beta expression in osteoblasts through the angiotensin II type 1 receptor. **J Cell Physiol** 211(2): 392-398

Barnett SB, Rott HD, ter Haar GR, Ziskin MC and Maeda K (1997). The sensitivity of biological tissue to ultrasound. **Ultrasound Med Biol** 23(6): 805-812

Barnett SB, Ter Haar GR, Ziskin MC, Rott HD, Duck FA and Maeda K (2000). International recommendations and guidelines for the safe use of diagnostic ultrasound in medicine. **Ultrasound Med Biol** 26(3): 355-366

Baron C, Aubry JF, Tanter M, Meairs S and Fink M (2009). Simulation of intracranial acoustic fields in clinical trials of sonothrombolysis. **Ultrasound Med Biol** 35(7): 1148-1158

Baume LJ (1980). The biology of pulp and dentine. A historic, terminologic-taxonomic, histologic-biochemical, embryonic and clinical survey. **Monogr Oral Sci** 8: 1-220

Bergenholtz G (1981). Inflammatory response of the dental pulp to bacterial irritation. **J Endod** 7(3): 100-104

Binder A, Hodge G, Greenwood AM, Hazleman BL and Page Thomas DP (1985). Is therapeutic ultrasound effective in treating soft tissue lesions? **Br Med J (Clin Res Ed)** 290(6467): 512-514

Blay J and Price RB (2010). Cellular inhibition produced by dental curing lights is a heating artifact. **J Biomed Mater Res B Appl Biomater** 93(2): 367-374

Blodgett DW (2002). Ultrasonic assessment of tooth structure. **Laser Tissue Interaction Xiii: Photochemical, Photothermal, and Photomechanical** 4617: 284-288

Bozec A, Bakiri L, Jimenez M, Schinke T, Amling M and Wagner EF (2010). Fra-2/AP-1 controls bone formation by regulating osteoblast differentiation and collagen production. **J Cell Biol** 190(6): 1093-1106

Bradnock B, Law HT and Roscoe K (1996). A Quantitative Comparative Assessment of the Immediate Response to High Frequency Ultrasound and Low Frequency Ultrasound ('Longwave Therapy') in the Treatment of Acute Ankle Sprains. **Physiotherapy** 82(2): 78-84

Buchaille R, Couble ML, Magloire H and Bleicher F (2000). A substractive PCR-based cDNA library from human odontoblast cells: identification of novel genes expressed in tooth forming cells. **Matrix Biol** 19(5): 421-430

Butler WT, Brunn JC and Qin C (2003). Dentin extracellular matrix (ECM) proteins: comparison to bone ECM and contribution to dynamics of dentinogenesis. **Connect Tissue Res** 44 Suppl 1: 171-178

Butler WT and Ritchie H (1995). The nature and functional significance of dentin extracellular matrix proteins. **Int J Dev Biol** 39(1): 169-179

Caldwell RC, Muntz ML, Gilmore RW and Pigman W (1957). Microhardness studies of intact surface enamel. **J Dent Res** 36(5): 732-738

Callam MJ, Harper DR, Dale JJ, Ruckley CV and Prescott RJ (1987). A controlled trial of weekly ultrasound therapy in chronic leg ulceration. **Lancet (London, England)** 2(8552): 204-206

Camps J, Dejou J, Remusat M and About I (2000). Factors influencing pulpal response to cavity restorations. **Dent Mater** 16(6): 432-440

Canalis E, McCarthy TL and Centrella M (1989). Effects of platelet-derived growth factor on bone formation in vitro. **Journal of cellular physiology** 140(3): 530-537

Canney MS, Bailey MR, Crum LA, Khokhlova VA and Sapozhnikov OA (2008). Acoustic characterization of high intensity focused ultrasound fields: A combined measurement and modeling approach. **Journal of the Acoustical Society of America** 124(4): 2406-2420

Carrigan PJ, Morse DR, Furst ML and Sinai IH (1984). A scanning electron microscopic evaluation of human dentinal tubules according to age and location. **J Endod** 10(8): 359-363

Carter DR, Fyhrie DP and Whalen RT (1987). Trabecular bone density and loading history: regulation of connective tissue biology by mechanical energy. **J Biomech** 20(8): 785-794

Casagrande L, Cordeiro MM, Nor SA and Nor JE (2011). Dental pulp stem cells in regenerative dentistry. **Odontology** 99(1): 1-7

Cassidy N, Fahey M, Prime SS and Smith AJ (1997). Comparative analysis of transforming growth factor-beta isoforms 1-3 in human and rabbit dentine matrices. **Arch Oral Biol** 42(3): 219-223

Chan CW, Qin L, Lee KM, Zhang M, Cheng JC and Leung KS (2006). Low intensity pulsed ultrasound accelerated bone remodeling during consolidation stage of distraction osteogenesis. **J Orthop Res** 24(2): 263-270

Chaussain C, Eapen AS, Huet E, Floris C, Ravindran S, Hao J, Menashi S and George A (2009). MMP2-cleavage of DMP1 generates a bioactive peptide promoting differentiation of dental pulp stem/progenitor cell. **Eur Cell Mater** 18: 84-95

Cherniavsky EA, Strakha IS, Adzerikho IE and Shkumatov VM (2011). Effects of low frequency ultrasound on some properties of fibrinogen and its plasminolysis. **BMC Biochem** 12: 60

Chetverikova EP, Pashovkin TN, Rosanova NA, Sarvazyan AP and Williams AR (1985). Interaction of therapeutic ultrasound with purified enzymes in vitro. **Ultrasonics** 23(4): 183-188

Child SZ, Hartman CL, Schery LA and Carstensen EL (1990). Lung damage from exposure to pulsed ultrasound. **Ultrasound Med Biol** 16(8): 817-825

Chin SP, Poey AC, Wong CY, Chang SK, Teh W, Mohr TJ and Cheong SK (2010). Cryopreserved mesenchymal stromal cell treatment is safe and feasible for severe dilated ischemic cardiomyopathy. **Cytotherapy** 12(1): 31-37

Chiu YC, Huang TH, Fu WM, Yang RS and Tang CH (2008). Ultrasound stimulates MMP-13 expression through p38 and JNK pathway in osteoblasts. **J Cell Physiol** 215(2): 356-365

Claes L and Willie B (2007). The enhancement of bone regeneration by ultrasound. **Prog Biophys Mol Biol** 93(1-3): 384-398

Coleman AJ, Choi MJ and Saunders JE (1996). Detection of acoustic emission from cavitation in tissue during clinical extracorporeal lithotripsy. **Ultrasound Med Biol** 22(8): 1079-1087

Coleman AJ, Kodama T, Choi MJ, Adams T and Saunders JE (1995). The cavitation threshold of human tissue exposed to 0.2-MHz pulsed ultrasound: preliminary measurements based on a study of clinical lithotripsy. **Ultrasound Med Biol** 21(3): 405-417

Connor CW and Hynynen K (2004). Patterns of thermal deposition in the skull during transcranial focused ultrasound surgery. **Ieee Transactions on Biomedical Engineering** 51(10): 1693-1706

Cooper PR, Takahashi Y, Graham LW, Simon S, Imazato S and Smith AJ (2010). Inflammation-regeneration interplay in the dentine-pulp complex. **J Dent** 38(9): 687-697

Cotton WR (1974). Bacterial contamination as a factor in healing of pulp exposures. **Oral Surg Oral Med Oral Pathol** 38(3): 441-450

Couble ML, Farges JC, Bleicher F, Perrat-Mabillon B, Boudeulle M and Magloire H (2000). Odontoblast differentiation of human dental pulp cells in explant cultures. **Calcif Tissue Int** 66(2): 129-138

Cox CF, Hafez AA, Akimoto N, Otsuki M and Mills JC (1999). Biological basis for clinical success: pulp protection and the tooth-restoration interface. **Pract Periodontics Aesthet Dent** 11(7): 819-826

Cox CF, Subay RK, Ostro E, Suzuki S and Suzuki SH (1996). Tunnel defects in dentin bridges: their formation following direct pulp capping. **Oper Dent** 21(1): 4-11

Cracknell AP (1980a). The propagation of ultrasound. **Ultrasonics** N. Mott and G. R. Noakes. London, Wykeham Publication**:** 11-37.

Cracknell AP (1980b). The attenuation of ultrasound. **Ultrasonics** N. Mott and G. R. Noakes. London, Wykeham Publication**:** 38-56.

Craig JA, Bradley J, Walsh DM, Baxter GD and Allen JM (1999). Delayed onset muscle soreness: lack of effect of therapeutic ultrasound in humans. **Arch Phys Med Rehabil** 80(3): 318-323

Craig RG and Peyton FA (1958). Elastic and mechanical properties of human dentin. **J Dent Res** 37(4): 710-718

Curie J and Curie P (1880). Développement, par pression, de l'électricité polaire dans les cristaux hémièdres à faces inclinées. **Comptes Rendus de l'Académie des Science** 91: 294-295

Curie J and Curie P (1881). Contractions et dilatations produites par des tensions dans les cristaux hémièdres à faces inclinées. **Comptes Rendus de l'Académie des Science** 93: 1137-1140

Daffertshofer M, Gass A, Ringleb P, Sitzer M, Sliwka U, Els T, Sedlaczek O, Koroshetz WJ and Hennerici MG (2005). Transcranial low-frequency ultrasound-mediated thrombolysis in brain ischemia: increased risk of hemorrhage with combined ultrasound and tissue plasminogen activator: results of a phase II clinical trial. **Stroke** 36(7): 1441-1446

Davies OG, Smith AJ, Cooper PR, Shelton RM and Scheven BA (2014). The effects of cryopreservation on cells isolated from adipose, bone marrow and dental pulp tissues. **Cryobiology** 69(2): 342-347

de Vicente JC, Cabo R, Ciriaco E, Laura R, Naves FJ, Silos-Santiago I and Vega JA (2002). Impaired dental cytodifferentiation in glial cell-line derived growth factor (GDNF) deficient mice. **Ann Anat** 184(1): 85-92

del Rio A, Perez-Jimenez R, Liu R, Roca-Cusachs P, Fernandez JM and Sheetz MP (2009). Stretching single talin rod molecules activates vinculin binding. **Science** 323(5914): 638-641

den Dekker E, Molin DG, Breikers G, van Oerle R, Akkerman JW, van Eys GJ and Heemskerk JW (2001). Expression of transient receptor potential mRNA isoforms and Ca(2+) influx in differentiating human stem cells and platelets. **Biochim Biophys Acta** 1539(3): 243-255

Deng CX, Sieling F, Pan H and Cui J (2004). Ultrasound-induced cell membrane porosity. **Ultrasound Med Biol** 30(4): 519-526

Derringer KA, Jaggers DC and Linden RW (1996). Angiogenesis in human dental pulp following orthodontic tooth movement. **J Dent Res** 75(10): 1761-1766

Deshpande AS, Fang PA, Zhang X, Jayaraman T, Sfeir C and Beniash E (2011). Primary structure and phosphorylation of dentin matrix protein 1 (DMP1) and dentin phosphophoryn (DPP) uniquely determine their role in biomineralization. **Biomacromolecules** 12(8): 2933-2945

Dhopatkar AA, Sloan AJ, Rock WP, Cooper PR and Smith AJ (2005). British Orthodontic Society, Chapman Prize Winner 2003. A novel in vitro culture model to investigate the reaction of the dentine-pulp complex to orthodontic force. **J Orthod** 32(2): 122-132

Dinno MA, Dyson M, Young SR, Mortimer AJ, Hart J and Crum LA (1989). The significance of membrane changes in the safe and effective use of therapeutic and diagnostic ultrasound. **Phys Med Biol** 34(11): 1543-1552

Doan N, Reher P, Meghji S and Harris M (1999). In vitro effects of therapeutic ultrasound on cell proliferation, protein synthesis, and cytokine production by human fibroblasts, osteoblasts, and monocytes. **J Oral Maxillofac Surg** 57(4): 409-419

Dobie K, Smith G, Sloan AJ and Smith AJ (2002). Effects of alginate hydrogels and TGF-beta 1 on human dental pulp repair in vitro. **Connect Tissue Res** 43(2-3): 387-390

Dominici M, Le Blanc K, Mueller I, Slaper-Cortenbach I, Marini F, Krause D, Deans R, Keating A, Prockop D and Horwitz E (2006). Minimal criteria for defining multipotent mesenchymal stromal cells. The International Society for Cellular Therapy position statement. **Cytotherapy** 8(4): 315-317

Downing DS and Weinstein A (1986). Ultrasound Therapy of Subacromial Bursitis - a Double-Blind Trial. **Physical Therapy** 66(2): 194-199

Drury JC (2005). Ultrasonics - Part 7. The ultrasonic beam. **Insight** 47(5): 297-299

Ducy P, Starbuck M, Priemel M, Shen J, Pinero G, Geoffroy V, Amling M and Karsenty G (1999). A Cbfa1-dependent genetic pathway controls bone formation beyond embryonic development. **Genes Dev** 13(8): 1025-1036

Dyson M, Franks C and Suckling J (1976). Stimulation of healing of varicose ulcers by ultrasound. **Ultrasonics** 14(5): 232-236

Eagle H (1973). The effect of environmental pH on the growth of normal and malignant cells. **J Cell Physiol** 82(1): 1-8

Ebenbichler GR, Erdogmus CB, Resch KL, Funovics MA, Kainberger F, Barisani G, Aringer M, Nicolakis P, Wiesinger GF, Baghestanian M, Preisinger E and Fialka-Moser V (1999). Ultrasound therapy for calcific tendinitis of the shoulder. **The New England journal of medicine** 340(20): 1533-1538

Ebenbichler GR, Resch KL, Nicolakis P, Wiesinger GF, Uhl F, Ghanem AH and Fialka V (1998). Ultrasound treatment for treating the carpal tunnel syndrome: randomised "sham" controlled trial. **BMJ (Clinical research ed)** 316(7133): 731-735

Edmonds PD and Sancier KM (1983). Evidence for free radical production by ultrasonic cavitation in biological media. **Ultrasound Med Biol** 9(6): 635-639

El-Bialy T, Lam B, Aldaghreer S and Sloan AJ (2011). The effect of low intensity pulsed ultrasound in a 3D ex vivo orthodontic model. **J Dent** 39(10): 693-699

El-Bialy TH, El-Moneim Zaki A and Evans CA (2003). Effect of ultrasound on rabbit mandibular incisor formation and eruption after mandibular osteodistraction. **Am J Orthod Dentofacial Orthop** 124(4): 427-434

El Karim IA, Linden GJ, Irwin CR and Lundy FT (2009). Neuropeptides regulate expression of angiogenic growth factors in human dental pulp fibroblasts. **J Endod** 35(6): 829-833

Eriksson SV, Lundeberg T and Malm M (1991). A Placebo Controlled Trial of Ultrasound Therapy in Chronic Leg Ulceration. **Scandinavian Journal of Rehabilitation Medicine** 23(4): 211-213

Everett T, McIntosh J and Grant A (1992). Ultrasound Therapy for persistent Post-natal Perineal Pain and Dyspareunia: A randomised placebo-controlled trial. **Physiotherapy** 10(4): 263-267

Falconer J, Hayes KW and Chang RW (1992). Effect of ultrasound on mobility in osteoarthritis of the knee. A randomized clinical trial. **Arthritis care and research : the official journal of the Arthritis Health Professions Association** 5(1): 29-35

Faraco IM, Jr. and Holland R (2001). Response of the pulp of dogs to capping with mineral trioxide aggregate or a calcium hydroxide cement. **Dent Traumatol** 17(4): 163-166

Feng JQ, Huang H, Lu Y, Ye L, Xie Y, Tsutsui TW, Kunieda T, Castranio T, Scott G, Bonewald LB and Mishina Y (2003). The Dentin matrix protein 1 (Dmp1) is specifically expressed in mineralized, but not soft, tissues during development. **J Dent Res** 82(10): 776-780

Feril LB, Jr. and Kondo T (2004). Biological effects of low intensity ultrasound: the mechanism involved, and its implications on therapy and on biosafety of ultrasound. **J Radiat Res** 45(4): 479-489

Ferracane JL, Cooper PR and Smith AJ (2010). Can interaction of materials with the dentin-pulp complex contribute to dentin regeneration? **Odontology** 98(1): 2-14

Ferracane JL, Cooper PR and Smith AJ (2013). Dentin matrix component solubilization by solutions of pH relevant to self-etching dental adhesives. **J Adhes Dent** 15(5): 407-412

Ferrara N, Gerber H-P and LeCouter J (2003). The biology of VEGF and its receptors. **Nature medicine** 9(6): 669-676

Finkelman RD, Mohan S, Jennings JC, Taylor AK, Jepsen S and Baylink DJ (1990). Quantitation of growth factors IGF-I, SGF/IGF-II, and TGF-beta in human dentin. **J Bone Miner Res** 5(7): 717-723

Fisher LW, Torchia DA, Fohr B, Young MF and Fedarko NS (2001). Flexible structures of SIBLING proteins, bone sialoprotein, and osteopontin. **Biochem Biophys Res Commun** 280(2): 460-465

Fitzgerald M (1979). Cellular mechanics of dentinal bridge repair using 3H-thymidine. **J Dent Res** 58(Spec Issue D): 2198-2206

Fitzgerald M, Chiego DJ, Jr. and Heys DR (1990). Autoradiographic analysis of odontoblast replacement following pulp exposure in primate teeth. **Arch Oral Biol** 35(9): 707-715

Fung CH, Cheung WH, Pounder NM, Harrison A and Leung KS (2014). Osteocytes exposed to far field of therapeutic ultrasound promotes osteogenic cellular activities in pre-osteoblasts through soluble factors. **Ultrasonics** 54(5): 1358-1365

Gale Z, Cooper PR and Scheven BA (2011). Effects of glial cell line-derived neurotrophic factor on dental pulp cells. **J Dent Res** 90(10): 1240-1245

Gao Q, Walmsley AD, Cooper PR and Scheven BA (2016). Ultrasound Stimulation of Different Dental Stem Cell Populations: Role of Mitogen-activated Protein Kinase Signaling. **J Endod** 42(3): 425-431

Garberoglio R and Brannstrom M (1976). Scanning electron microscopic investigation of human dentinal tubules. **Arch Oral Biol** 21(6): 355-362

Garrido C, Gurbuxani S, Ravagnan L and Kroemer G (2001). Heat shock proteins: endogenous modulators of apoptotic cell death. **Biochem Biophys Res Commun** 286(3): 433-442

Geiger B, Bershadsky A, Pankov R and Yamada KM (2001). Transmembrane crosstalk between the extracellular matrix--cytoskeleton crosstalk. **Nat Rev Mol Cell Biol** 2(11): 793-805

Ghorayeb SR, Bertoncini CA and Hinders MK (2008). Ultrasonography in dentistry. **IEEE Trans Ultrason Ferroelectr Freq Control** 55(6): 1256-1266

Ghorayeb SR, Patel US, Walmsley AD and Scheven BA (2013). Biophysical characterization of low-frequency ultrasound interaction with dental pulp stem cells. **J Ther Ultrasound** 1: 12

Gleizal A, Li S, Pialat JB and Beziat JL (2006). Transcriptional expression of calvarial bone after treatment with low-intensity ultrasound: an in vitro study. **Ultrasound Med Biol** 32(10): 1569-1574

Gluhak-Heinrich J, Ye L, Bonewald LF, Feng JQ, MacDougall M, Harris SE and Pavlin D (2003). Mechanical loading stimulates dentin matrix protein 1 (DMP1) expression in osteocytes in vivo. **J Bone Miner Res** 18(5): 807-817

Goldberg HA, Warner KJ, Stillman MJ and Hunter GK (1996). Determination of the hydroxyapatite-nucleating region of bone sialoprotein. **Connect Tissue Res** 35(1-4): 385-392

Goldberg M, Farges JC, Lacerda-Pinheiro S, Six N, Jegat N, Decup F, Septier D, Carrouel F, Durand S, Chaussain-Miller C, Denbesten P, Veis A and Poliard A (2008). Inflammatory and immunological aspects of dental pulp repair. **Pharmacol Res** 58(2): 137-147

Goldberg M, Kulkarni AB, Young M and Boskey A (2011). Dentin: structure, composition and mineralization. **Front Biosci (Elite Ed)** 3: 711-735

Goldberg M and Smith AJ (2004). Cells and Extracellular Matrices of Dentin and Pulp: A Biological Basis for Repair and Tissue Engineering. **Crit Rev Oral Biol Med** 15(1): 13-27

Gorter de Vries I, Quartier E, Boute P, Wisse E and Coomans D (1987). Immunocytochemical localization of osteocalcin in developing rat teeth. **J Dent Res** 66(3): 784-790

Gosain A and DiPietro LA (2004). Aging and wound healing. **World J Surg** 28(3): 321-326

Goss SA, Frizzell LA and Dunn F (1979). Ultrasonic absorption and attenuation in mammalian tissues. **Ultrasound Med Biol** 5(2): 181-186

Graham L, Cooper PR, Cassidy N, Nor JE, Sloan AJ and Smith AJ (2006). The effect of calcium hydroxide on solubilisation of bio-active dentine matrix components. **Biomaterials** 27(14): 2865-2873

Grant A, Sleep J, McIntosh J and Ashurst H (1989). Ultrasound and pulsed electromagnetic energy treatment for perineal trauma. A randomized placebo-controlled trial. **Br J Obstet Gynaecol** 96(4): 434-439

Gregory CA, Gunn WG, Peister A and Prockop DJ (2004). An Alizarin red-based assay of mineralization by adherent cells in culture: comparison with cetylpyridinium chloride extraction. **Anal Biochem** 329(1): 77-84

Griffin XL, Parsons N, Costa ML and Metcalfe D (2014). Ultrasound and shockwave therapy for acute fractures in adults. **Cochrane Database Syst Rev** 6: CD008579

Gronthos S, Brahim J, Li W, Fisher LW, Cherman N, Boyde A, DenBesten P, Robey PG and Shi S (2002). Stem cell properties of human dental pulp stem cells. **J Dent Res** 81(8): 531-535

Gronthos S, Mankani M, Brahim J, Robey PG and Shi S (2000). Postnatal human dental pulp stem cells (DPSCs) in vitro and in vivo. **Proc Natl Acad Sci U S A** 97(25): 13625-13630

Gwinnett AJ (1992). Structure and Composition of Enamel. **Operative Dentistry**: 10-17

Haker E and Lundeberg T (1991). Pulsed ultrasound treatment in lateral epicondylalgia. **Scand J Rehabil Med** 23(3): 115-118

Hall A and Girkin JM (2004). A review of potential new diagnostic modalities for caries lesions. **J Dent Res** 83 Spec No C: C89-94

Hanks CT, Fang D, Sun Z, Edwards CA and Butler WT (1998). Dentin-specific proteins in MDPC-23 cell line. **Eur J Oral Sci** 106 Suppl 1: 260-266

Hannemann PF, Mommers EH, Schots JP, Brink PR and Poeze M (2014). The effects of low-intensity pulsed ultrasound and pulsed electromagnetic fields bone growth stimulation in acute fractures: a systematic review and meta-analysis of randomized controlled trials. **Arch Orthop Trauma Surg** 134(8): 1093-1106

Harle J, Mayia F, Olsen I and Salih V (2005). Effects of ultrasound on transforming growth factor-beta genes in bone cells. **Eur Cell Mater** 10: 70-76; discussion 76

Harle J, Salih V, Knowles JC, Mayia F and Olsen I (2001). Effects of therapeutic ultrasound on osteoblast gene expression. **J Mater Sci Mater Med** 12(10-12): 1001-1004

Harris SE, Gluhak-Heinrich J, Harris MA, Yang W, Bonewald LF, Riha D, Rowe PS, Robling AG, Turner CH, Feng JQ, McKee MD and Nicollela D (2007). DMP1 and MEPE expression are elevated in osteocytes after mechanical loading in vivo: theoretical role in controlling mineral quality in the perilacunar matrix. **J Musculoskelet Neuronal Interact** 7(4): 313-315

Hashish I, Hai HK, Harvey W, Feinmann C and Harris M (1988). Reduction of postoperative pain and swelling by ultrasound treatment: a placebo effect. **Pain** 33(3): 303-311

Hashish I, Harvey W and Harris M (1986). Anti-inflammatory effects of ultrasound therapy: evidence for a major placebo effect. **British journal of rheumatology** 25(1): 77-81

Hasson S, Mundorf R, Barnes W, Williams J and Fujii M (1990). Effect of pulsed ultrasound versus placebo on muscle soreness perception and muscular performance. **Scandinavian journal of rehabilitation medicine** 22(4): 199-205

Hayes BT, Merrick MA, Sandrey MA and Cordova ML (2004). Three-MHz Ultrasound Heats Deeper Into the Tissues Than Originally Theorized. **J Athl Train** 39(3): 230-234

Hayton MJ, Dillon JP, Glynn D, Curran JM, Gallagher JA and Buckley KA (2005). Involvement of adenosine 5'-triphosphate in ultrasound-induced fracture repair. **Ultrasound Med Biol** 31(8): 1131-1138

He G, Dahl T, Veis A and George A (2003). Dentin matrix protein 1 initiates hydroxyapatite formation in vitro. **Connect Tissue Res** 44 Suppl 1: 240-245

Heckman JD, Ryaby JP, McCabe J, Frey JJ and Kilcoyne RF (1994). Acceleration of tibial fracture-healing by non-invasive, low-intensity pulsed ultrasound. **J Bone Joint Surg Am** 76(1): 26-34

Hensel K, Mienkina MP and Schmitz G (2011). Analysis of ultrasound fields in cell culture wells for in vitro ultrasound therapy experiments. **Ultrasound Med Biol** 37(12): 2105-2115

Higgins A, Glover M, Yang Y, Bayliss S, Meads C and Lord J (2014). EXOGEN ultrasound bone healing system for long bone fractures with non-union or delayed healing: a NICE medical technology guidance. **Appl Health Econ Health Policy** 12(5): 477-484

Hill CR (1971). Ultrasonic Exposure Thresholds for Changes in Cells and Tissues. **Journal of the Acoustical Society of America** 50(1): 90-&

Hu CC, Zhang C, Qian Q and Tatum NB (1998). Reparative dentin formation in rat molars after direct pulp capping with growth factors. **J Endod** 24(11): 744-751

Huiskes R, Ruimerman R, van Lenthe GH and Janssen JD (2000). Effects of mechanical forces on maintenance and adaptation of form in trabecular bone. **Nature** 405(6787): 704-706

Hykes DL, Hedrick WR and Starchman DE (1985). **Ultrasound Physics and Intrumentation** New York, Churchill Livingstone.

Ikeda K, Takayama T, Suzuki N, Shimada K, Otsuka K and Ito K (2006). Effects of low-intensity pulsed ultrasound on the differentiation of C2C12 cells. **Life Sci** 79(20): 1936-1943

Ingber D (1991). Integrins as mechanochemical transducers. **Current opinion in cell biology** 3(5): 841-848

Ito M, Azuma Y, Ohta T and Komoriya K (2000). Effects of ultrasound and 1,25-dihydroxyvitamin D3 on growth factor secretion in co-cultures of osteoblasts and endothelial cells. **Ultrasound in medicine & biology** 26(1): 161-166

Johns LD (2002). Nonthermal Effects of Therapeutic Ultrasound: The Frequency Resonance Hypothesis. **J Athl Train** 37(3): 293-299

Jones GL, Walton R, Czernuszka J, Griffiths SL, El Haj AJ and Cartmell SH (2010). Primary human osteoblast culture on 3D porous collagen-hydroxyapatite scaffolds. **Journal of Biomedical Materials Research Part A** 94a(4): 1244-1250

Joule J (1842). On a new class of magnetic forces. **Annals of Electricity, Magnetism, and Chemistry** 8: 219-224

Kakehashi S, Stanley HR and Fitzgerald RJ (1965). The Effects of Surgical Exposures of Dental Pulps in Germ-Free and Conventional Laboratory Rats. **Oral Surg Oral Med Oral Pathol** 20: 340-349

Kang KS, Hong JM, Kang JA, Rhie JW and Cho DW (2013). Osteogenic differentiation of human adipose-derived stem cells can be accelerated by controlling the frequency of continuous ultrasound. **J Ultrasound Med** 32(8): 1461-1470

Kang KS, Lee SJ, Lee H, Moon W and Cho DW (2011). Effects of combined mechanical stimulation on the proliferation and differentiation of pre-osteoblasts. **Experimental and Molecular Medicine** 43(6): 367-373

Khambay BS and Walmsley AD (1999). Acoustic microstreaming: detection and measurement around ultrasonic scalers. **J Periodontol** 70(6): 626-631

Khan Y and Laurencin CT (2008). Fracture repair with ultrasound: clinical and cell-based evaluation. **J Bone Joint Surg Am** 90 Suppl 1: 138-144

Kilian O, Flesch I, Wenisch S, Taborski B, Jork A, Schnettler R and Jonuleit T (2004). Effects of platelet growth factors on human mesenchymal stem cells and human endothelial cells in vitro. **Eur J Med Res** 9(7): 337-344

Kline LW and Yu DC (2009). Effects of calcitonin, calcitonin gene-related peptide, human recombinant bone morphogenetic protein-2, and parathyroid hormone-related protein on endodontically treated ferret canines. **J Endod** 35(6): 866-869

Komori T, Yagi H, Nomura S, Yamaguchi A, Sasaki K, Deguchi K, Shimizu Y, Bronson RT, Gao YH, Inada M, Sato M, Okamoto R, Kitamura Y, Yoshiki S and Kishimoto T (1997). Targeted disruption of Cbfa1 results in a complete lack of bone formation owing to maturational arrest of osteoblasts. **Cell** 89(5): 755-764

Kuang Z, Yao S, Keizer DW, Wang CC, Bach LA, Forbes BE, Wallace JC and Norton RS (2006). Structure, dynamics and heparin binding of the C-terminal domain of insulin-like growth factor-binding protein-2 (IGFBP-2). **J Mol Biol** 364(4): 690-704

Kwon SM, Kim SA, Yoon JH and Ahn SG (2010). Transforming growth factor beta1-induced heat shock protein 27 activation promotes migration of mouse dental papilla-derived MDPC-23 cells. **J Endod** 36(8): 1332-1335

Lacey DL, Timms E, Tan HL, Kelley MJ, Dunstan CR, Burgess T, Elliott R, Colombero A, Elliott G, Scully S, Hsu H, Sullivan J, Hawkins N, Davy E, Capparelli C, Eli A, Qian YX, Kaufman S, Sarosi I, Shalhoub V, Senaldi G, Guo J, Delaney J and Boyle WJ (1998). Osteoprotegerin ligand is a cytokine that regulates osteoclast differentiation and activation. **Cell** 93(2): 165-176

Lagneaux L, de Meulenaer EC, Delforge A, Dejeneffe M, Massy M, Moerman C, Hannecart B, Canivet Y, Lepeltier MF and Bron D (2002). Ultrasonic low-energy treatment: a novel approach to induce apoptosis in human leukemic cells. **Exp Hematol** 30(11): 1293-1301

Laird WR and Walmsley AD (1991). Ultrasound in dentistry. Part 1--Biophysical interactions. **J Dent** 19(1): 14-17

Lea SC, Price GJ and Walmsley AD (2005). A study to determine whether cavitation occurs around dental ultrasonic scaling instruments. **Ultrason Sonochem** 12(3): 233-236

Lee DH, Lim BS, Lee YK and Yang HC (2006). Effects of hydrogen peroxide (H2O2) on alkaline phosphatase activity and matrix mineralization of odontoblast and osteoblast cell lines. **Cell Biol Toxicol** 22(1): 39-46

Lee HJ, Choi BH, Min BH, Son YS and Park SR (2006). Low-intensity ultrasound stimulation enhances chondrogenic differentiation in alginate culture of mesenchymal stem cells. **Artif Organs** 30(9): 707-715

Lees S (1971). Ultra-sonics in hard tissues. **Int Dent J** 21(4): 403-417

Lesot H, Beguekirn C, Kubler MD, Meyer JM, Smith AJ, Cassidy N, Ruch JV, Aubin JE, Goldberg M and Magloire H (1993). Experimental Induction of Odontoblast Differentiation and Stimulation during Reparative Processes. **Cells and Materials** 3(2): 201-217

Levin LG, Rudd A, Bletsa A and Reisner H (1999). Expression of IL-8 by cells of the odontoblast layer in vitro. **Eur J Oral Sci** 107(2): 131-137

Li JK, Chang WH, Lin JC, Ruaan RC, Liu HC and Sun JS (2003). Cytokine release from osteoblasts in response to ultrasound stimulation. **Biomaterials** 24(13): 2379-2385

Liedert A, Kaspar D, Blakytny R, Claes L and Ignatius A (2006). Signal transduction pathways involved in mechanotransduction in bone cells. **Biochem Biophys Res Commun** 349(1): 1-5

Louw TM, Budhiraja G, Viljoen HJ and Subramanian A (2013). Mechanotransduction of ultrasound is frequency dependent below the cavitation threshold. **Ultrasound Med Biol** 39(7): 1303-1319

Lu H, Qin L, Lee K, Cheung W, Chan K and Leung K (2009). Identification of genes responsive to low-intensity pulsed ultrasound stimulations. **Biochem Biophys Res Commun** 378(3): 569-573

Lundeberg T, Abrahamsson P and Haker E (1988). A Comparative-Study of Continuous Ultrasound, Placebo Ultrasound and Rest in Epicondylalgia. **Scandinavian Journal of Rehabilitation Medicine** 20(3): 99-101

Lundeberg T, Nordstrom F, Brodda-Jansen G, Eriksson SV, Kjartansson J and Samuelson UE (1990). Pulsed ultrasound does not improve healing of venous ulcers. **Scand J Rehabil Med** 22(4): 195-197

Macdonald KK, Cheung CY and Anseth KS (2007). Cellular delivery of TGFbeta1 promotes osteoinductive signalling for bone regeneration. **J Tissue Eng Regen Med** 1(4): 314-317

MacDougall M, Gu TT, Luan X, Simmons D and Chen J (1998). Identification of a novel isoform of mouse dentin matrix protein 1: spatial expression in mineralized tissues. **J Bone Miner Res** 13(3): 422-431

MacDougall M, Simmons D, Luan X, Nydegger J, Feng J and Gu TT (1997). Dentin phosphoprotein and dentin sialoprotein are cleavage products expressed from a single transcript coded by a gene on human chromosome 4. Dentin phosphoprotein DNA sequence determination. **J Biol Chem** 272(2): 835-842

Macione J, Long D, Nesbitt S, Wentzell S, Yokota H, Pandit V and Kotha S (2015). Stimulation of osteoblast differentiation with guided ultrasound waves. **J Ther Ultrasound** 3: 12

Maddi A, Hai H, Ong ST, Sharp L, Harris M and Meghji S (2006). Long wave ultrasound may enhance bone regeneration by altering OPG/RANKL ratio in human osteoblast-like cells. **Bone** 39(2): 283-288

Malcolm AL and ter Haar GR (1996). Ablation of tissue volumes using high intensity focused ultrasound. **Ultrasound Med Biol** 22(5): 659-669

Malizos KN, Hantes ME, Protopappas V and Papachristos A (2006). Low-intensity pulsed ultrasound for bone healing: an overview. **Injury** 37 Suppl 1: S56-62

Malone AM, Anderson CT, Tummala P, Kwon RY, Johnston TR, Stearns T and Jacobs CR (2007). Primary cilia mediate mechanosensing in bone cells by a calcium-independent mechanism. **Proc Natl Acad Sci U S A** 104(33): 13325-13330

Man J, Shelton RM, Cooper PR and Scheven BA (2012). Low-intensity low-frequency ultrasound promotes proliferation and differentiation of odontoblast-like cells. **J Endod** 38(5): 608-613

Marchioni C, Riccardi E, Spinelli S, Dell'Unto F, Grimaldi P, Bedini A, Giliberti C, Giuliani L, Palomba R and Congiu Castellano A (2009). Structural changes induced in proteins by therapeutic ultrasounds. **Ultrasonics** 49(6-7): 569-576

Marotti J, Heger S, Tinschert J, Tortamano P, Chuembou F, Radermacher K and Wolfart S (2013). Recent advances of ultrasound imaging in dentistry--a review of the literature. **Oral Surg Oral Med Oral Pathol Oral Radiol** 115(6): 819-832

Marsh PD and Bradshaw DJ (1995). Dental plaque as a biofilm. **J Ind Microbiol** 15(3): 169-175

Marvel S, Okrasinski S, Bernacki SH, Loboa E and Dayton PA (2010). The development and validation of a LIPUS system with preliminary observations of ultrasonic effects on human adult stem cells. **IEEE Trans Ultrason Ferroelectr Freq Control** 57(9): 1977-1984

Mason TJ (2011). Therapeutic ultrasound an overview. **Ultrason Sonochem** 18(4): 847-852

Matthews BG, Naot D, Callon KE, Musson DS, Locklin R, Hulley PA, Grey A and Cornish J (2014). Enhanced osteoblastogenesis in three-dimensional collagen gels. **Bonekey Rep** 3: 560

Mazzoleni G, Di Lorenzo D and Steimberg N (2009). Modelling tissues in 3D: the next future of pharmaco-toxicology and food research? **Genes and Nutrition** 4(1): 13-22

McDannold N, Zhang Y and Vykhodtseva N (2016). Nonthermal ablation in the rat brain using focused ultrasound and an ultrasound contrast agent: long-term effects. **J Neurosurg**: 1-10

Mcdiarmid T, Burns PN and Machin D (1984). Ultrasound in the Treatment of Superficial Pressure Sores - a Clinical-Trial. **Clinical Physics and Physiological Measurement** 5(1): 40-40

McLachlan JL, Smith AJ, Sloan AJ and Cooper PR (2003). Gene expression analysis in cells of the dentine-pulp complex in healthy and carious teeth. **Arch Oral Biol** 48(4): 273-283

McLachlan Z, Milne EJ, Lumley J and Walker BL (1991). Ultrasound treatment for breast engorgement: A randomised double blind trial. **The Australian journal of physiotherapy** 37(1): 23-28

Meckel AH, Griebstein WJ and Neal RJ (1965). Structure of mature human dental enamel as observed by electron microscopy. **Arch Oral Biol** 10(5): 775-783

Mehier-Humbert S, Bettinger T, Yan F and Guy RH (2005). Plasma membrane poration induced by ultrasound exposure: implication for drug delivery. **J Control Release** 104(1): 213-222

Melin M, Joffre-Romeas A, Farges JC, Couble ML, Magloire H and Bleicher F (2000). Effects of TGFbeta1 on dental pulp cells in cultured human tooth slices. **J Dent Res** 79(9): 1689-1696

Mente J, Geletneky B, Ohle M, Koch MJ, Friedrich Ding PG, Wolff D, Dreyhaupt J, Martin N, Staehle HJ and Pfefferle T (2010). Mineral trioxide aggregate or calcium hydroxide direct pulp capping: an analysis of the clinical treatment outcome. **J Endod** 36(5): 806-813

Miller DL, Smith NB, Bailey MR, Czarnota GJ, Hynynen K, Makin IR and Bioeffects Committee of the American Institute of Ultrasound in M (2012). Overview of therapeutic ultrasound applications and safety considerations. **J Ultrasound Med** 31(4): 623-634

Mitragotri S (2005). Healing sound: the use of ultrasound in drug delivery and other therapeutic applications. **Nat Rev Drug Discov** 4(3): 255-260

Mitsiadis TA and Luukko K (1995). Neurotrophins in odontogenesis. **Int J Dev Biol** 39(1): 195-202

Mitsiadis TA and Rahiotis C (2004). Parallels between tooth development and repair: conserved molecular mechanisms following carious and dental injury. **J Dent Res** 83(12): 896-902

Mjor IA (1966). Microradiography of Human Coronal Dentine. **Archives of Oral Biology** 11(2): 225-&

Mjor IA (2002). Pulp-dentin biology in restorative dentistry. Part 7: The exposed pulp. **Quintessence Int** 33(2): 113-135

Morris HL, Reed CI, Haycock JW and Reilly GC (2010). Mechanisms of fluid-flow-induced matrix production in bone tissue engineering. **Proc Inst Mech Eng H** 224(12): 1509-1521

Morse DR (1991). Age-related changes of the dental pulp complex and their relationship to systemic aging. **Oral Surg Oral Med Oral Pathol** 72(6): 721-745

Moses KD, Butler WT and Qin C (2006). Immunohistochemical study of small integrin-binding ligand, N-linked glycoproteins in reactionary dentin of rat molars at different ages. **Eur J Oral Sci** 114(3): 216-222

Moxham BJ, Webb PP, Benjamin M and Ralphs JR (1998). Changes in the cytoskeleton of cells within the periodontal ligament and dental pulp of the rat first molar tooth during ageing. **Eur J Oral Sci** 106 Suppl 1: 376-383

Mukai S, Ito H, Nakagawa Y, Akiyama H, Miyamoto M and Nakamura T (2005). Transforming growth factor-beta1 mediates the effects of low-intensity pulsed ultrasound in chondrocytes. **Ultrasound in medicine & biology** 31(12): 1713-1721

Murray PE, About I, Lumley PJ, Franquin JC, Remusat M and Smith AJ (2000). Human odontoblast cell numbers after dental injury. **Journal of Dentistry** 28(4): 277-285

Murray PE, About I, Lumley PJ, Franquin JC, Remusat M and Smith AJ (2002a). Cavity remaining dentin thickness and pulpal activity. **Am J Dent** 15(1): 41-46

Murray PE, Stanley HR, Matthews JB, Sloan AJ and Smith AJ (2002b). Age-related odontometric changes of human teeth. **Oral Surg Oral Med Oral Pathol Oral Radiol Endod** 93(4): 474-482

Murray PE, Windsor LJ, Smyth TW, Hafez AA and Cox CF (2002c). Analysis of pulpal reactions to restorative procedures, materials, pulp capping, and future therapies. **Crit Rev Oral Biol Med** 13(6): 509-520

Myers JC, Chu ML, Faro SH, Clark WJ, Prockop DJ and Ramirez F (1981). Cloning a cDNA for the pro-alpha 2 chain of human type I collagen. **Proc Natl Acad Sci U S A** 78(6): 3516-3520

Nagasaki R, Mukudai Y, Yoshizawa Y, Nagasaki M, Shiogama S, Suzuki M, Kondo S, Shintani S and Shirota T (2015). A Combination of Low-Intensity Pulsed Ultrasound and Nanohydroxyapatite Concordantly Enhances Osteogenesis of Adipose-Derived Stem Cells From Buccal Fat Pad. **Cell Med** 7(3): 123-131

Nair PN, Duncan HF, Pitt Ford TR and Luder HU (2008). Histological, ultrastructural and quantitative investigations on the response of healthy human pulps to experimental capping with mineral trioxide aggregate: a randomized controlled trial. **Int Endod J** 41(2): 128-150

Nakashima M (1994). Induction of dentin formation on canine amputated pulp by recombinant human bone morphogenetic proteins (BMP)-2 and -4. **J Dent Res** 73(9): 1515-1522

Nakashima M, Tachibana K, Iohara K, Ito M, Ishikawa M and Akamine A (2003). Induction of reparative dentin formation by ultrasound-mediated gene delivery of growth/differentiation factor 11. **Hum Gene Ther** 14(6): 591-597

Nalbandian J, Gonzales F and Sognnaes RF (1960). Sclerotic age changes in root dentin of human teeth as observed by optical, electron, and x-ray microscopy. **J Dent Res** 39: 598-607

Narita H, Itoh S, Imazato S, Yoshitake F and Ebisu S (2010). An explanation of the mineralization mechanism in osteoblasts induced by calcium hydroxide. **Acta Biomater** 6(2): 586-590

Naruse K, Miyauchi A, Itoman M and Mikuni-Takagaki Y (2003). Distinct anabolic response of osteoblast to low-intensity pulsed ultrasound. **J Bone Miner Res** 18(2): 360-369

National Institute for Health and Clinical Excellence (2010). Low-intensity pulsed ultrasound to promote fracture healing. **NICE Guideline** (IPG374)

Nosrat CA, Fried K, Ebendal T and Olson L (1998). NGF, BDNF, NT3, NT4 and GDNF in tooth development. **Eur J Oral Sci** 106 Suppl 1: 94-99

Nussbaum EL and Locke M (2007). Heat shock protein expression in rat skeletal muscle after repeated applications of pulsed and continuous ultrasound. **Arch Phys Med Rehabil** 88(6): 785-790

Nyborg WL (1982). Ultrasonic microstreaming and related phenomena. **Br J Cancer Suppl** 5: 156-160

Nykanen M (1995). Pulsed ultrasound treatment of the painful shoulder a randomized, double-blind, placebo-controlled study. **Scand J Rehabil Med** 27(2): 105-108

O'Brien WD (2007). Ultrasound-biophysics mechanisms. **Prog Biophys Mol Biol** 93(1-3): 212-255

O'Leary R, Sved AM, Davies EH, Leighton TG, Wilson M and Kieser JB (1997). The bactericidal effects of dental ultrasound on Actinobacillus actinomycetemcomitans and Porphyromonas gingivalis. An in vitro investigation. **J Clin Periodontol** 24(6): 432-439

O'Reilly MA, Huang Y and Hynynen K (2010). The impact of standing wave effects on transcranial focused ultrasound disruption of the blood-brain barrier in a rat model. **Phys Med Biol** 55(18): 5251-5267

Ock SA and Rho GJ (2011). Effect of dimethyl sulfoxide (DMSO) on cryopreservation of porcine mesenchymal stem cells (pMSCs). **Cell Transplant** 20(8): 1231-1239

Okiji T and Yoshiba K (2009). Reparative dentinogenesis induced by mineral trioxide aggregate: a review from the biological and physicochemical points of view. **Int J Dent** 2009: 464280

Otto F, Thornell AP, Crompton T, Denzel A, Gilmour KC, Rosewell IR, Stamp GW, Beddington RS, Mundlos S, Olsen BR, Selby PB and Owen MJ (1997). Cbfa1, a candidate gene for cleidocranial dysplasia syndrome, is essential for osteoblast differentiation and bone development. **Cell** 89(5): 765-771

Padilla F, Puts R, Vico L and Raum K (2014). Stimulation of bone repair with ultrasound: a review of the possible mechanic effects. **Ultrasonics** 54(5): 1125-1145

Papagerakis P, Berdal A, Mesbah M, Peuchmaur M, Malaval L, Nydegger J, Simmer J and Macdougall M (2002). Investigation of osteocalcin, osteonectin, and dentin sialophosphoprotein in developing human teeth. **Bone** 30(2): 377-385

Parvizi J, Parpura V, Greenleaf JF and Bolander ME (2002). Calcium signaling is required for ultrasound-stimulated aggrecan synthesis by rat chondrocytes. **J Orthop Res** 20(1): 51-57

Pashley DH (1996). Dynamics of the pulpo-dentin complex. **Crit Rev Oral Biol Med** 7(2): 104-133

Patel US, Ghorayeb SR, Yamashita Y, Atanda F, Walmsley AD and Scheven BA (2015). Ultrasound field characterization and bioeffects in multiwell culture plates. **J Ther Ultrasound** 3: 8

Paula-Silva FW, Ghosh A, Silva LA and Kapila YL (2009). TNF-alpha promotes an odontoblastic phenotype in dental pulp cells. **J Dent Res** 88(4): 339-344

Perry MJ, Parry LK, Burton VJ, Gheduzzi S, Beresford JN, Humphrey VF and Skerry TM (2009). Ultrasound mimics the effect of mechanical loading on bone formation in vivo on rat ulnae. **Med Eng Phys** 31(1): 42-47

Plaskett C, Tiidus PM and Livingston L (1999). Ultrasound treatment does not affect postexercise muscle strength recovery or soreness. **Journal of Sport Rehabilitation** 8(1): 1-9

Plotino G, Pameijer CH, Grande NM and Somma F (2007). Ultrasonics in endodontics: a review of the literature. **J Endod** 33(2): 81-95

Pounder NM and Harrison AJ (2008). Low intensity pulsed ultrasound for fracture healing: a review of the clinical evidence and the associated biological mechanism of action. **Ultrasonics** 48(4): 330-338

Qin C, Brunn JC, Jones J, George A, Ramachandran A, Gorski JP and Butler WT (2001). A comparative study of sialic acid-rich proteins in rat bone and dentin. **Eur J Oral Sci** 109(2): 133-141

Reher P, Doan N, Bradnock B, Meghji S and Harris M (1998). Therapeutic ultrasound for osteoradionecrosis: an in vitro comparison between 1 MHz and 45 kHz machines. **Eur J Cancer** 34(12): 1962-1968

Reher P, Doan N, Bradnock B, Meghji S and Harris M (1999). Effect of ultrasound on the production of IL-8, basic FGF and VEGF. **Cytokine** 11(6): 416-423

Reher P, Elbeshir el NI, Harvey W, Meghji S and Harris M (1997). The stimulation of bone formation in vitro by therapeutic ultrasound. **Ultrasound Med Biol** 23(8): 1251-1258

Reher P, Harris M, Whiteman M, Hai HK and Meghji S (2002). Ultrasound stimulates nitric oxide and prostaglandin E-2 production by human osteoblasts. **Bone** 31(1): 236-241

Ren L, Yang Z, Song J, Wang Z, Deng F and Li W (2013). Involvement of p38 MAPK pathway in low intensity pulsed ultrasound induced osteogenic differentiation of human periodontal ligament cells. **Ultrasonics** 53(3): 686-690

Richard C, Lee HS and Guyomar D (2004). Thermo-mechanical stress effect on 1-3 piezocomposite power transducer performance. **Ultrasonics** 42(1-9): 417-424

Ritchie HH, Pinero GJ, Hou H and Butler WT (1995). Molecular analysis of rat dentin sialoprotein. **Connect Tissue Res** 33(1-3): 73-79

Robertson VJ (2002). Dosage and treatment response in randomized clinical trials of therapeutic ultrasound. **Physical Therapy in Sport** 3(3): 124-133

Robling AG, Castillo AB and Turner CH (2006). Biomechanical and molecular regulation of bone remodeling. **Annu Rev Biomed Eng** 8: 455-498

Roche C and West J (1984). A controlled trial investigating the effect of ultrasound on venous ulcers referred from general practitioners. **Physiotherapy** 70: 475-477

Roussignol X, Currey C, Duparc F and Dujardin F (2012). Indications and results for the Exogen ultrasound system in the management of non-union: a 59-case pilot study. **Orthop Traumatol Surg Res** 98(2): 206-213

Rubin C, Bolander M, Ryaby JP and Hadjiargyrou M (2001). The use of low-intensity ultrasound to accelerate the healing of fractures. **J Bone Joint Surg Am** 83-A(2): 259-270

Rubin CT and Lanyon LE (1984). Regulation of bone formation by applied dynamic loads. **J Bone Joint Surg Am** 66(3): 397-402

Rubin H (1971). pH and population density in the regulation of animal cell multiplication. **J Cell Biol** 51(3): 686-702

Rutherford RB, Wahle J, Tucker M, Rueger D and Charette M (1993). Induction of reparative dentine formation in monkeys by recombinant human osteogenic protein-1. **Arch Oral Biol** 38(7): 571-576

Saito K, Nakatomi M, Ida-Yonemochi H, Kenmotsu S and Ohshima H (2011). The expression of GM-CSF and osteopontin in immunocompetent cells precedes the odontoblast differentiation following allogenic tooth transplantation in mice. **J Histochem Cytochem** 59(5): 518-529

Saito K, Nakatomi M, Ida-Yonemochi H and Ohshima H (2016). Osteopontin Is Essential for Type I Collagen Secretion in Reparative Dentin. **J Dent Res** 95(9): 1034-1041

Sakai VT, Cordeiro MM, Dong Z, Zhang Z, Zeitlin BD and Nor JE (2011). Tooth slice/scaffold model of dental pulp tissue engineering. **Adv Dent Res** 23(3): 325-332

Sakurakichi K, Tsuchiya H, Uehara K, Yamashiro T, Tomita K and Azuma Y (2004). Effects of timing of low-intensity pulsed ultrasound on distraction osteogenesis. **J Orthop Res** 22(2): 395-403

Sant'Anna EF, Leven RM, Virdi AS and Sumner DR (2005). Effect of low intensity pulsed ultrasound and BMP-2 on rat bone marrow stromal cell gene expression. **J Orthop Res** 23(3): 646-652

Saqqur M, Tsivgoulis G, Nicoli F, Skoloudik D, Sharma VK, Larrue V, Eggers J, Perren F, Charalampidis P, Storie D, Shuaib A and Alexandrov AV (2014). The role of sonolysis and

sonothrombolysis in acute ischemic stroke: a systematic review and meta-analysis of randomized controlled trials and case-control studies. **J Neuroimaging** 24(3): 209-220

Sarvazyan AP, Rudenko OV and Nyborg WL (2010). Biomedical applications of radiation force of ultrasound: historical roots and physical basis. **Ultrasound Med Biol** 36(9): 1379-1394

Saunders O, Clift S and Duck F (2004). Ultrasound transducer self heating: development of 3-D finite-element models. **AMUM 2004: Advanced Metrology for Ultrasound in Medicine 2004** 1: 72-77

Sawada T, Ishikawa T, Shintani S and Yanagisawa T (2012). Ultrastructural immunolocalization of dentin matrix protein 1 on Sharpey's fibers in monkey tooth cementum. **Biotech Histochem** 87(5): 360-365

Scheven BA, Man J, Millard JL, Cooper PR, Lea SC, Walmsley AD and Smith AJ (2009a). VEGF and odontoblast-like cells: stimulation by low frequency ultrasound. **Arch Oral Biol** 54(2): 185-191

Scheven BA, Millard JL, Cooper PR, Lea SC, Walmsley AD and Smith AJ (2007). Short-term in vitro effects of low frequency ultrasound on odontoblast-like cells. **Ultrasound Med Biol** 33(9): 1475-1482

Scheven BA, Shelton RM, Cooper PR, Walmsley AD and Smith AJ (2009b). Therapeutic ultrasound for dental tissue repair. **Med Hypotheses** 73(4): 591-593

Schumann D, Kujat R, Zellner J, Angele MK, Nerlich M, Mayr E and Angele P (2006). Treatment of human mesenchymal stem cells with pulsed low intensity ultrasound enhances the chondrogenic phenotype in vitro. **Biorheology** 43(3-4): 431-443

Seltzer S, Bender IB and Ziontz M (1963). The Dynamics of Pulp Inflammation: Correlations between Diagnostic Data and Actual Histologic Findings in the Pulp. **Oral Surg Oral Med Oral Pathol** 16: 969-977

Senawongse P, Otsuki M, Tagami J and Mjor IA (2008). Morphological characterization and permeability of attrited human dentine. **Arch Oral Biol** 53(1): 14-19

Simon SR, Tomson PL and Berdal A (2014). Regenerative endodontics: regeneration or repair? **J Endod** 40(4 Suppl): S70-75

Singh RS, Culjat MO, Grundfest WS, Brown ER and White SN (2008). Tissue mimicking materials for dental ultrasound. **J Acoust Soc Am** 123(4): EL39-44

Six N, Decup F, Lasfargues JJ, Salih E and Goldberg M (2002). Osteogenic proteins (bone sialoprotein and bone morphogenetic protein-7) and dental pulp mineralization. **J Mater Sci Mater Med** 13(2): 225-232

Sloan AJ, Moseley R, Dobie K, Waddington RJ and Smith AJ (2002). TGF-beta latency-associated peptides (LAPs) in human dentin matrix and pulp. **Connect Tissue Res** 43(2-3): 381-386

Sloan AJ, Shelton RM, Hann AC, Moxham BJ and Smith AJ (1998). An in vitro approach for the study of dentinogenesis by organ culture of the dentine-pulp complex from rat incisor teeth. **Arch Oral Biol** 43(6): 421-430

Sloan AJ and Smith AJ (1999). Stimulation of the dentine-pulp complex of rat incisor teeth by transforming growth factor-beta isoforms 1-3 in vitro. **Arch Oral Biol** 44(2): 149-156

Sloan AJ and Smith AJ (2007). Stem cells and the dental pulp: potential roles in dentine regeneration and repair. **Oral Dis** 13(2): 151-157

Sloan AJ and Waddington RJ (2009). Dental pulp stem cells: what, where, how? **Int J Paediatr Dent** 19(1): 61-70

Smith AJ (2002). Pulpal responses to caries and dental repair. **Caries Res** 36(4): 223-232

Smith AJ, Cassidy N, Perry H, Begue-Kirn C, Ruch JV and Lesot H (1995). Reactionary dentinogenesis. **Int J Dev Biol** 39(1): 273-280

Smith AJ and Lesot H (2001a). Induction and regulation of crown dentinogenesis: embryonic events as a template for dental tissue repair? **Crit Rev Oral Biol Med** 12(5): 425-437

Smith AJ, Matthews JB and Hall RC (1998). Transforming growth factor-beta1 (TGF-beta1) in dentine matrix. Ligand activation and receptor expression. **Eur J Oral Sci** 106 Suppl 1: 179-184

Smith AJ, Murray PE, Sloan AJ, Matthews JB and Zhao S (2001b). Trans-dentinal stimulation of tertiary dentinogenesis. **Adv Dent Res** 15: 51-54

Smith AJ, Scheven BA, Takahashi Y, Ferracane JL, Shelton RM and Cooper PR (2012a). Dentine as a bioactive extracellular matrix. **Arch Oral Biol** 57(2): 109-121

Smith AJ, Tobias RS, Cassidy N, Plant CG, Browne RM, Beguekirn C, Ruch JV and Lesot H (1994). Odontoblast Stimulation in Ferrets by Dentin Matrix Components. **Archives of Oral Biology** 39(1): 13-22

Smith AJ, Tobias RS, Plant CG, Browne RM, Lesot H and Ruch JV (1990). In vivo morphogenetic activity of dentine matrix proteins. **J Biol Buccale** 18(2): 123-129

Spath L, Rotilio V, Alessandrini M, Gambara G, De Angelis L, Mancini M, Mitsiadis TA, Vivarelli E, Naro F, Filippini A and Papaccio G (2010). Explant-derived human dental pulp stem cells enhance differentiation and proliferation potentials. **J Cell Mol Med** 14(6B): 1635-1644

Speed CA (2001). Therapeutic ultrasound in soft tissue lesions. **Rheumatology (Oxford)** 40(12): 1331-1336

Sreenath T, Thyagarajan T, Hall B, Longenecker G, D'Souza R, Hong S, Wright JT, MacDougall M, Sauk J and Kulkarni AB (2003). Dentin sialophosphoprotein knockout mouse teeth display widened predentin zone and develop defective dentin mineralization similar to human dentinogenesis imperfecta type III. **J Biol Chem** 278(27): 24874-24880

Staines M, Robinson WH and Hood JAA (1981). Spherical Indentation of Tooth Enamel. **Journal of Materials Science** 16(9): 2551-2556

Stanislawski L, Carreau JP, Pouchelet M, Chen ZH and Goldberg M (1997). In vitro culture of human dental pulp cells: some aspects of cells emerging early from the explant. **Clin Oral Investig** 1(3): 131-140

Stanley HR, Conti AJ and Graham C (1975). Conservation of human research teeth by controlling cavity depth. **Oral Surg Oral Med Oral Pathol** 39(1): 151-156

Staquet MJ, Durand SH, Colomb E, Romeas A, Vincent C, Bleicher F, Lebecque S and Farges JC (2008). Different roles of odontoblasts and fibroblasts in immunity. **J Dent Res** 87(3): 256-261

Stocum DL (2001). Stem cells in regenerative biology and medicine. **Wound Repair Regen** 9(6): 429-442

Su CH, Chang CY, Wang HH, Wu YJ, Bettinger T, Tsai CH and Yeh HI (2010). Ultrasonic microbubble-mediated gene delivery causes phenotypic changes of human aortic endothelial cells. **Ultrasound Med Biol** 36(3): 449-458

Sun S, Liu Y, Lipsky S and Cho M (2007). Physical manipulation of calcium oscillations facilitates osteodifferentiation of human mesenchymal stem cells. **FASEB J** 21(7): 1472-1480

Suzuki A, Takayama T, Suzuki N, Sato M, Fukuda T and Ito K (2009). Daily low-intensity pulsed ultrasound-mediated osteogenic differentiation in rat osteoblasts. **Acta Biochim Biophys Sin (Shanghai)** 41(2): 108-115

Symons NBB (1961). A Histochemical Study of the Intertubular and Peritubular Matrices in Normal Human Dentine. **Archives of Oral Biology** 5(3-4): 241-&

Takayama S, Reed JC and Homma S (2003). Heat-shock proteins as regulators of apoptosis. **Oncogene** 22(56): 9041-9047

Takayama T, Suzuki N, Ikeda K, Shimada T, Suzuki A, Maeno M, Otsuka K and Ito K (2007). Low-intensity pulsed ultrasound stimulates osteogenic differentiation in ROS 17/2.8 cells. **Life Sci** 80(10): 965-971

Takeuchi R, Ryo A, Komitsu N, Mikuni-Takagaki Y, Fukui A, Takagi Y, Shiraishi T, Morishita S, Yamazaki Y, Kumagai K, Aoki I and Saito T (2008). Low-intensity pulsed

ultrasound activates the phosphatidylinositol 3 kinase/Akt pathway and stimulates the growth of chondrocytes in three-dimensional cultures: a basic science study. **Arthritis Res Ther** 10(4): R77

Tang CH, Yang RS, Huang TH, Lu DY, Chuang WJ, Huang TF and Fu WM (2006). Ultrasound stimulates cyclooxygenase-2 expression and increases bone formation through integrin, focal adhesion kinase, phosphatidylinositol 3-kinase, and Akt pathway in osteoblasts. **Mol Pharmacol** 69(6): 2047-2057

Tartaix PH, Doulaverakis M, George A, Fisher LW, Butler WT, Qin C, Salih E, Tan M, Fujimoto Y, Spevak L and Boskey AL (2004). In vitro effects of dentin matrix protein-1 on hydroxyapatite formation provide insights into in vivo functions. **J Biol Chem** 279(18): 18115-18120

Taylor AC (1962). Responses of cells to pH changes in the medium. **J Cell Biol** 15: 201-209

Ten Cate AR (1998). **Oral Histology: Development, Structure and Function** London, Mosby.

ter Haar G (1999). Therapeutic ultrasound. **Eur J Ultrasound** 9(1): 3-9

ter Haar G (2007). Therapeutic applications of ultrasound. **Prog Biophys Mol Biol** 93(1-3): 111-129

ter Haar G (2011a). Ultrasonic imaging: safety considerations. **Interface Focus** 1(4): 686-697

ter Haar G, Daniels S, Eastaugh KC and Hill CR (1982). Ultrasonically induced cavitation in vivo. **Br J Cancer Suppl** 5: 151-155

ter Haar G, Dyson M and Oakley EM (1987). The use of ultrasound by physiotherapists in Britain, 1985. **Ultrasound Med Biol** 13(10): 659-663

ter Haar G, Shaw A, Pye S, Ward B, Bottomley F, Nolan R and Coady AM (2011b). Guidance on reporting ultrasound exposure conditions for bio-effects studies. **Ultrasound Med Biol** 37(2): 177-183

ter Haar GR and Daniels S (1981). Evidence for ultrasonically induced cavitation in vivo. **Phys Med Biol** 26(6): 1145-1149

ter Riet G, Kessels AG and Knipschild P (1996). A randomized clinical trial of ultrasound in the treatment of pressure ulcers. **Phys Ther** 76(12): 1301-1311

Tezvergil-Mutluay A, Mutluay M, Seseogullari-Dirihan R, Agee KA, Key WO, Scheffel DL, Breschi L, Mazzoni A, Tjaderhane L, Nishitani Y, Tay FR and Pashley DH (2013). Effect of phosphoric acid on the degradation of human dentin matrix. **J Dent Res** 92(1): 87-91

Thirumala S, Gimble JM and Devireddy RV (2010). Evaluation of methylcellulose and dimethyl sulfoxide as the cryoprotectants in a serum-free freezing media for cryopreservation of adipose-derived adult stem cells. **Stem Cells Dev** 19(4): 513-522

Thyagarajan T, Sreenath T, Cho A, Wright JT and Kulkarni AB (2001). Reduced expression of dentin sialophosphoprotein is associated with dysplastic dentin in mice overexpressing transforming growth factor-beta 1 in teeth. **Journal of Biological Chemistry** 276(14): 11016-11020

Tobita K, Ohnishi I, Matsumoto T, Ohashi S, Bessho M, Kaneko M, Matsuyama J and Nakamura K (2011). Effect of low-intensity pulsed ultrasound stimulation on callus remodelling in a gap-healing model: evaluation by bone morphometry using three-dimensional quantitative micro-CT. **J Bone Joint Surg Br** 93(4): 525-530

Tomson PL, Grover LM, Lumley PJ, Sloan AJ, Smith AJ and Cooper PR (2007). Dissolution of bio-active dentine matrix components by mineral trioxide aggregate. **J Dent** 35(8): 636-642

Toyosawa S, Kanatani N, Shintani S, Kobata M, Yuki M, Kishino M, Ijuhin N and Komori T (2004b). Expression of dentin matrix protein 1 (DMP1) during fracture healing. **Bone** 35(2): 553-561

Toyosawa S, Okabayashi K, Komori T and Ijuhin N (2004a). mRNA expression and protein localization of dentin matrix protein 1 during dental root formation. **Bone** 34(1): 124-133

Tziafas D (2004). The future role of a molecular approach to pulp-dentinal regeneration. **Caries Res** 38(3): 314-320

Tziafas D, Smith AJ and Lesot H (2000). Designing new treatment strategies in vital pulp therapy. **J Dent** 28(2): 77-92

Unsworth J, Kaneez S, Harris S, Ridgway J, Fenwick S, Chenery D and Harrison A (2007). Pulsed low intensity ultrasound enhances mineralisation in preosteoblast cells. **Ultrasound Med Biol** 33(9): 1468-1474

Unterbrink A, O'Sullivan M, Chen S and MacDougall M (2002). TGF beta-1 downregulates DMP-1 and DSPP in odontoblasts. **Connect Tissue Res** 43(2-3): 354-358

Vaezy S, Martin R and Crum L (2001). High intensity focused ultrasound: a method of hemostasis. **Echocardiography** 18(4): 309-315

Vakil N and Everbach EC (1993). Transient acoustic cavitation in gallstone fragmentation: a study of gallstones fragmented in vivo. **Ultrasound Med Biol** 19(4): 331-342

Vogel C and Marcotte EM (2012). Insights into the regulation of protein abundance from proteomic and transcriptomic analyses. **Nature reviews Genetics** 13(4): 227-232

Wagner AC, Weber H, Jonas L, Nizze H, Strowski M, Fiedler F, Printz H, Steffen H and Goke B (1996). Hyperthermia induces heat shock protein expression and protection against cerulein-induced pancreatitis in rats. **Gastroenterology** 111(5): 1333-1342

Wakefield LM, Winokur TS, Hollands RS, Christopherson K, Levinson AD and Sporn MB (1990). Recombinant latent transforming growth factor beta 1 has a longer plasma half-life in rats than active transforming growth factor beta 1, and a different tissue distribution. **J Clin Invest** 86(6): 1976-1984

Walmsley AD (1988). Applications of ultrasound in dentistry. **Ultrasound Med Biol** 14(1): 7-14

Walmsley AD, Laird WR and Williams AR (1984). A model system to demonstrate the role of cavitational activity in ultrasonic scaling. **J Dent Res** 63(9): 1162-1165

Walmsley AD, Laird WRE and Lumley PJ (1992). Ultrasound in Dentistry .2. Periodontology and Endodontics. **Journal of Dentistry** 20(1): 11-17

Wang F-S, Kuo Y-R, Wang C-J, Yang KD, Chang P-R, Huang Y-T, Huang H-C, Sun Y-C, Yang Y-J and Chen Y-J (2004). Nitric oxide mediates ultrasound-induced hypoxia-inducible factor-1alpha activation and vascular endothelial growth factor-A expression in human osteoblasts. **Bone** 35(1): 114-123

Watabe H, Furuhama T, Tani-Ishii N and Mikuni-Takagaki Y (2011). Mechanotransduction activates alpha(5)beta(1) integrin and PI3K/Akt signaling pathways in mandibular osteoblasts. **Exp Cell Res** 317(18): 2642-2649

Watanabe Y, Matsushita T, Bhandari M, Zdero R and Schemitsch EH (2010). Ultrasound for fracture healing: current evidence. **J Orthop Trauma** 24 Suppl 1: S56-61

Watmough DJ, Davies HM, Quan KM, Wytch R and Williams AR (1991). Imaging microbubbles and tissues using a linear focussed scanner operating at 20 MHz: possible implications for the detection of cavitation thresholds. **Ultrasonics** 29(4): 312-318

Wei FY, Leung KS, Li G, Qin J, Chow SK, Huang S, Sun MH, Qin L and Cheung WH (2014). Low intensity pulsed ultrasound enhanced mesenchymal stem cell recruitment through stromal derived factor-1 signaling in fracture healing. **PLoS One** 9(9): e106722

Whitney NP, Lamb AC, Louw TM and Subramanian A (2012). Integrin-mediated mechanotransduction pathway of low-intensity continuous ultrasound in human chondrocytes. **Ultrasound Med Biol** 38(10): 1734-1743

Whittaker DK and Kneale MJ (1979). The dentine-predentine interface in human teeth. A scanning electron microscope study. **Br Dent J** 146(2): 43-46

Williams AR and Chater BV (1980). Mammalian platelet damage in vitro by an ultrasonic therapeutic device. **Arch Oral Biol** 25(3): 175-179

Williamson JD and Cox P (1968). Use of a new buffer in the culture of animal cells. **The Journal of general virology** 2(2): 309-312

Wu J and Nyborg WL (2006). **Emerging Therapeutic Ultrasound** Singapore, World Scientific Publishing Co. Pte. Ltd.

Wu J and Nyborg WL (2008). Ultrasound, cavitation bubbles and their interaction with cells. **Adv Drug Deliv Rev** 60(10): 1103-1116

Xia P, Ren S, Lin Q, Cheng K, Shen S, Gao M and Li X (2015). Low-Intensity Pulsed Ultrasound Affects Chondrocyte Extracellular Matrix Production via an Integrin-Mediated p38 MAPK Signaling Pathway. **Ultrasound Med Biol** 41(6): 1690-1700

Yang RS, Lin WL, Chen YZ, Tang CH, Huang TH, Lu BY and Fu WM (2005). Regulation by ultrasound treatment on the integrin expression and differentiation of osteoblasts. **Bone** 36(2): 276-283

Ye L, Zhang S, Ke H, Bonewald LF and Feng JQ (2008). Periodontal breakdown in the Dmp1 null mouse model of hypophosphatemic rickets. **J Dent Res** 87(7): 624-629

Zeqiri B (2007). Metrology for ultrasonic applications. **Prog Biophys Mol Biol** 93(1-3): 138-152

Zhao S, Sloan AJ, Murray PE, Lumley PJ and Smith AJ (2000). Ultrastructural localisation of TGF-beta exposure in dentine by chemical treatment. **Histochem J** 32(8): 489-494

Zhou YF (2011). High intensity focused ultrasound in clinical tumor ablation. **World J Clin Oncol** 2(1): 8-27

APPENDIX I

Research Papers

- **Patel US**, Ghorayeb SR, Yamashita Y, Atanda F, Walmsley AD & Scheven BA. Ultrasound field characterization and bioeffects in multiwall culture plates. Journal of Therapeutic Ultrasound Jun 2015, 3(8).
- Ghorayeb SR, **Patel US**, Walmsley AD & Scheven BA. Biophysical characterization of low-frequency ultrasound interaction with dental pulp stem cells. Journal of Therapeutic Ultrasound Aug 2013, 1(12).

Conference Presentations

- **Patel US**, Walmsley AD & Scheven BA. An in vitro set-up to study low-frequency ultrasound effects on dental cells. Ultrasonics Industries Association, Glasgow, UK, 2011 (oral presentation).
- **Patel US**, Walmsley AD & Scheven BA. Low-frequency Ultrasound Stimulates Proliferation of Odontoblast-like Cells *in vitro*. International Association for Dental Research, Barcelona, Spain, 2010 (poster presentation).
- **Patel US**, Walmsley AD & Scheven BA. Travelling Ultrasound: Transference in Multiwell Plates. College of Medical and Dental Sciences Research Gala, University of Birmingham, UK, 2010 (poster presentation).
- **Patel US**, Walmsley AD & Scheven BA. Ultrasound Induced Dental Regeneration. Graduate School Poster Conference, University of Birmingham, UK, 2009 (poster presentation – won first prize).